Co-funded by the European Union

MINISTRY OF AGRICULTURE AND FOOD

MARITIME, FISHERIES AND AQUACULTURE PROGRAMME

PELAGIC TRAWL SURVEYS IN THE BULGARIAN MARINE AREA, NOVEMBER 2024

SCIENTIFIC REPORT

--www.eufunds.bg--

Project No. BG14MFOP001-1.002-0001 "Collection, management and use of data for the purposes of scientific analysis and implementation of the Common Fisheries Policy for the period 2023-2024", financed by the Maritime, Fisheries and Aquaculture Programme, co-financed by the European Union through the European Fund for maritime, fisheries and aquaculture fund.

Co-funded by the European Union

MINISTRY OF AGRICULTURE AND FOOD

MARITIME, FISHERIES AND AQUACULTURE PROGRAMME

This study was carried out thanks to the financial support of the European Commission under REGULATION (EU) 2017/1004 OF THE EUROPEAN PARLIAMENT AND OF THE COUNCIL of 17 May 2017 on the establishment of a Union framework for the collection, management and use of data in the fisheries sector and support for scientific advice regarding the common fisheries policy and repealing Council Regulation (EC) No 199/2008 (recast), the National Agency for Fisheries and Aquaculture – Ministry of Agriculture, Bulgaria and Institute of Oceanology – Bulgarian Academy of Sciences, Varna, Bulgaria.

Project No. BG14MFOP001-1.002-0001 "Collection, management and use of data for the purposes of scientific analysis and implementation of the Common Fisheries Policy for the period 2023-2024", financed by the Maritime, Fisheries and Aquaculture Programme, co-financed by the European Union through the European Fund for maritime, fisheries and aquaculture fund.

The survey was carried out in November 2024 in the Bulgarian Black Sea area on board of R/V HAITHABU in execution of the National Program of Bulgaria for data collection.

BULGARIAN ACADEMY OF SCIENCES

INSTITUTE OF OCEANOLOGY

VARNA

AUTHORS: Assoc. Prof. Violin Raykov, Assoc. Prof. Maria Yankova, Prof. Petya Ivanova, Assoc. Prof. Veselina Mihneva, Assoc. Prof. Dimitar Dimitrov, Assoc. Prof. Kremena Stefanova, Chief Asst. Elitsa Stefanova, Dr. Ilian Kotsev, Assoc. Prof. Nina Dzhembekova, Chief Asst. Ivelina Zlateva, Nelly Valcheva (technician), Dobroslav Dechev (technician), Hristiyana Stamatova (technician), Svetla Koleva (technician), Yordan Raev (PhD student), Konstantin Petrov (PhD student), Yordan Yordanov (logistics).

Table of content

Project No. BG14MFOP001-1.002-0001 "Collection, management and use of data for the purposes of scientific analysis and implementation of the Common Fisheries Policy for the period 2023-2024", financed by the Maritime, Fisheries and Aquaculture Programme, co-financed by the European Union through the European Fund for maritime, fisheries and aquaculture fund.

Project No. BG14MFOP001-1.002-0001 "Collection, management and use of data for the purposes of scientific analysis and implementation of the Common Fisheries Policy for the period 2023-2024", financed by the Maritime, Fisheries and Aquaculture Programme, co-financed by the European Union through the European Fund for maritime, fisheries and aquaculture fund.

1. Material and Methods

Pelagic trawl survey was accomplished following the National Programs for Data Collection in the Fisheries sector of Bulgaria. The study was conducted in November 2024, in the Bulgarian Black Sea area, enclosed between Durankulak and Ahtopol (42°05' and 43°45' N and 27°55' and 29°55' E), with a total length of the coastline of 370 km (Fig. 1.1).

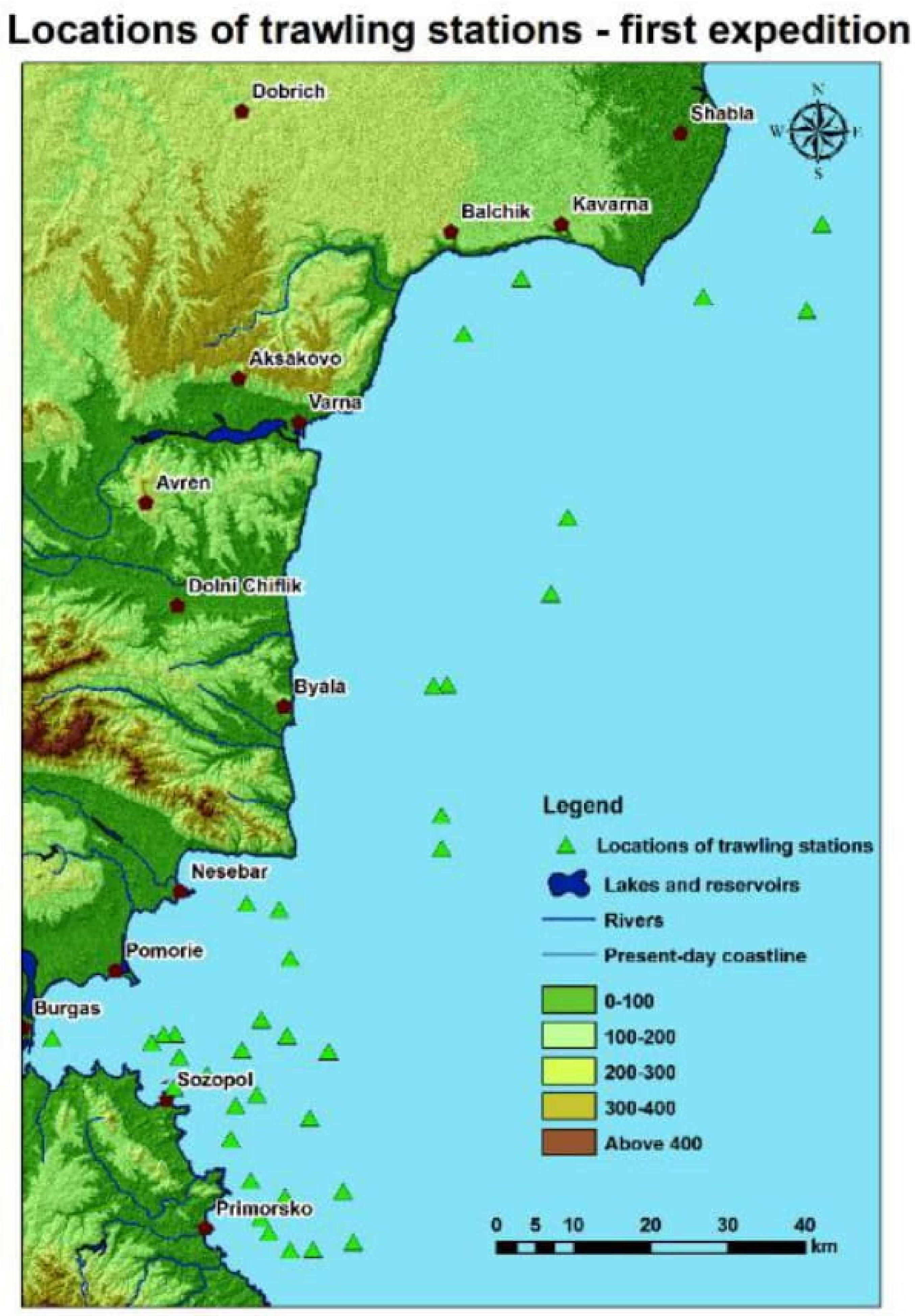

Figure 1.1. Location of the stations in November 2024

The pelagic trawl survey (OTM) was carried out on board the research vessel "HaitHabu". During the survey, a total of 36 trawls were carried out. The trawling was performed during the day with a duration of 30–40 minutes, depending on the hydro-meteorological conditions, at an average speed of 2.7 knots (variation in the range 2.7–2.9).

The size of the pelagic trawl are as follows:

- Pelagic trawl type 50/35 – 74 m;
- Headroap length – 40 m;
- Horizontal opening – 16 m;
- Vertical opening – 7 m;
- Mesh size – 7×7 mm;
- Effective part of trawl – 27 m;
- Pelagic doors – 3.5 m^2.

The following types of data were collected:

- Coordinates and duration of each trawl;
- Total catch weight;
- Separation of catches by species;
- Composition of by-catch.

The biological analysis is based on the biomass of the species found during the study. Additionally, an analysis of the distribution and abundance of the other species caught as by-catch is presented.

1.1. Sampling design

In order to determine the abundance of the reference species (*Sprattus sprattus*) in the Bulgarian part of the Black Sea, a standard stratified survey methodology was used (Gulland, 1966). The study area is divided into three subgroups depending on depth: **Stratum 1** (15–30 m), **Stratum 2** (30–50 m), and **Stratum 3** (50–100 m). The research area in Bulgarian waters was further divided into 128 non-overlapping polygons of equal size, located at depths between 15 and 100 m. Samplimg was conducted at 36 randomly selected sites using pelagic trawling.

Each field is a rectangle with dimensions 5′′ latitude x 5′′ longitude and an area of approximately 62.58 km^2 (measured using GIS), which is large enough to allow trawling for a corresponding duration in the meridional direction. The fields are grouped into larger —referred to as layers— whose geographical and depth boundaries are determined based on the distribution and density of the species observed during the survey. Only one trawl was conducted in each field, lasting between 30 and 40 minutes at a speed of 2.7–2.9 knots (Picture 1.1.1.).

Picture 1.1.1. Catch in trawl

1.2. Onboard sample processing

The specimens processed during the survey are presented in Table 1.2.1.

Table 1.2.1. Number of processed individuals

Species	Number
sprat	12
whiting	1200
red mullet	1200
horse mackerel	1500
anchovy	-

The data from each trawl included measurements of the following parameters (Gulland, 1966):

- Depth, measured using the vessel's echo sounder;
- GPS coordinates of start and end haul points;
- Haul duration;
- Abundance of species caught;
- Weight of the total sprat catch;
- Abundance and weight of other species;
- Species composition of the by-catch.

A 4% formaldehyde solution prepared with seawater was used to preserve the stomach contents.

1.3. Laboratory analyses

The processing of the samples collected on board continued under laboratory conditions, focusing on determining the age and nutritional composition of the stomach contents of sprat.

Age was determined based on the analysis of otoliths under a binocular microscope.

Project No. BG14MFOP001-1.002-0001 "Collection, management and use of data for the purposes of scientific analysis and implementation of the Common Fisheries Policy for the period 2023-2024", financed by the Maritime, Fisheries and Aquaculture Programme, co-financed by the European Union through the European Fund for maritime, fisheries and aquaculture fund.

The dietary spectrum was assessed by soritn the stomach contents into taxonomic groups, identified to the lowest possible taxonomic level.

1.4. Statistical analyses

Swept area method

This method is based on near-bottom trawling (protrawled area), a widely used direct technique for estimating the instantaneous biomass of benthic organisms (Fig. 1.4.1, 1.4.2).

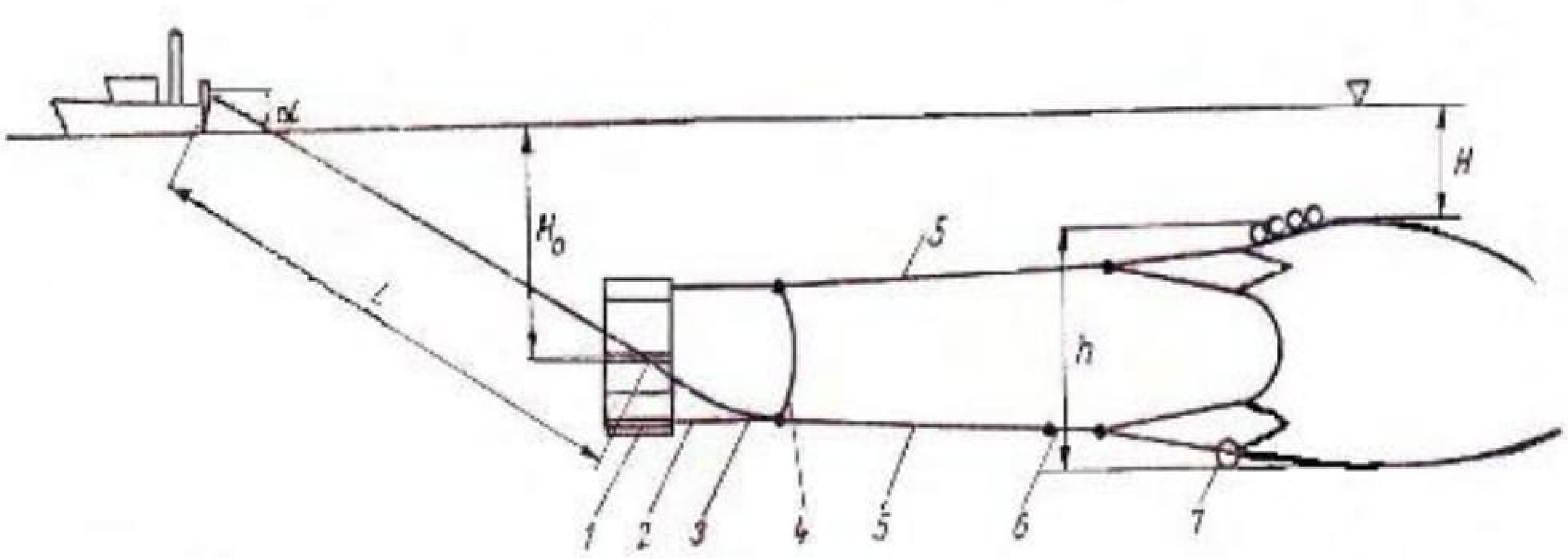

Figure 1.4.1. Scheme of the trawl, used in the Swept area method (according to Grudev et al., 1981) 1 - trawl door; 2 - conjections; 3 - transitional wire; 4 - compensator; 5 - wires; 6 - extention cord; 7- deepener

In Figure 1.4.2. the scheme of the so-called bathy-pelagic trawl for catching sprat is represented.

Project No. BG14MFOP001-1.002-0001 "Collection, management and use of data for the purposes of scientific analysis and implementation of the Common Fisheries Policy for the period 2023-2024", financed by the Maritime, Fisheries and Aquaculture Programme, co-financed by the European Union through the European Fund for maritime, fisheries and aquaculture fund.

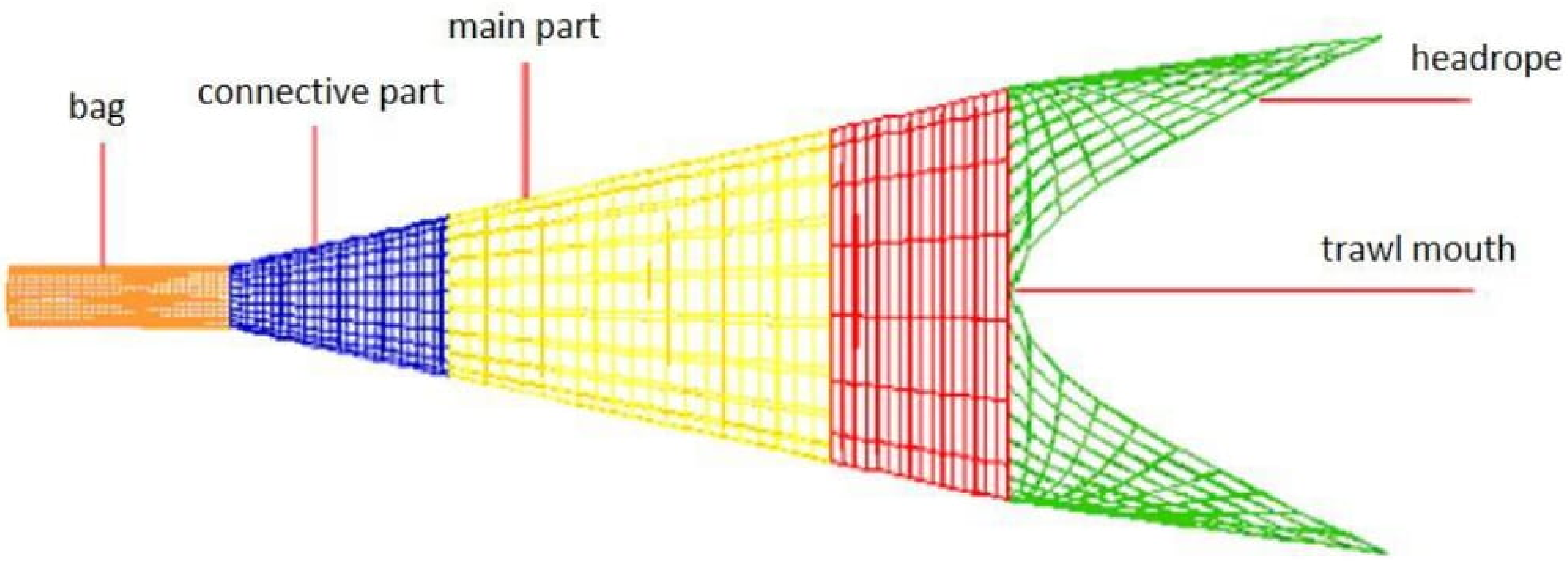

Figure 1.4.2. Scheme of bathy-pelagic trawl for sprat catch

The main point of the method: the trawl doors are designed to drag along the seafloor for defined distance. Trawling area is calculated as follows:

$$(1)\quad a = D * hr * X2$$
$$D = V * t$$

(where: a – trawling area, V – trawling velocity, hr* X2 – trawl door distance, t – trawling duration (h), D – dragged distance on the seafloor;

$$(2)\ D = 60 * \sqrt{(Lat_1 - Lat_2)^2 + (Lon_2 - Lon_1) * \cos(0.5 * (Lat_1 + Lat_2))}$$
$$(3)\ D = \sqrt{VS^2 + CS^2 + 2 * VS * CS * \cos(dirV - dirC)},$$

where, VS is vessel velocity, CS – present velocity (knots), dir$V$ vessel course (degrees), and $dirC$ – present course (degrees).

Stock biomass is calculated using catch per unit area, as a fraction of catch per unit effort from the dragged area:

$$(4)\ \left(\frac{C_{w/t}}{a/t}\right) = C_{w/a} kg/sq.km$$

where: *Cw/t* – catch per unit effort, a/t – trawling area (km^2) per unit time;

Stock biomass of the given species per each stratum could be calculated as follows:

(5) $$B = (\overline{C_{w/a}}) * A$$

where: $\overline{C_{w/a}}$ - mean CPUA for total trawling number in each stratum, A- area of the stratum.
The variance of biomass estimate for each stratum is (equation 4):

(6) $$VAR(B) = A^2 * \frac{1}{n} * \frac{1}{n-1} * \sum_{i=1}^{n} \left[Ca(i) - \overline{Ca}\right]^2$$

The total area of the investigated region is equal to the sum of areas of each stratum:
A = A1+A2+A3

Average weighted catch per whole aquatic territory is calculated as follows:

(7) $$\overline{Ca}(A) = Ca1 * A1 + Ca2 * A2 + Ca3 * A3 / A$$

where: Ca1- catch per unit area in stratum 1, A1 – an area of stratum 1, etc., A- size of total area.

Accordingly, total stock biomass for the whole marine area:

(8) $$B = \overline{Ca}(A) * A$$

where: $\overline{Ca}(A)$ - average weighted catch per whole investigated marine area, A – total investigated marine area.

Estimation of Maximum Sustainable Yield (MSY)
The Gulland's formula for virgin stocks is used:

(9) MSY = 0.5*M*Bv

where: M – coefficient of natural mortality; Bv – virgin stock biomass.

A relative yield-per-recruit model with uncertainties:

(10)
$$Y'/R = E * U^{M/k} \left\{ 1 - \frac{3U}{(1+m)} + \frac{3U^2}{(1+2m)} - \frac{U^3}{(1+3m)} \right\}$$

where: U = 1-(Lc/L∞)
m = (1-E)/(M/k) = k/Z
E = F/Z – exploitation coefficient

Converted catch curve

Several methods are available for estimating total mortality (Z) from length-frequency data. Reliable estimates of Z can be obtained from the mean length of a representative sample or from the slope of a cumulative Jones' plot. A variety of approaches have been developed to analyze length-frequency data, which serve as the functional equivalent of age-structured catch curves. These "length-converted catch curves" are based on assumptions similar to those used in age-structured catch curve analyses.

1.5. Age estimation

Calcified structures (CS) are commonly used to determine age. Aging in fish means the presence of CS visible as opaque and transparent areas. Calcified age-determining structures in fish are various: otoliths (statoliths), dorsal vertebrae, spines, and opercular bones. In some species, so called "sagittae" are used. The most important aspects (difficulties, extraction, storage, method of preparation, criteria for age determination) regarding age analysis are discussed by species. Otoliths play a role in balance, movement, and sound perception. They are most commonly used for age determination, growth and mortality studies. In bony fish, otoliths are the primary CS for age determination and are widely used in ichthyology. On the other hand, when analyzing O_2 isotopes, both species migrations and stock identification are determined. Otoliths serve as balance in space and as hearing organs for fish. Based on the shape and size of the otoliths, the feeding habits of the fish are also determined (Kasapoglu and Duzgunes, 2014). Researchers used reference collections and photographs of otoliths in publications to aid identification (Picture 1.5.1). Otoliths have a characteristic shape that is highly specific but varies greatly among species.

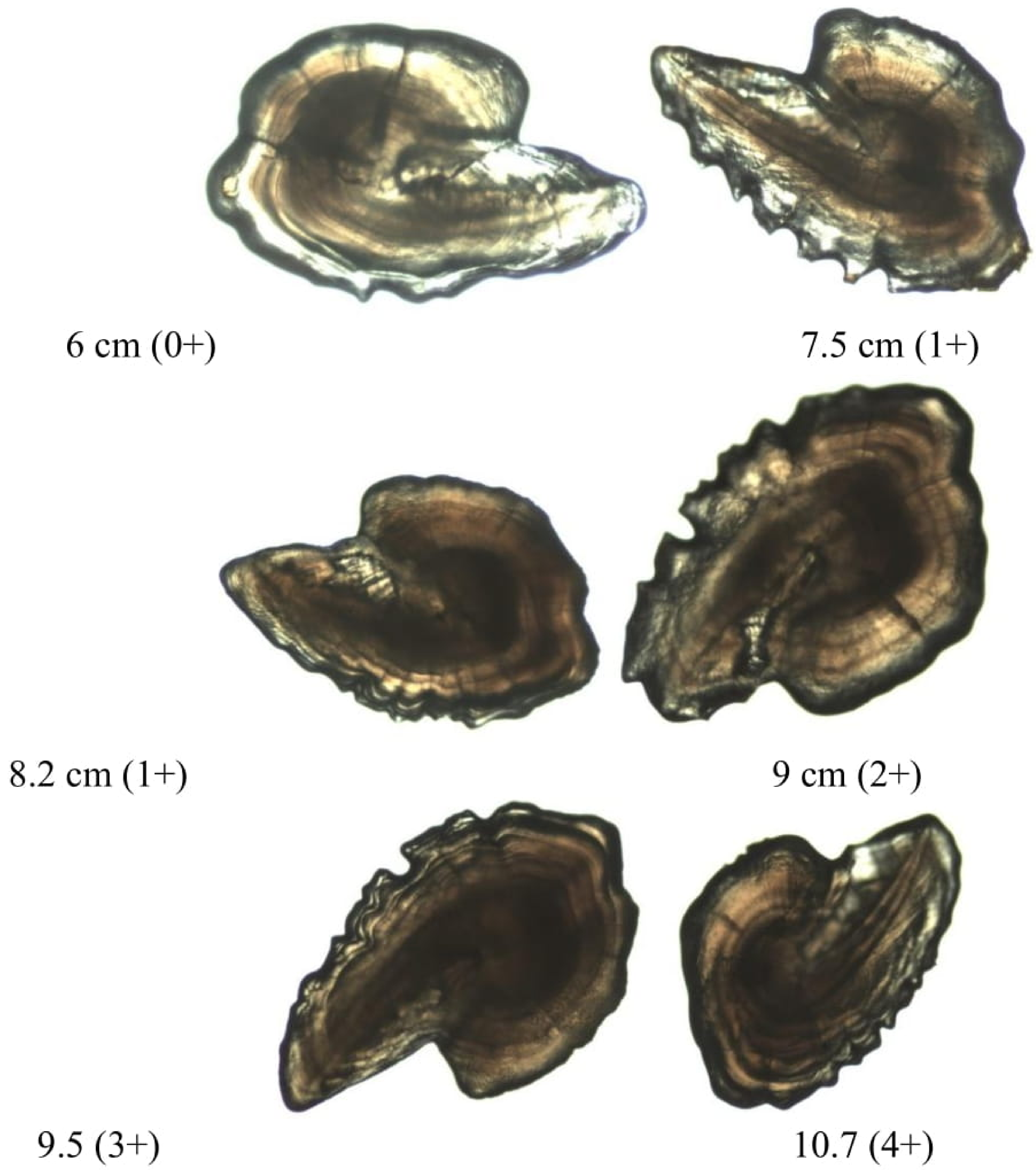

Picture 1.5.1. Otoliths of sprat

Project No. BG14MFOP001-1.002-0001 "Collection, management and use of data for the purposes of scientific analysis and implementation of the Common Fisheries Policy for the period 2023-2024", financed by the Maritime, Fisheries and Aquaculture Programme, co-financed by the European Union through the European Fund for maritime, fisheries and aquaculture fund.

Otoliths are three types, located on the left and right sides of the head in semi rings: "sagitta" in the sacculus, "lapillus" in the lagenar, and "asteriscus" in the utricular channels. The location, size, and shape of these three types differ by species, the largest is "sagitta" and the smallest is "asteriscus". So, "sagitta" is the one that is mostly used in age determination of bony fishes. Other reasons for using otoliths to determine age are:

- Their formation in the embryonic phase, which shows all the changes in the life cycle of the fish.
- Their presence in fish which have no scales.
- Achieving better results than those of scale analysis, especially when it comes to older fish.
- No recovery or regeneration.
- Having the same structure in all the individuals of the same species (Jearld, 1983).

On the other hand, their disadvantages are the need to dissect the fish and some problems in age determination due to crystal-like formations by irregular $CaCO_3$ accumulations on the otoliths.

1.5.1. Preparation for otolith extraction

It is very important to have a representative sample from which the otoliths will be extracted, and their number depends on the size of the respective species. For smaller species, fewer otoliths are taken. According to availability, 5 specimens from each size group are set aside for age determination. For each fish total length (±0.1 cm), total weight (±0.01 g), sex, maturation stage (I-V), and gonad weight (±0.01 g) are recorded.

Sagittal otoliths of each fish are removed by cutting the head over the eyes after all individual measurements. The fish is then rinsed and placed in 96% ethyl alcohol to remove organic debris and finally stored with a sample number for other operational information.

1.5.2. Preparation of the otoliths for the age determination

Otoliths are placed in small black convex laboratory glasses containing 96% ethyl alcohol for age determination under a binocular stereo microscope with side and top illumination (Polat and Beamish, 1992). The magnification used depends on the size of the otolith, with 4× magnification being optimal for sprat.

1.5.3. Age determination and analysis of annual rings

The first step is to identify the location of the center and the first age ring. The observation of consecutive rings, whether continuous or not, is then essential. It is important to determine whether the fish is still growing or has reached the end of its growth period by examining the characteristics of the otolith's outer ring to see if it is opaque or hyaline. After these steps, the otoliths can be read following standardized protocols, which are very import for providing accurate age data, determining realistic population parameters, and reduce abnormal procedures and biases through standardized age reading criteria.

Isometric growth is observed in the sprat's left and right otoliths. These are small, transparent structures (Fig. 1.5.3.1). They feature distinct summer and winter rings, along with a central core. Additionally, spring rings—opaque—and late autumn rings—hyaline—are considered during age determination (Pısıl, 2006).

Sprattus sprattus

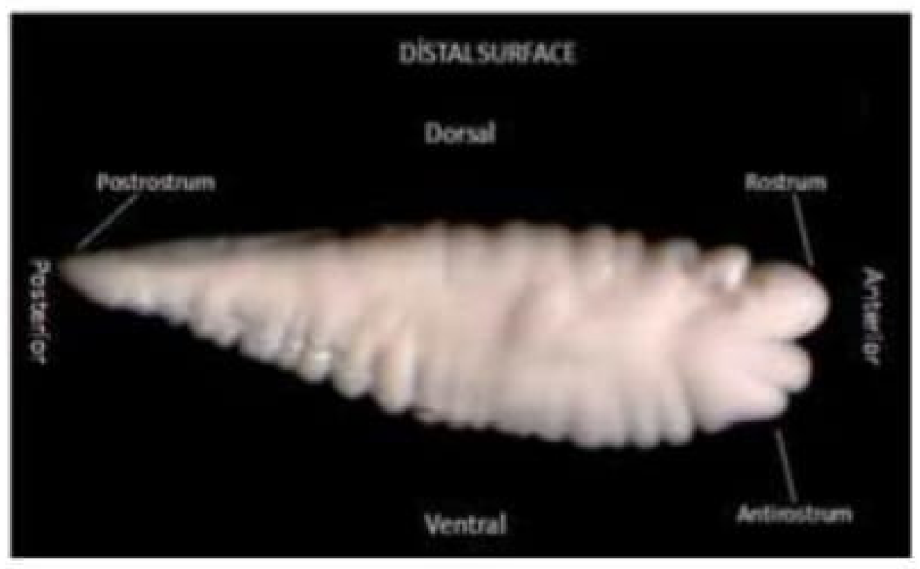

Merlangius merlangus

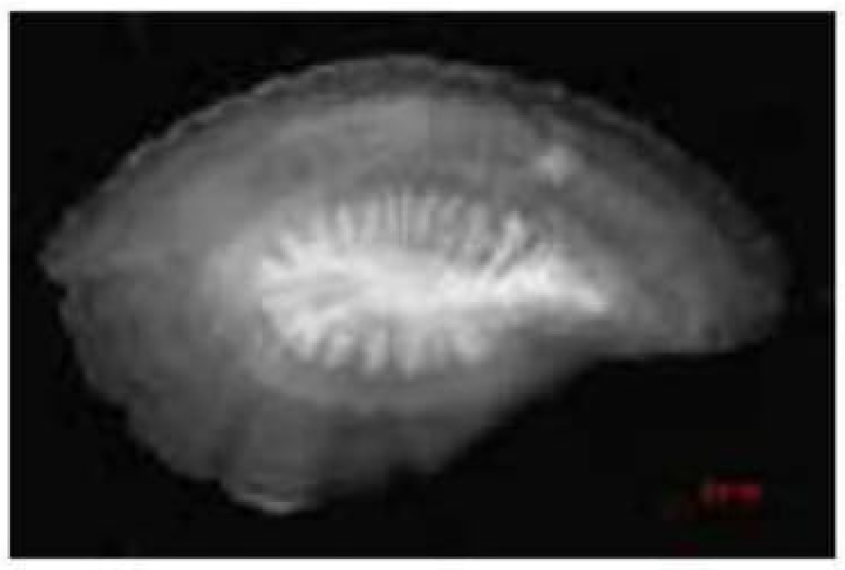

Trachurus mediterraneus

Mullus barbatus

Figure 1.5.3.1. Sprat, whiting, horse mackerel, and red mullet otoliths

1.5.4. Age reading protocol for sprat

1. The dissected otoliths are rinsed, treated with 96% ethyl alcohol, and stored dry.
2. Age determination is performed by an expert by immersing the entire otolith in 96% ethyl alcohol, then placing it in a convex glass under reflected light against a dark background.
3. Magnification is selected based on the size of the otolith. The aim is to avoid increasing magnification excessively, as this may reveal rings that are not representative for age determination in larger otoliths. A magnification of 4× is optimal for visualizing the hyaline zones in sprat otoliths.
4. Otolith are observed from their distal surface.
5. January 1st of the respective year is considered the hatching date for sprat.
6. A central point surrounded by hyaline rings forms after the yolk sac and the initiation of free feeding. The next opaque ring is known as "first year growth". This ring retains its circular shape in the postrostrum region. Together with this ring and the next hyaline ring, they form a "V" shape in the rostrum and are accepted as first-year rings.
7. Small, continuous concentric rings near the true hyaline ring as part of the same age mark. These may appear as either very small opaque rings within the hyaline band or as small hyaline rings near the outer edge of an opaque ring.
8. Sprat and some other short-lived species exhibit very rapid growth, particularly in their first years. After the second year, the width of the growth rings narrows significantly, which should be considered when counting rings in older specimens.

The number of small and weak hyaline rings—known as false rings—in the opaque region is generally low, and distinguishing them from true age rings is relatively easy. However, when numerous and indistinguishable, such otoliths should not be used.

1.6. Sex and maturity estimation

1.6.1. Maturity stages

It is very important to use standardized maturity scales for sprat (and all species) to assess sampling strategies and determine the appropriate timing for accurate maturity classification in both sexes. In sprat, the small gonad size and batch spawnings of multiple egg cohorts over an extended period pose significant challenges for standardizing the maturity scale.

Project No. BG14MFOP001-1.002-0001 "Collection, management and use of data for the purposes of scientific analysis and implementation of the Common Fisheries Policy for the period 2023-2024", financed by the Maritime, Fisheries and Aquaculture Programme, co-financed by the European Union through the European Fund for maritime, fisheries and aquaculture fund.

According to ICES (2011), standardized sexual maturity scale for sprat includes six stages for both males and females (Fig. 1.6.1.1, Table 1.6.1.1).

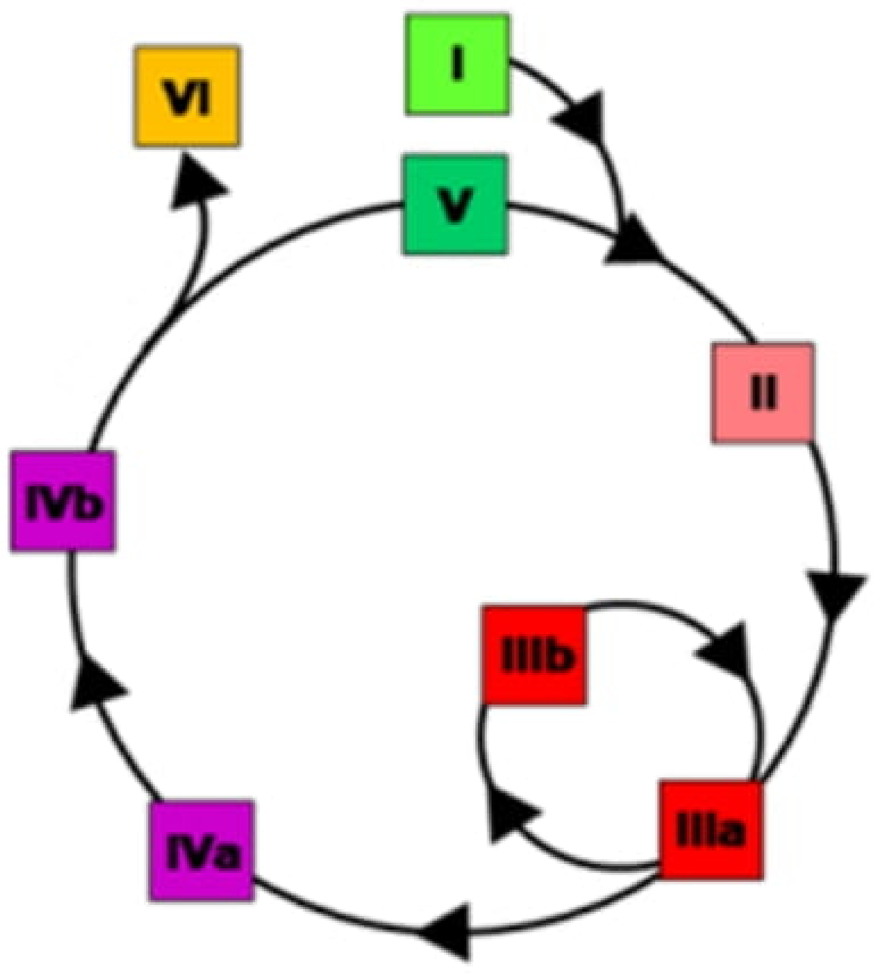

Figure 1.6.1.1. Scale with six maturity stages in sprat (Name of the stages are given in Table 1.6.1.1)

In particular, specimens without visible gland development were grouped into the "Immature" and "Preparation" categories. The spawning stage was subdivided into an inactive spawning stage (maturation and re-maturation, characterized by visible gamete development) and an active spawning stage, indicated by the presence of hydrated eggs. Integrating maturation and re-maturation into the spawning stage allows for more accurate identification of maturing and spawning individuals within the population.

Table 1.6.1.1. Macroscopic and histological characteristics of gonad developmental stages

Stages	*Macroscopic Characteristics*	*Histological characteristics*
FEMALES (OG: Oogonia, PG1: Early previtellogenic oocytes, PG2: Late previtellogenic oocytes, CA: Cortil alveoli oocytes, VT1: Early vitellogenic oocytes, VT2: Mid vitellogenic oocytes, VT3: Late vitellogenic oocytes, HYD: Hydrated oocytes, POF: Postovulatory follicles, SSB: Spawning stock biomass).		
I-Immature	*Juvenile: ovaries threadlike and small; transparent to wine red and translucent in color; sex difficult to determine; distinguishable from testes by a more tubular shape; oocytes not visible to the naked eye*	*OG+/-PGI*
II. Preparation	*The transition from immature to early maturing; oocytes not visible to the naked eye; ovaries yellow-orange to*	*PG1, PG2, CA*

	bright red; ovaries occupy up to half of the abdominal cavity. This stage is not included in SSB.	
III. Spawning *a. Inactive*	*Maturing and re-maturing: yolked opaque oocytes visible to the naked eye; ovaries change from semi-transparent to opaque yellow-orange or reddish as more oocytes enter the yolk stage; ovaries occupy at least half of the body cavity; re-maturing ovaries may be red to grey-red or purple in color and less firm than an ovary maturing the first batch, few hydrated oocytes may be left*	*PG1, PG2, CA, VT1, VT2, VT3, +/- POF*
b. Active	*Spawning active. Hydrated eggs are visible among yolked opaque oocytes; hydrates oocytes may be running; ovaries fill the body cavity; overall color varies from yellowish to reddish.*	*PG1, PG2, CA, VT1,VT2, VT3, HYD, POF*
IV.a. Cessation	*Baggy appearance; bloodshot; grey-red translucent in color; atretic oocytes appear as opaque irregular grains; few residual eggs may remain*	*PG1, PG2, POF, atretic oocytes, residual HYD*
IV.b. Recovery	*Ovaries appear firmer and membranes thicker than in sub-stage IV.a; these characteristics together with the slightly larger size distinguish this stage from the virgin stage; ovaries appear empty and there are no residual eggs; transparent to wine red translucent in color*	*PG1, PG2, atretic VT oocytes*
V. Resting	*Ovaries appear more tubular and firmer; oocytes not visible to the naked eye; transparent or grey-white to wine red with well-developed blood supply; this stage leads to stage II.*	*PG1, PG2 +/- atretic oocytes*
VI. Abnormal	*a) infection; b) intersex - both female and male tissues can be recognized; c) one lobe degenerated; d) stone roe (filled with connective tissue); e) other*	*Abnormal tissue*
MALES (SG: Spermatogonia; PS: Primary spermatocytes; SS: Secondary spermatocytes; ST: Spermatids; SZ: Spermatozoa; SSB: Spawning stock biomass)		
I. Immature	*Juvenile: Testes threadlike and small; white-grey to grey-brown; difficult to determine sex, but distinguishable from ovaries by a more lanceolate shape (knife-shaped edge of the distal part of the lobe).*	*SG, PS*
II. Preparation	*The transition from immature to mature: Testes easily distinguishable from ovaries by lanceolate shape; sperm development not visible;* *reddish grey to creamy translucent in color; testes occupy up to ½ of the abdominal cavity; this stage is not included in SSB.*	*SG, PS, SS, potentially few ST*
III. Spawning *a. Inactive*	*Maturing and re-maturing: Testes occupy at least half of the body cavity and grow to almost the length of the body cavity; the empty sperm duct may be visible; color varies from reddish light grey, creamy to white; edges may still be translucent at the beginning of the stage, otherwise*	*SG, PS, SS, ST, SZ*

	opaque; re-maturing testes may be irregularly colored with reddish or brownish blotches and grey at the lower edge with partly whitish remains of sperm	
b. Active	*Spawning active: testes fill the body cavity; Sperm duct filled and distended throughout the entire length; sperm runs freely or will run from the sperm duct, if transected; color varies from light grey to white..*	*SG, PS, SS, ST, SZ*
IV.a. Cessation	*Baggy appearance (like an empty bag when cut open); bloodshot; grey to reddish-brown translucent in color; residual sperm may be visible in the sperm duct.*	*SG, PS, atretic SS, ST and SZ*
IV.b. Recovery	*Testes appear firmer and the testes membrane appears thicker than in stage IVa due to contraction of the testes membrane; these characteristics together with the slightly larger size distinguish this stage from the virgin stage; testes appear empty and no residual sperm is visible in the sperm duct; reddish grey to greyish translucent in color.*	*SG, PS, potentially SS, atretic SZ*
V. Resting	*Testes appear firmer, development of a new line of germ cells; grey in color; this stage leads to stage II.*	*SG, PS, SS*
VI. Abnormal	*a) infection; b) intersex - both female and male tissues can be recognized; c) one lobe degenerated; d) other.*	*e.g. oocytes visible among spermatogenic tissues*

1.7. Batch fecundity

All fish were measured to the nearest 1 mm in total length (TL) and weighed to the nearest 1 gram. The gonads were examined under a microscope for external characteristics such as hardness and color to determine the stage of maturity. The sex ratio was also calculated in this study as the number of males / the number of females (Simon et al., 2012). Females were identified through macroscopic observation of a mature ovary (Laevastu, 1965). Fecundity rates can vary considerably during the short spawning season—starting low, peaking during peak spawning, and declining again toward the end. Batch fecundity of sprat was determined using the Hydrated Oocyte Method (Hunter et al., 1985). Fat, hydrated females were used. After sampling, their body cavity was opened and preserved in a buffered formalin solution (Hunter et al., 1985). The ovary-free female weight and the ovary weight were recorded. Three tissue samples of approximately 50 mg were taken from different parts of the ovary, and their exact weights were measured. The number of hydrated oocytes in each of the three subsamples was then counted under a binocular microscope. Hydrated oocytes are easily distinguished from other oocyte types by their large size, translucent appearance, and wrinkled surace resulting from formalin preservation. Batch fecundity was estimated based on the average number of hydrated oocytes per unit weight of the three subsamples.

Gonadosomatic Index (GSI) is determined monthly. GSI is calculated as:

$$GSI = \frac{GW}{SW} X\ 100$$

where GW is gonads weight and SW is somatic weight (represents the BW without GW).

For the estimation of sprat growth rate, the von Bertalanffy growth function (1938) is used, (according to Sparre, Venema, 1998):

(11) $L_t = L_\infty \left\{1 - \exp\left[-k\left(t - t_0\right)\right]\right\}$

(12) $W_t = W_\infty \left\{1 - \exp\left[-k\left(t - t_0\right)\right]\right\}^n$

Where: L_t, W_t are the length and weight of the fish at age t years; L_∞, W_∞ – asymptotic length and weight, k – curvature parameter, t_o – the initial condition parameter.

The length-weight relationship is obtained by the following equation:

(13) $W_t = qL_t^n$

where q – condition factor, constant in a length-weight relationship; n – constant in a length-weight relationship.

Coefficient of natural mortality (M), Pauly's empirical formula (1979, 1980) is applied:

(14) $\log M = -0.0066 - 0.279 * \log L_\infty + 0.6543 * \log k + 0.4634 * \log T^\circ C$

(15) $\log M = -0{\cdot}2107 - 0{\cdot}0824 \log W_\infty + 0{\cdot}6757 \log K + 0{\cdot}4627 \log T°C$

Where: L_∞, W_∞ and κ – parameters in von Bertalanffy growth function, $T^\circ C$ – an average annual temperature of the water (environmental parameter of the studied species).

1.8. Maximum Sustainable Catch (MSY)

The maximum sustainable catch was estimated as follow:

B msy = 0.5* B (t)

According to FAO (1995), following the precautionary approach:

B pr (2/3MSY)

1.9. Planktivorous fish species feeding

The study of the feeding habits of planktivorous fish (horse mackere, and sprat) in the western part of the Black Sea is based on the analysis of the stomach contents of **132 specimens (120 horse mackerel and 12 sprat)** collected between November 16 - 27, 2024.

During this period, data on the composition and quantity of mesozooplankton in the marine environment were also collected, as this group of organisms forms the main food base of the fish species studied.

The coordinates of the study area and descriptions of the data are presented in Table 1.9.1.

Table 1.9.1. Study areas in November 2024

Date	Trawl №	Coordinates		Depth (m)	Temperature (°C)
		Latitude	Longitude		
16.11.2024	T7	42.670	27.816	24	8.4
16.11.2024	T9	42.636	27.738	25	10.8
17.11.2024	T10	42.666	27.842	25	12
17.11.2024	T13	42.912	28.169	45	12.8
18.11.2024	T15	43.377	28.783	75	10.8
18.11.2024	T17	43.366	28.341	17	9.6
19.11.2024	T19	43.233	28.062	23	11.2
19.11.2024	T21	42.800	28.008	34	10.8
20.11.2024	T23	42.687	27.854	20	11.2
25.11.2024	T25	42.561	27.823	34	9.6
25.11.2024	T29	42.647	27.752	23	7.6
26.11.2024	T31	42.540	27.920	44	11.6
27.11.2024	T33	42.446	28.003	49	10

From the trawl catch, approximately 10/11 live fish specimens were separated and fixed with 10% formaldehyde solution. Under laboratory conditions, the absolute length (TL, with an accuracy of 0.1 cm) and weight (with an accuracy of 0.01 g) of the collected specimens were measured. The stomachs of the studied organisms were weighed using an analytical balance (accuracy, 0.0001 g). The food mass of each fish specimen was calculated as the difference between the weights of full and empty stomachs.

To determine the species composition of the food and the number of food objects, the stomach contents were examined under a microscope. Prey biomass in fish stomachs was calculated by multiplying the number of zooplankton organisms by their individual weights.

The following indices were defined.

1. Index of stomach fullness (ISF) as a percentage of body mass: (weight of stomach contents/weight of fish body) × 100

2. Index of relative importance (IRI; Pinkas et al., 1971): IRI = (N + M) × FO, where N is the proportion of the taxon (species) of the prey in the food by number, M is the proportion of the taxon (species) of the prey in the food by biomass, and FO is the frequency of occurrence of the taxon (species).

Zooplankton samples were collected from the entire water layer (surface–bottom) with a plankton net with an inlet diameter of d = 36 cm and an aperture of 150 µm and fixed on board the ship with a 4% formalin-seawater solution (Korshenko & Aleksandrov, 2013). The zooplankton species composition was determined according to the Manuals for the Black and Azov Seas (Mordukhay-Boltovsky et al., 1968) and the quantity in a Bogorov chamber, according to the methodology of Korshenko and Aleksandrov (2013). Cluster analyses method (PRIMER 7.0.17) was used for grouping of data on sprat food composition from different stations and depths.

2. Results

2.1. Species diversity

A total of 24 species were identified during the study, including 17 fish, 2 crustaceans, 2 molluscs, and 3 macrozooplankton species. The most common species in the trawl catches (based on presence/absence) were *Trachurus mediterraneus* (45.76%), *Mullus barbatus*

(24.66%), and *Merlangius merlangus* (10.4%). *Sprattus sprattus* was observed only sporadically in the catches. Other species, such as *Alosa immaculata*, *Neogobius melanostomus*, *Gobius niger*, *Mesogobius batrachocephalus*, *Zosterisessor ophiocephalus*, *Raja clavata*, *Dasyatis pastinaca*, *Pegusa lascaris*, *Uranoscopus scaber*, *Trachinus draco*, *Scophthalmus maximus*, *Squalus acanthias*, and *Acipenser stellatus*, had a negligible presence in the catches.

2.2. Horse mackerel (*Trachurus mediterraneus*)

2.2.1. Distribution

Horse mackerel is a migratory species along the Bulgarian coast. It is a carnivorous fish and plays an important role in the food chain, serving as prey for larger predators such as turbot and dolphins. Horse mackerel was significantly represented in the catches in November 2024.

2.2.2. Horse mackerel biomass by strata

The total area surveyed was 8010.24 km², and the total biomass of horse mackerel was estimated at 3093.2 tonnes (Table 2.2.2.1; Table 2.2.2.2; Fig. 2.2.2.1; Fig. 2.2.2.2). The densest aggregations were observed off the coast of Byala and in Nesebar Bay. The highest biomass was recorded in the 30–50 m depth stratum, with 2138 tonnes, followed by 1511.348 tonnes (15–30 m) and 1281.708 tonnes (50–100 m).

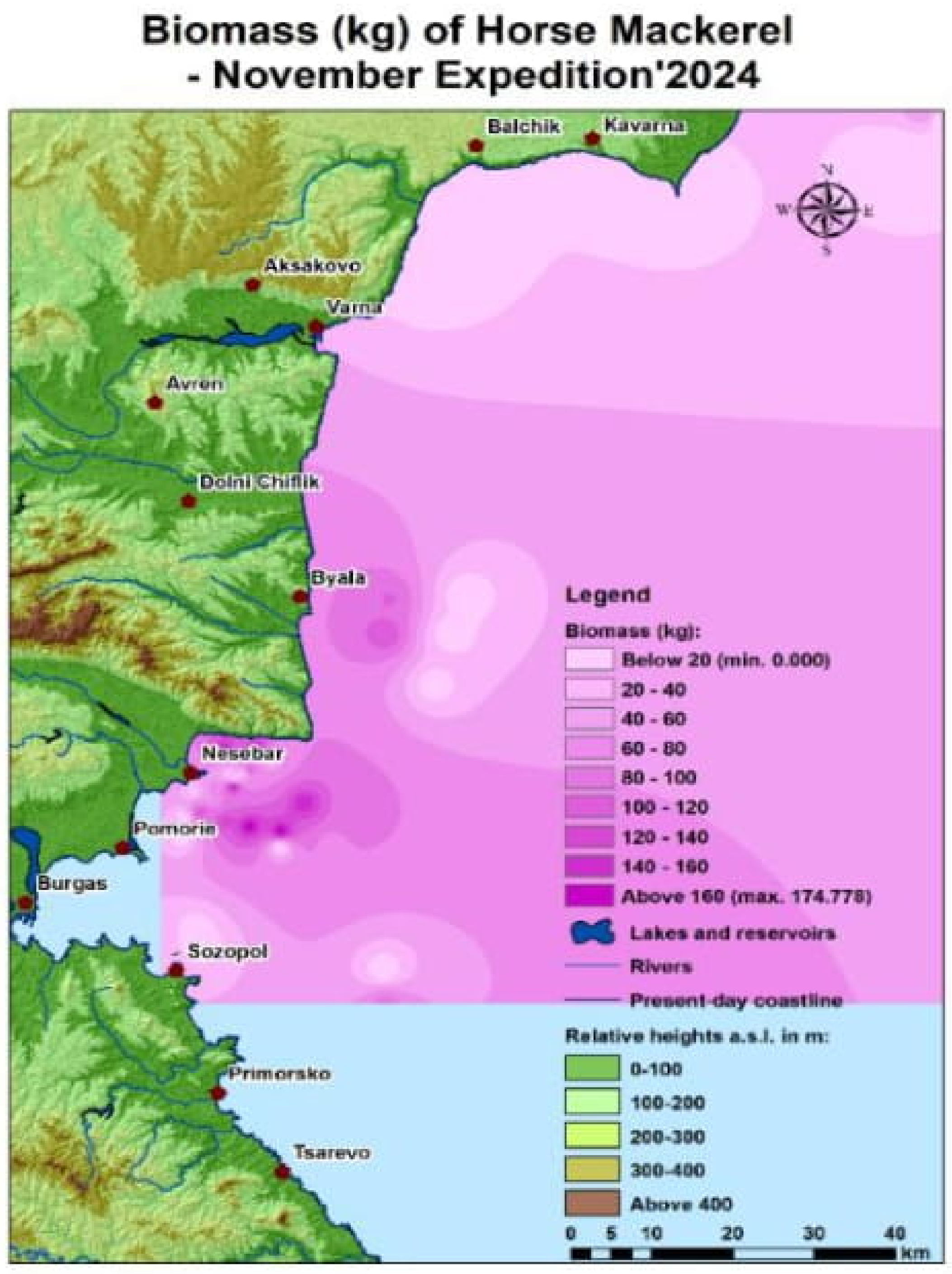

Figure 2.2.2.1. Horse mackerel biomass by strata, November 2024

Table 2.2.2.1. Swept area method for stock survey in November 2024 – average values of catch per unit area (CPUA), biomass (kg), Ax – area and number of fields

CPUA average	Strata	Biomass (kg)	Ax Surface	Number of stations
731.838	15−30	1511.348	2065.14	33
1178.246	30−50	2138.304	1814.82	29
310.32	50−100	1281.708	4130.28	66
		4931.36	8010.24	128

Project No. BG14MFOP001-1.002-0001 "Collection, management and use of data for the purposes of scientific analysis and implementation of the Common Fisheries Policy for the period 2023-2024", financed by the Maritime, Fisheries and Aquaculture Programme, co-financed by the European Union through the European Fund for maritime, fisheries and aquaculture fund.

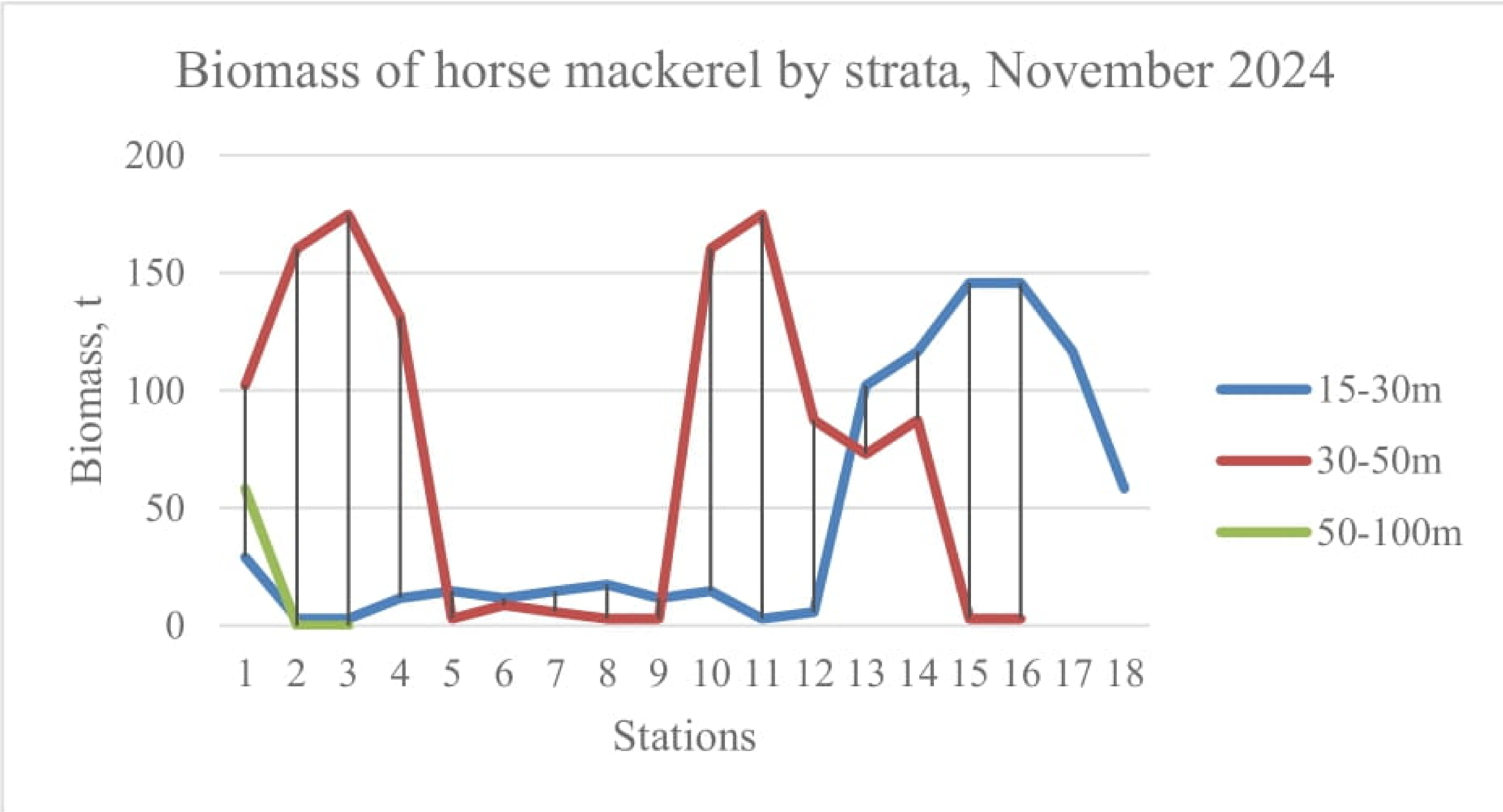

Figure 2.2.2.2. Horse mackerel biomass (kg) by strata in November 2024

Table 2.2.2.2. Descriptive statistics of horse mackerel CPUA indices (t) in November 2024

	15–30 m	30–50 m	50–100 m
Average	731.838	1178.2463	310.32
Standard error	199.86737	280.11813	310.32
Median	232.74	1280.07	0
Fashion	46.548	46.548	0
Standard deviation	847.96542	1120.4725	537.49001
Variation	719045.35	1255458.6	288895.51
Excess	−0.6615785	−1.6613722	#DIV/0!
Asymmetry	1.0357367	0.2672106	1.7320508
Range	2280.852	2746.332	930.96001
Minimum	46.548	46.548	0
Maximum	2327.4	2792.88	930.96001
Amount	13173.084	18851.94	930.96001
Number	18	16	3
Greatest Value (1)	2327.4	2792.88	930.96001
Smallest value (1)	46.548	46.548	0
Confidence level (95.0%)	421.68328	597.05765	1335.1992

2.2.3. Catch per unit area (CPUA)

Horse mackerel was recorded at the highest densities in the waters off Byala, Nesebar Bay, the "Elenite" resort, Pomorie, Sozopol, and Burgas Bay (Fig. 2.2.3.1).

The highest values of CPUA were registered in the 30–50 m depth layer, reaching 1178.3 kg.km^{-2}, with an average value of 731 kg.km^{-2}. In the 15–30 m and 50–100 m depth layers, the species was recorded in individual trawls with values of 731 kg.km^{-2} and 310.3 kg.km^{-2}, respectively (Fig. 2.2.3.1).

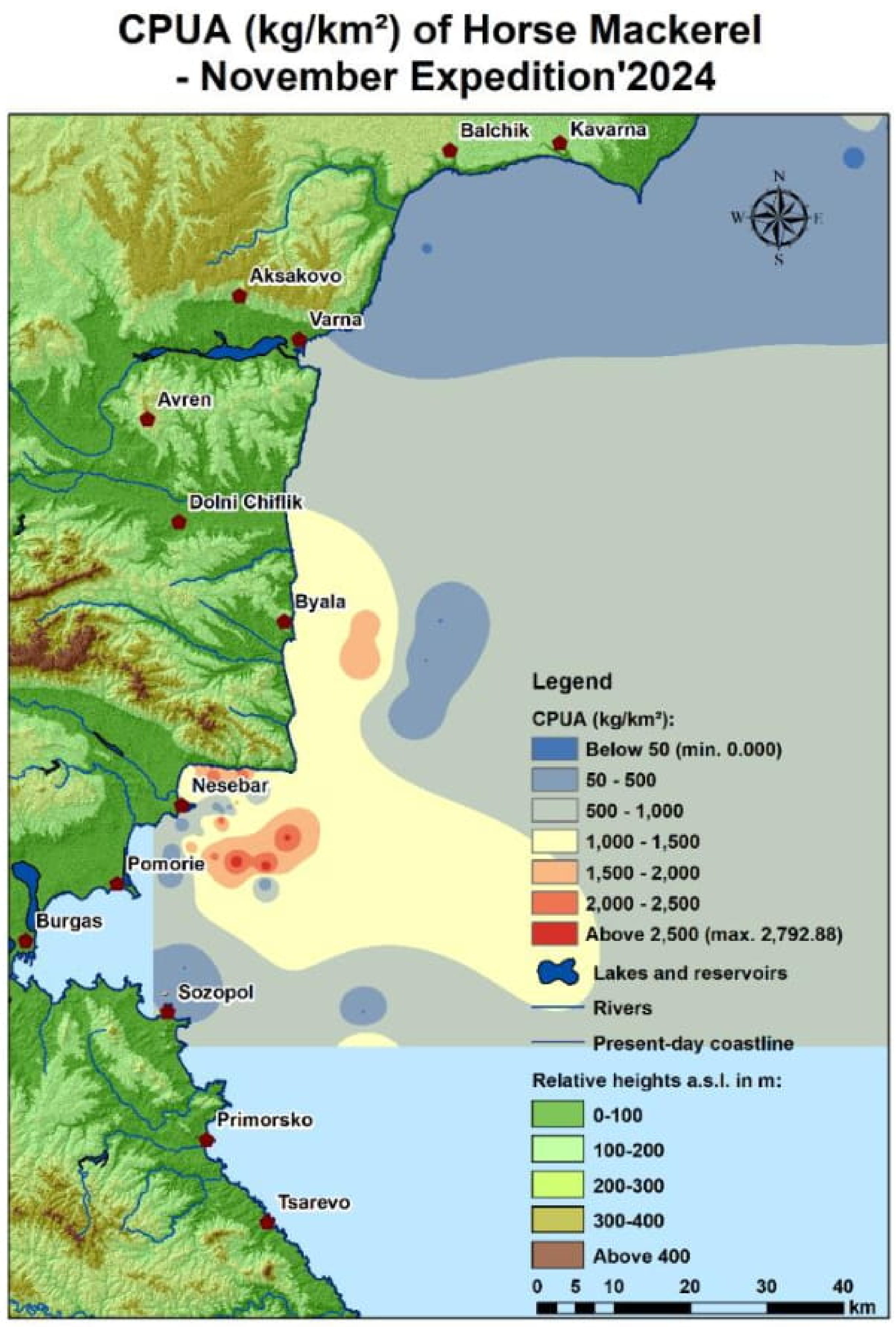

Figure 2.2.3.1. Catch per unit area (CPUA kg.km^{-2}), November 2024

2.2.4. Catch per unit effort (CPUE)

The catch per unit effort (CPUE) for the species is presented graphically in Figure 2.2.4.1. The highest CPUE values (kg.h^{-1}) were observed off Nesebar Bay, Byala, "Elenite" resort, Pomorie, and Burgas Bay.

CPUE (kg/h) of horse mackerel - First expedition

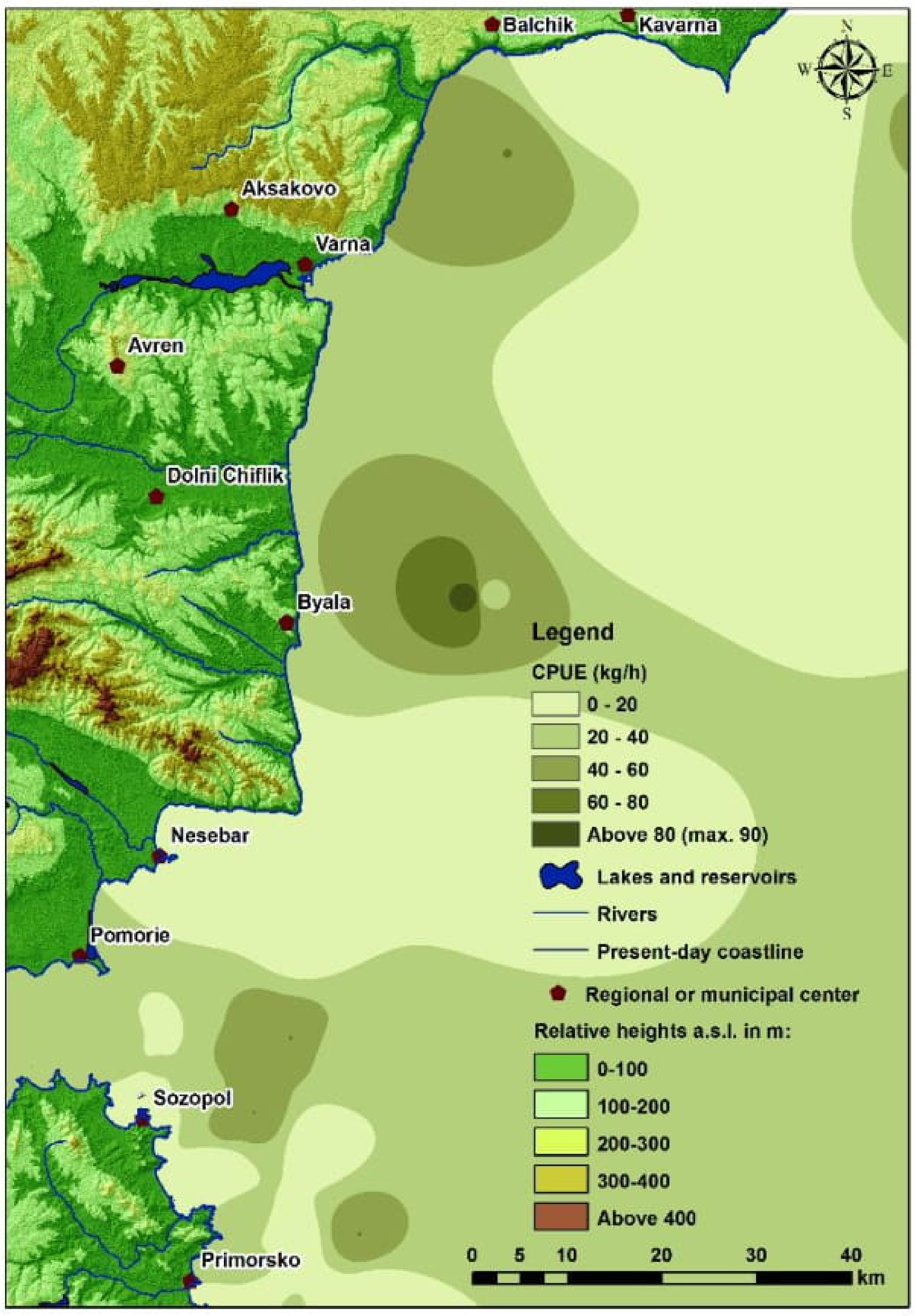

Figure 2.2.4.1. Catch per unit effort (CPUE kg.h^{-1}) for horse mackerel by strata

2.2.5. Lenght-weight relationship

The length-weight relationship in horse mackerel is described by the model $W = 0.009^{*}.L^{2.99}$, allometric growth coefficient >3, the resulting nonlinear length-weight relationship model has a high degree of determination ($R^2 = 0.997$) (Fig. 2.2.5.1.).

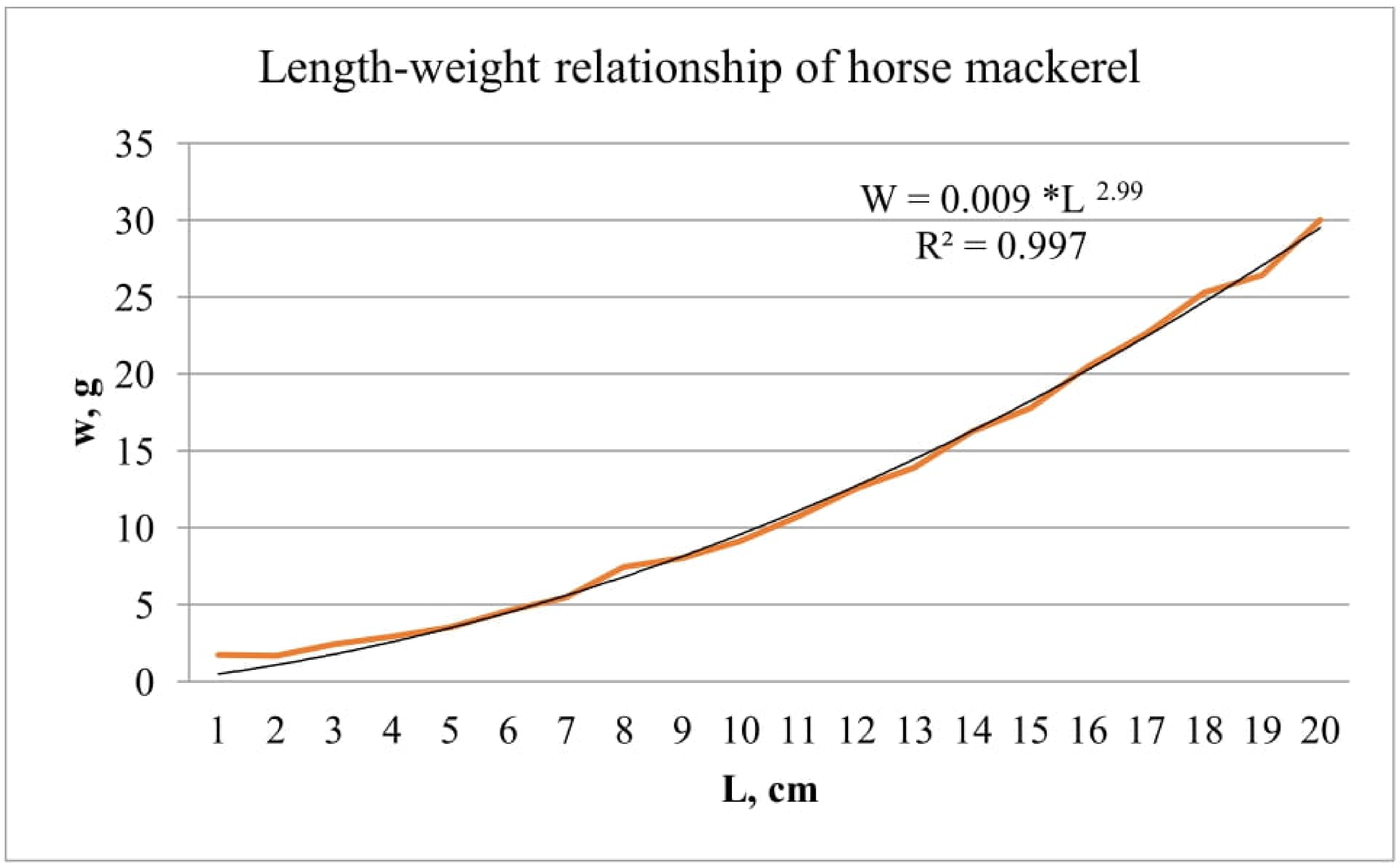

Figure 2.2.5.1. Length-weight relationship of horse mackerel in November 2024

The size structure of the horse mackerel stock is presented in Figure 2.2.5.2. The length distribution in the horse mackerel samples is normal (gaus), with 1 peak – bell-shaped, as the most common lengths in the samples were in the range 10.5–13.5 cm. A peak was observed in the 12.5 cm size group (1500 ind.) (Фиг. 2.2.5.2).

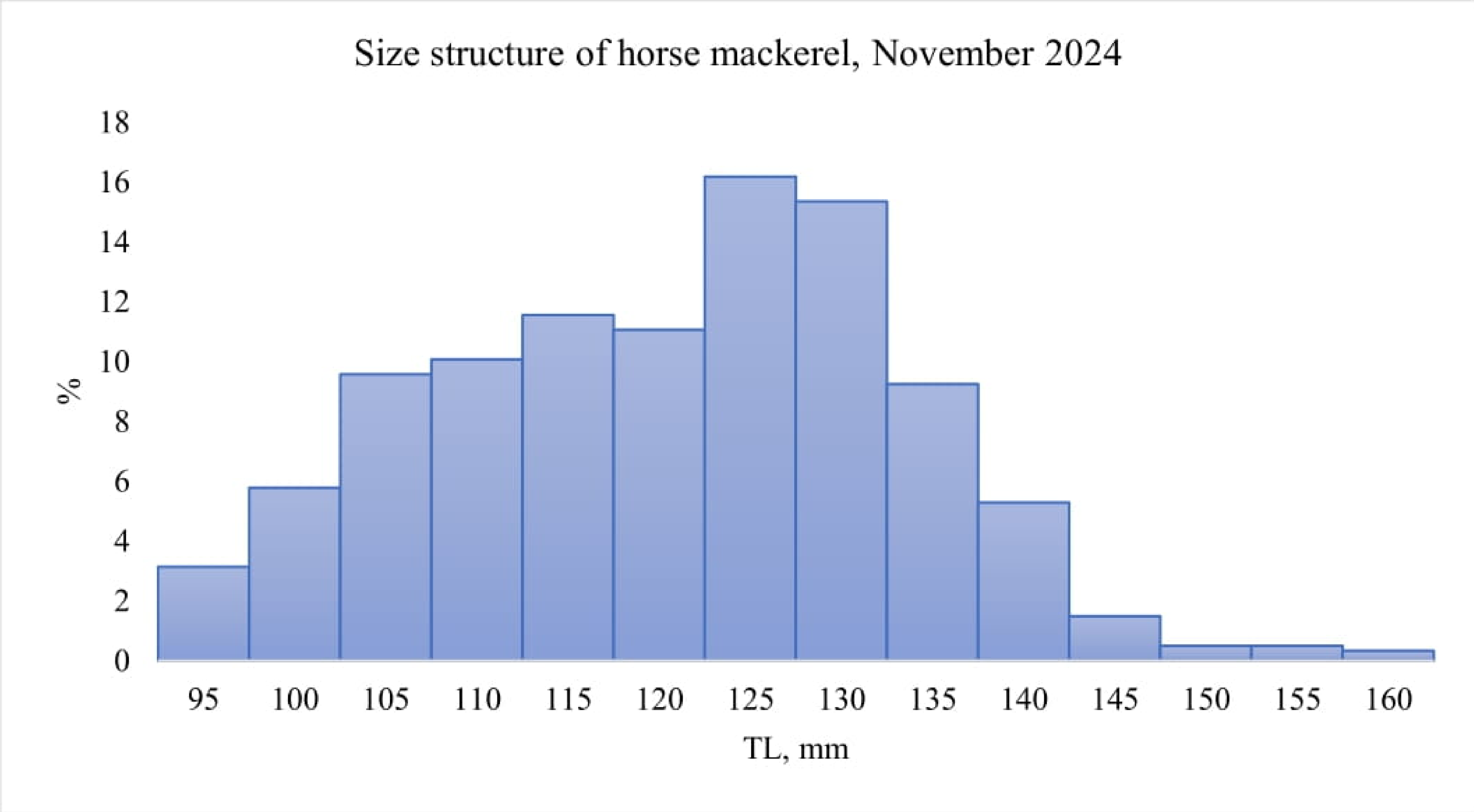

Figure 2.2.5.2. Size structure of horse mackerel in November 2024

Average weight varied from 7.3 to 29.9 g (Fig. 2.2.5.3.).

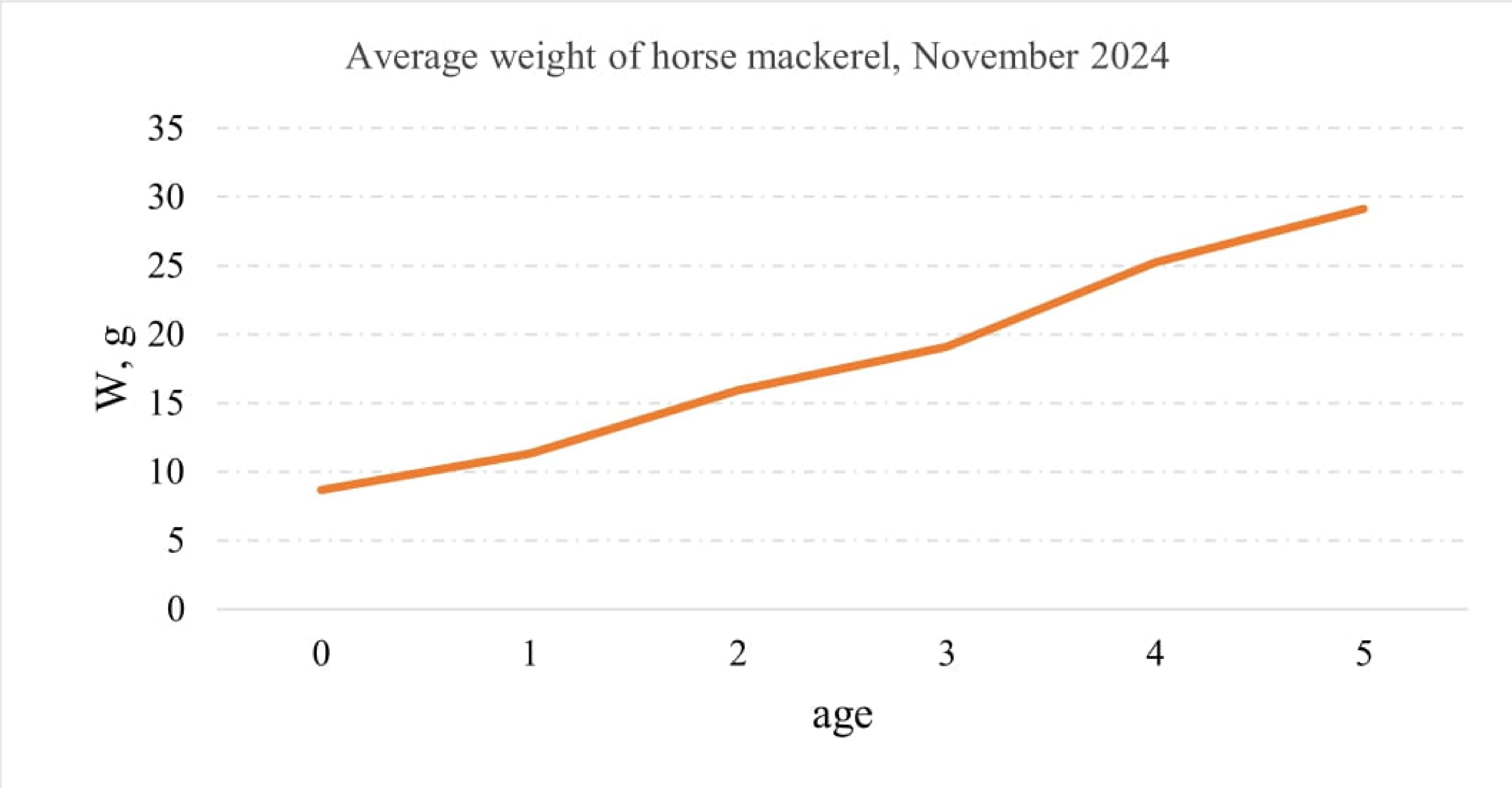

Figure 2.2.5.3. Weight structure of horse mackerel in November 2024

Project No. BG14MFOP001-1.002-0001 "Collection, management and use of data for the purposes of scientific analysis and implementation of the Common Fisheries Policy for the period 2023-2024", financed by the Maritime, Fisheries and Aquaculture Programme, co-financed by the European Union through the European Fund for maritime, fisheries and aquaculture fund.

The dominant age group of horse mackerel during the study period was 2-2+ years (37.33%), followed by age group 1-1+ years (26%). The replenishment was represented by 7.66%. The age structure of the horse mackerel varies from 0 to 5+ years, with a significant presence of the 3-3+years age group, comprising 21.33% of the total (Fig. 2.2.5.4.).

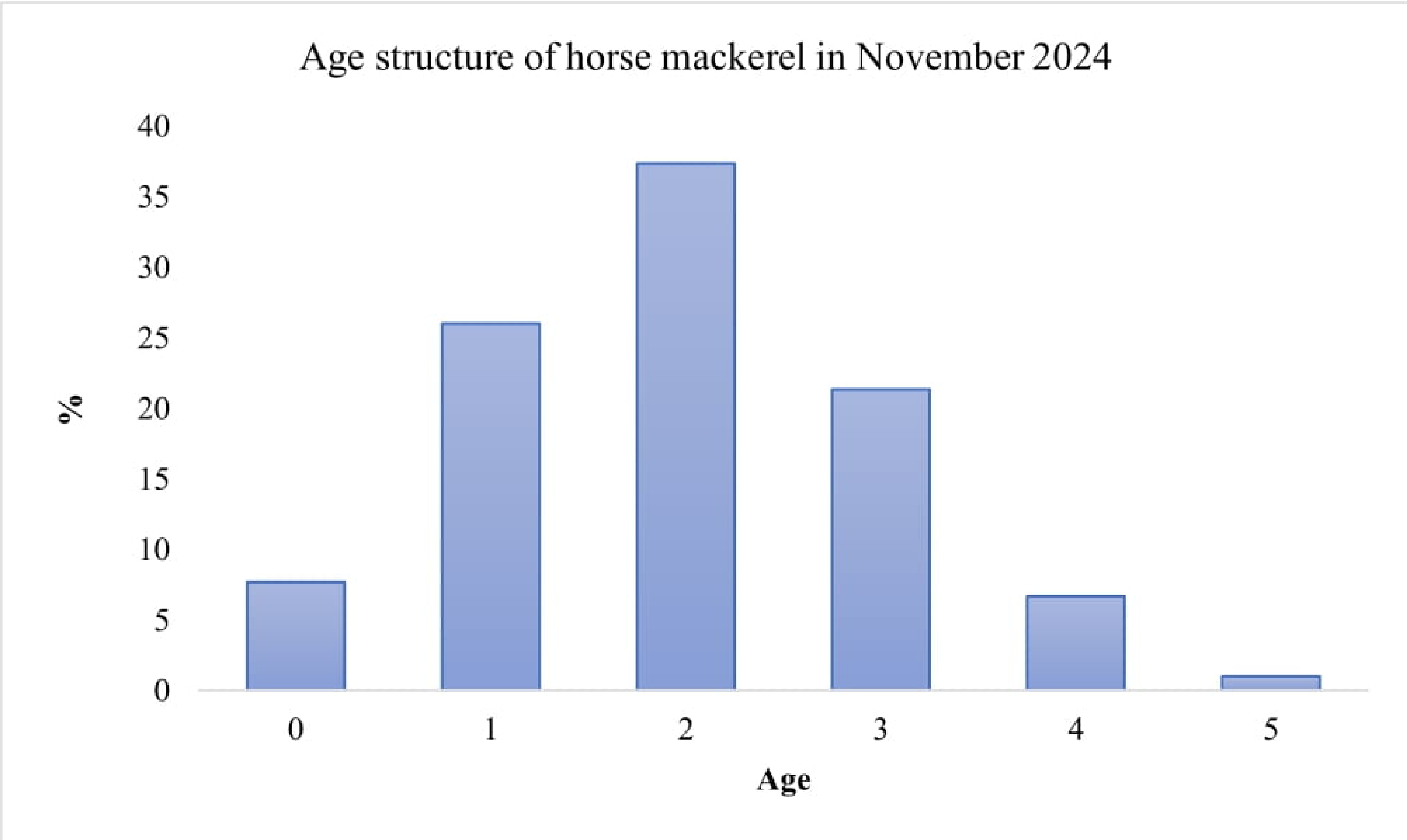

Figure 2.2.5.4. Age structure of horse mackerel in November 2024

2.2.6. Individual growth

The growth parameters of horse mackerel (1500 ind.), calculated using the von Bertalanffy model, show an asymptotic length of 22.45 cm and higher values of the coefficient determining the rate of reaching the asymptote (Table 2.2.6.1.).

Project No. BG14MFOP001-1.002-0001 "Collection, management and use of data for the purposes of scientific analysis and implementation of the Common Fisheries Policy for the period 2023-2024", financed by the Maritime, Fisheries and Aquaculture Programme, co-financed by the European Union through the European Fund for maritime, fisheries and aquaculture fund.

Table 2.2.6.1. Von Bertalanffy Growth Model (VBGF) for horse mackerel

Species	Asymptotic lenght	Growth rate	Growth parameter	Growth coefficient	Allometric coefficient
Trachurus mediterraneus	**L_∞ = 22.45**	**K = 0.342**	**t_0 = -0.015**	**a = 0.0057**	**n = 2.9802**

2.2.7. Abundance and biomass by length and age classes

In November 2024, the 12.5 cm size class had the highest percentage representation in the catches, followed by the 10.5 cm size class (Fig. 2.2.7.1).

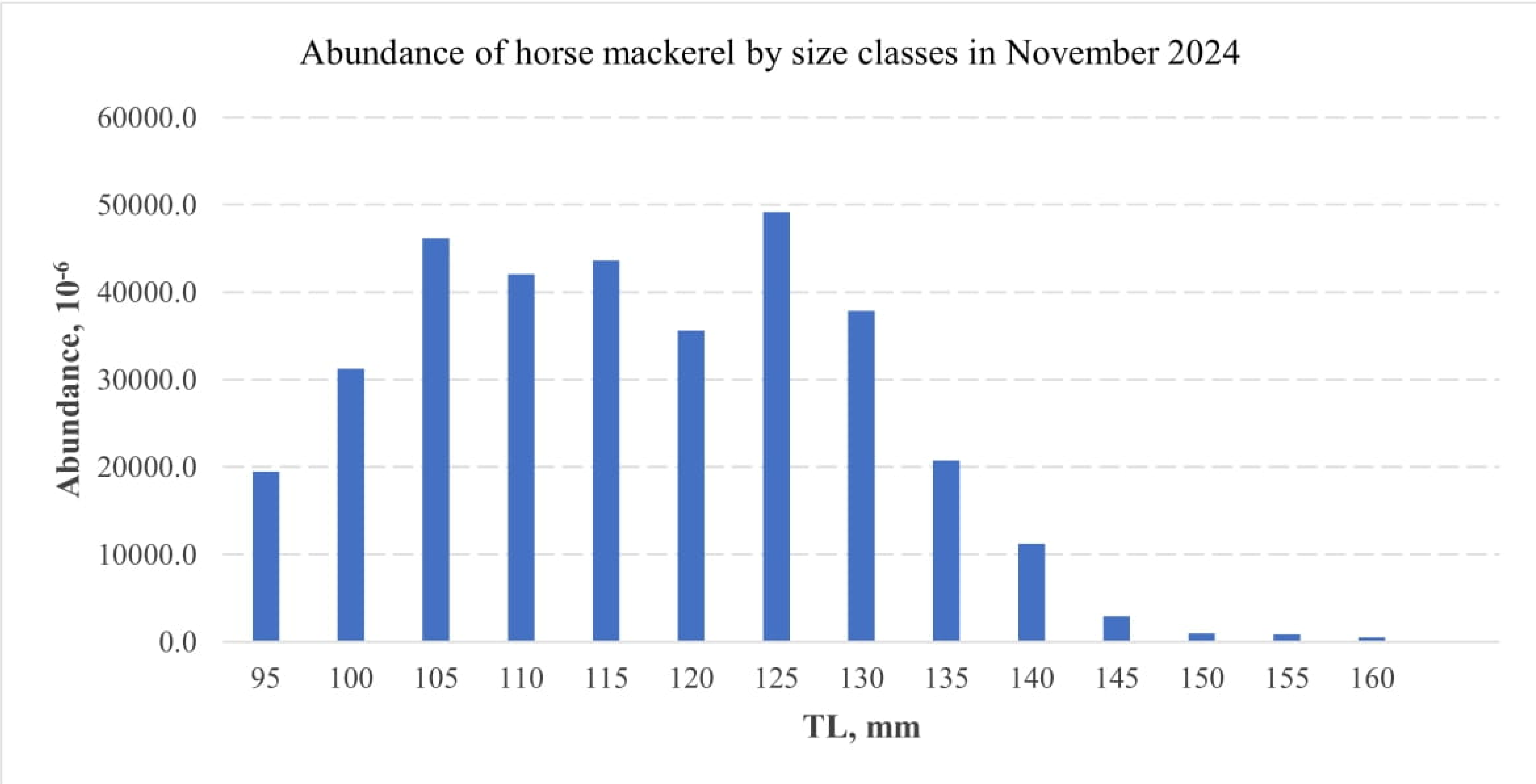

Figure 2.2.7.1. Abundance of horse mackerel by size classes in November 2024

Analysis of the age structure of the catch showed that age groups 1–1+ and 2–2+ had high abundance indices and dominated the catches (Fig. 2.2.7.2). The age groups recorded in the catches ranged from 0 to 5+ years.

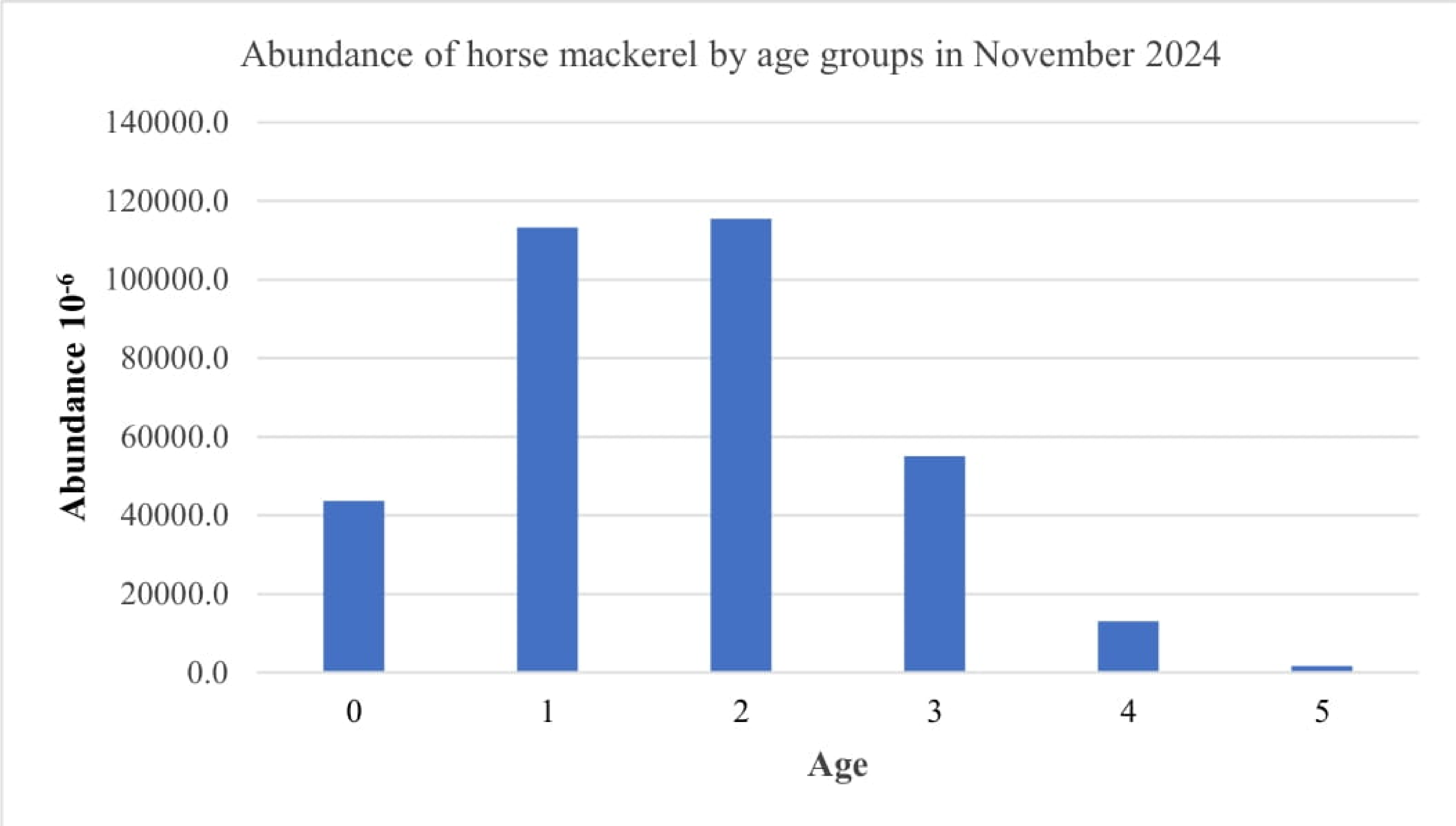

Figure 2.2.7.2. Abundance of horse mackerel by age groups in November 2024

Biomass, similar to abundance, was dominated by the 125 mm size group, followed by the 130 mm size group (Fig. 2.2.7.3). Figure 2.2.7.4 presents the distribution of biomass by age group. In November 2024, age groups 1–1+ years, and especially 2–2+ years, had a significantly higher share in the catches compared to other age groups.

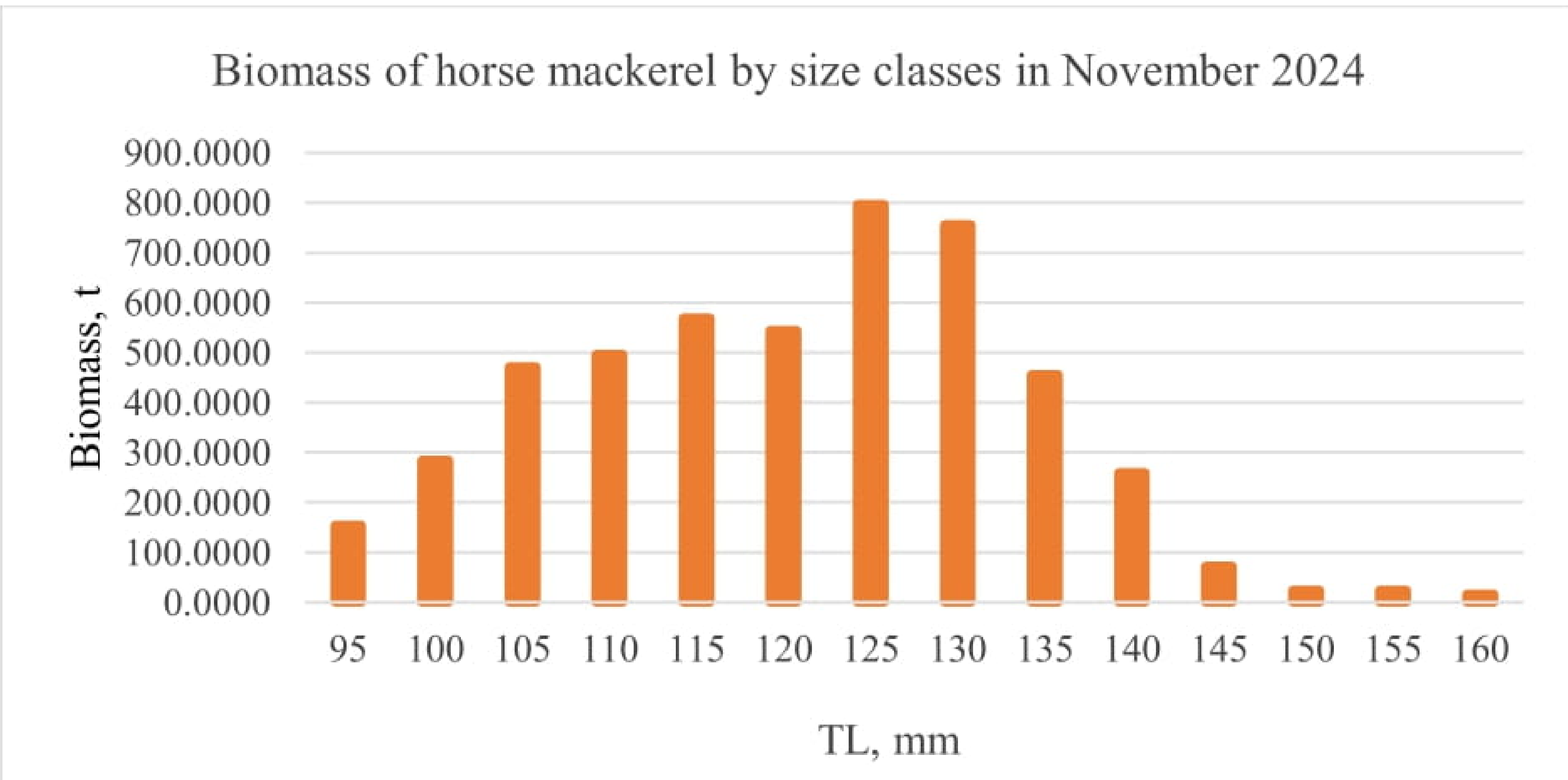

Figure 2.2.7.3. Biomass of horse mackerel by size classes in November 2024

Project No. BG14MFOP001-1.002-0001 "Collection, management and use of data for the purposes of scientific analysis and implementation of the Common Fisheries Policy for the period 2023-2024", financed by the Maritime, Fisheries and Aquaculture Programme, co-financed by the European Union through the European Fund for maritime, fisheries and aquaculture fund.

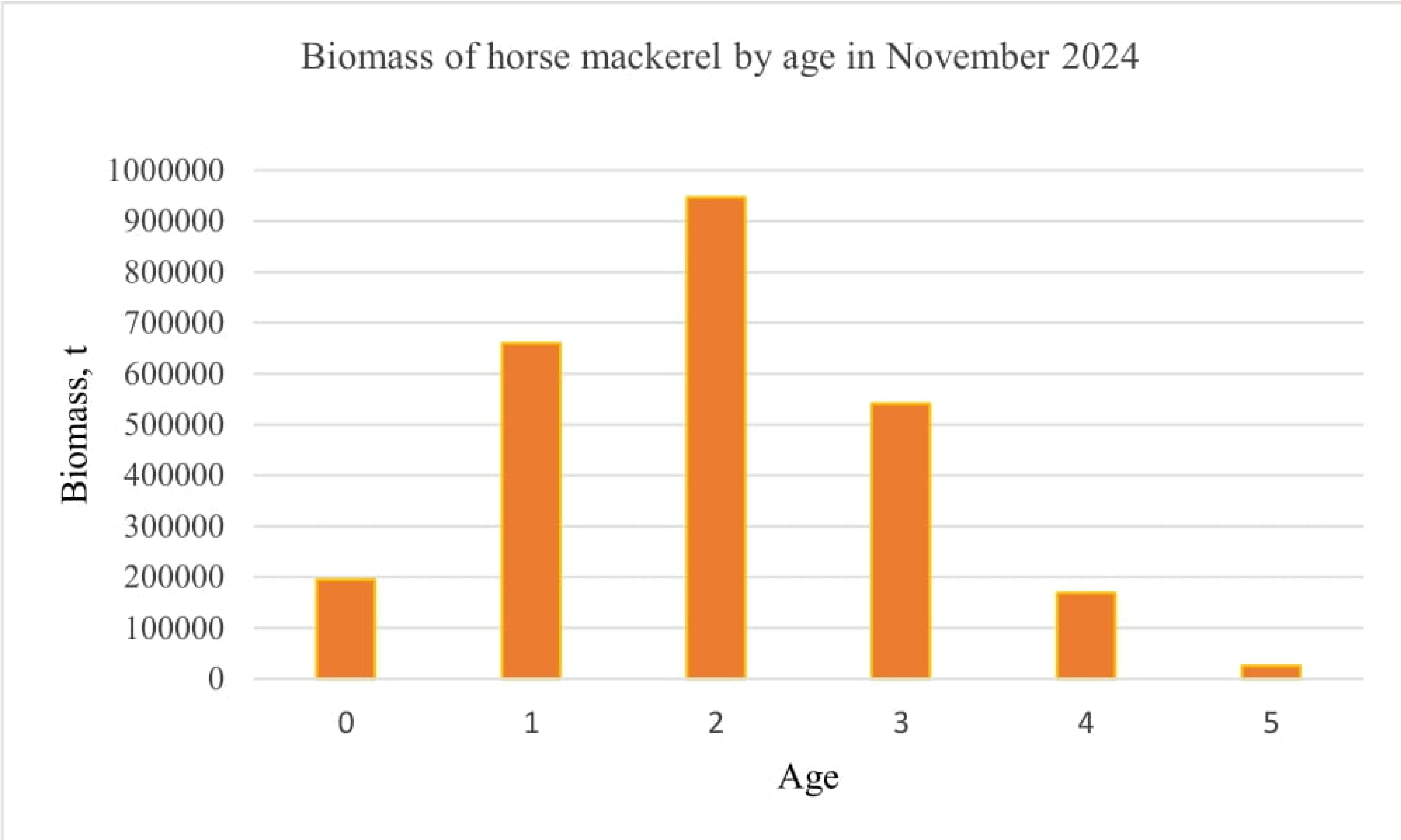

Figure 2.2.7.4. БиомасаBiomass of horse mackerel by age groups in November 2024

The sex ratio (250 individuals) of horse mackerel was 32% males and 68% females (Fig. 2.2.7.5).

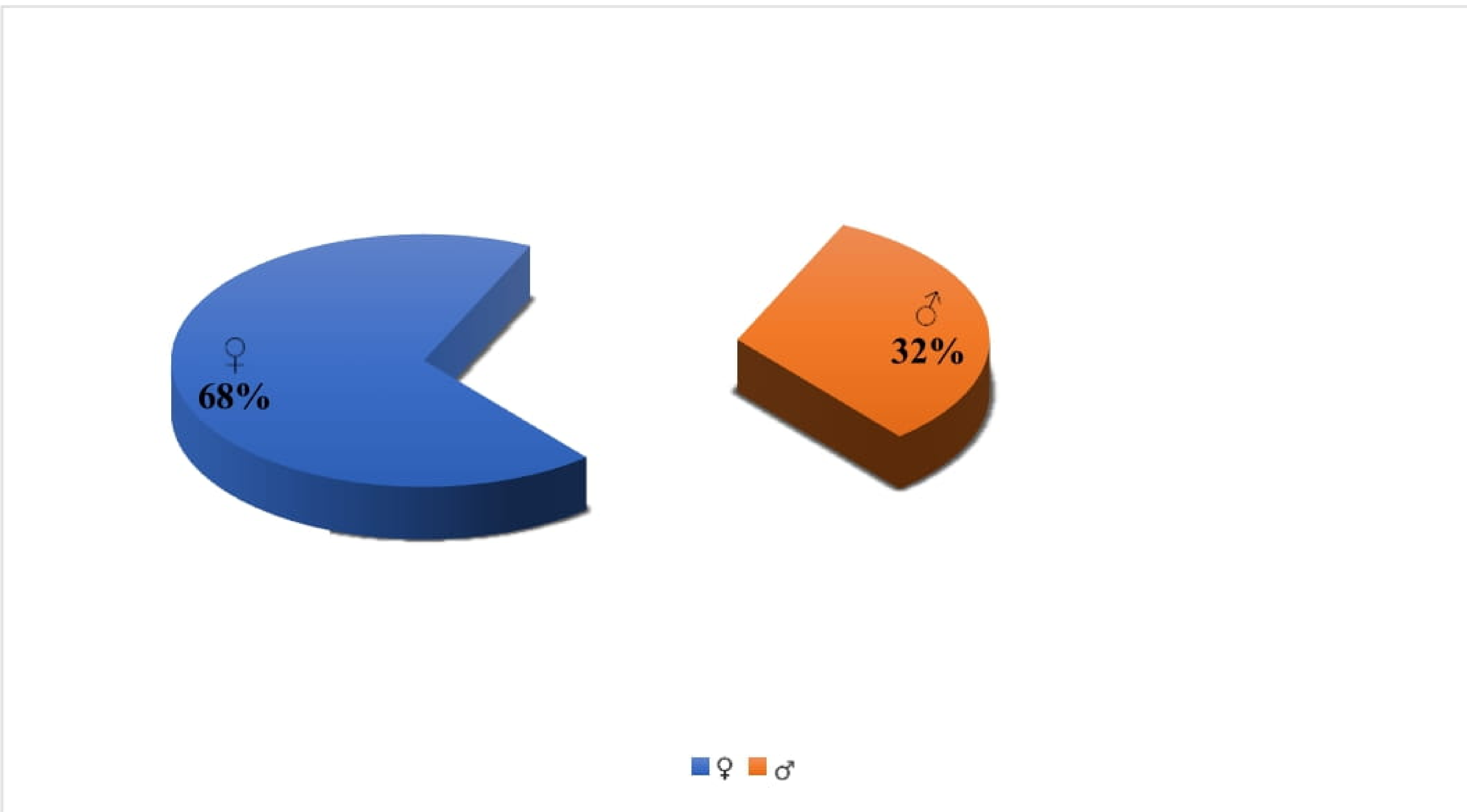

Figure 2.2.7.5. Sex ratio (females – ♀, males – ♂) of horse mackerel, November 2024.

Project No. BG14MFOP001-1.002-0001 "Collection, management and use of data for the purposes of scientific analysis and implementation of the Common Fisheries Policy for the period 2023-2024", financed by the Maritime, Fisheries and Aquaculture Programme, co-financed by the European Union through the European Fund for maritime, fisheries and aquaculture fund.

The sexual maturity of the analyzed species by size classes is presented in Figure 2.2.7.6, and by age groups in Figure 2.2.7.7.

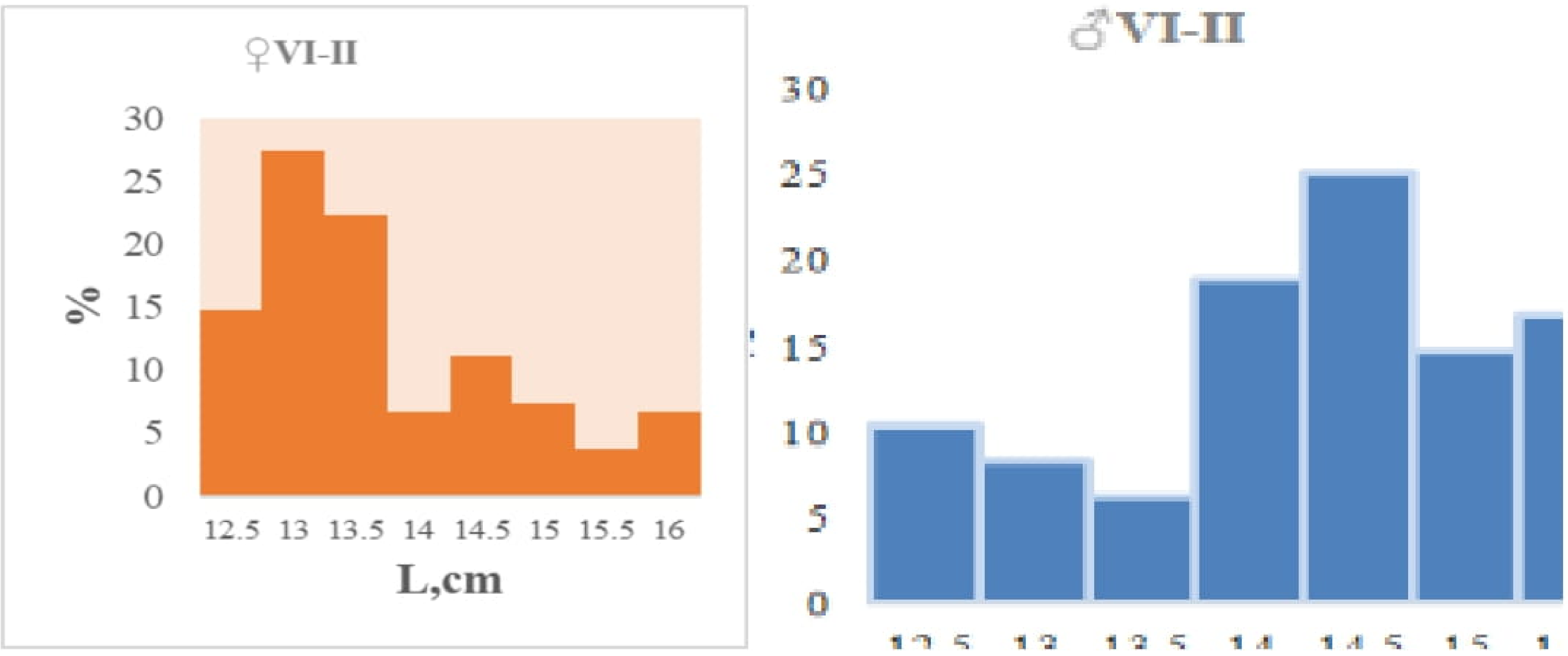

Figure 2.2.7.6. Sexual maturity of horse mackerel by size groups in November 2024

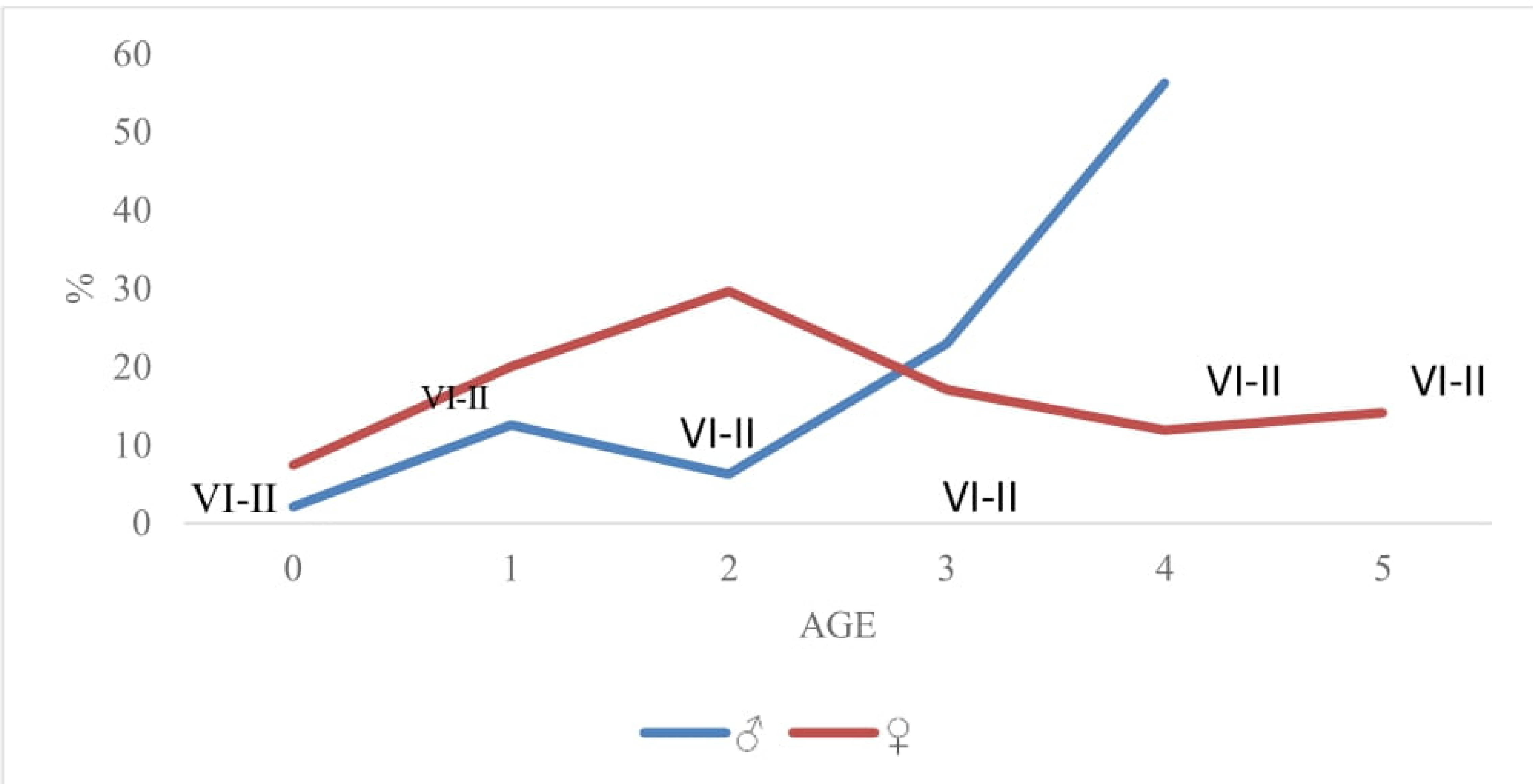

Figure 2.2.7.7. Sexual maturity of horse mackerel by age

The gonadosomatic index (GSI, %) of horse mackerel based on 250 individuals measured, is indicative of a later stage of spawning. An R^2 value of 0.3353 (Fig. 2.2.7.8) shows a strong correlation between gonad weight and the gonadosomatic index, which indicates mass spawning activity and active sexual maturity of the reproductive organs during the study period.

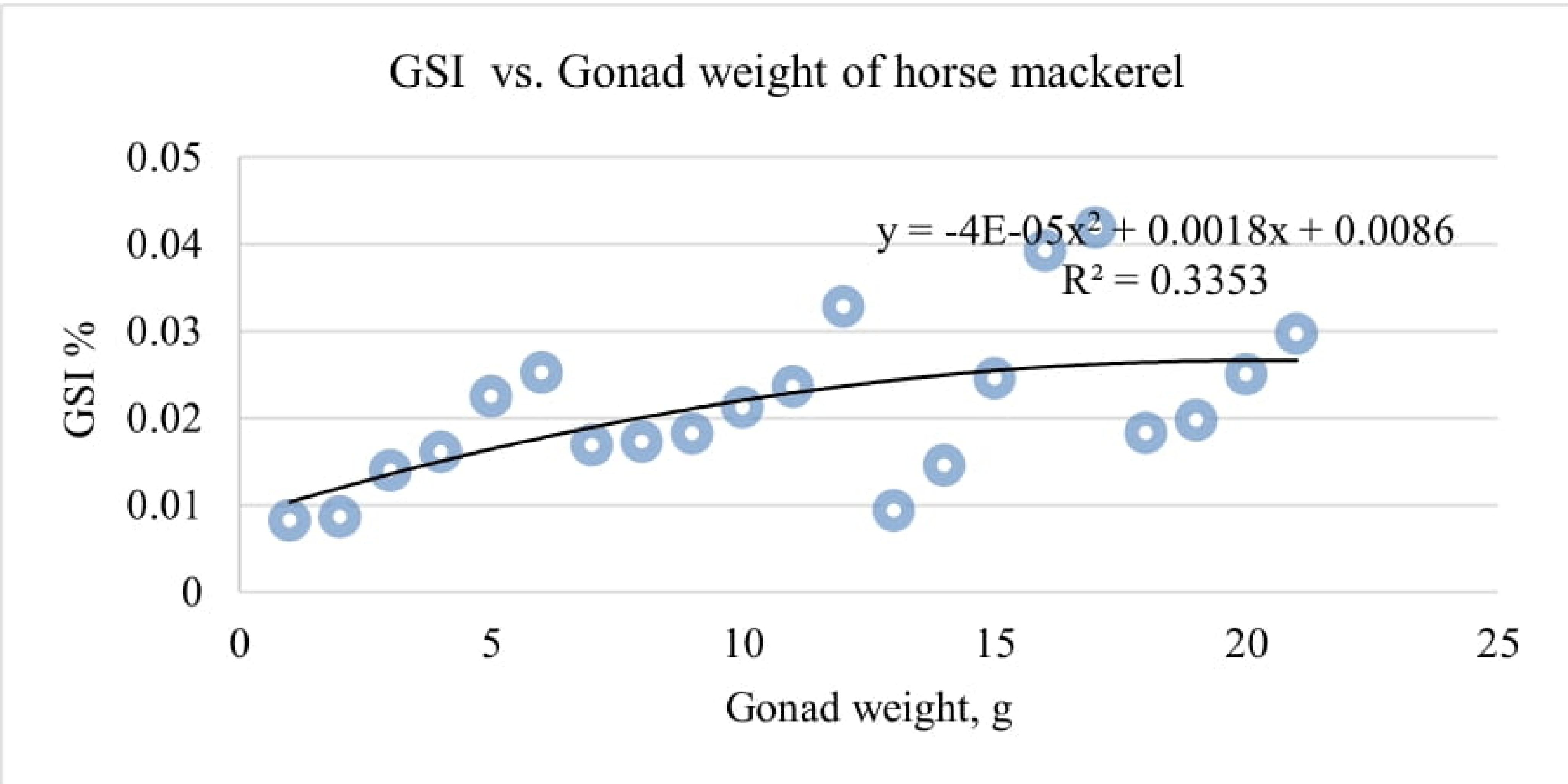

Figure 2.2.7.8. Gonadosomatic index of horse mackerel during the study period (GSI, % vs. Gonad weight)

2.2.8 Absolute and relative fecundity of horse mackerel

Absolute fecundity (measured on 250 ind) at length of 15 cm was the highest: 46 700 cavier grains. In terms of relative fecundity, the highest was detected at 12.5 cm TL individuals: 1275. The mean values of absolute and relative fecundity of the whiting were as follows: 27333 and 1011.93 (Table 2.2.8.1).

Project No. BG14MFOP001-1.002-0001 "Collection, management and use of data for the purposes of scientific analysis and implementation of the Common Fisheries Policy for the period 2023-2024", financed by the Maritime, Fisheries and Aquaculture Programme, co-financed by the European Union through the European Fund for maritime, fisheries and aquaculture fund.

Table 2.2.8.1. Absolute and relative fecundity of horse mackerel

Size class	Mean weight (w,g)	Mean length	absolute fecundity (number of cavier grains	relative fecundity	No. ♀
10	7.79	9.71	8250±212	1059.05±111	30
10.5	8.93	10.44	8512±118	953.19±95	30
11	11.04	11.25	9835±242	890.85±48	30
11.5	16.53	11.62	11706±355	708.17±51	30
12	18.02	11.99	14800±405	821.31±66	30
12.5	22.06	12.44	28120±1205	1274.71±155	30
13	29.16	13.02	36035±1435	1235.77±168	30
13.5	40.99	13.44	44200±1954	1078.31±112	25
14	42.22	14	46000±1600	1089.53±125	5
14.5	46.01	14.44	46500±1717	1010.65±48	5
15	46.25	15.01	46700±2241	1009.73±61	5
			mean 27333	mean 1011.93	250

2.3. Red mullet (*Mullus barbatus*)

2.3.1. Biomass of red mullet

The total surveyed area was 8010.24 km², and the total biomass of red mullet was 496 tonnes (Table 2.3.1.1). The species was recorded at 24 stations (out of a total of 36). The densest aggregations were observed off Cape Kaliakra, in Nesebar Bay, Burgas Bay, and west of Sozopol. A biomass peak was recorded in the 15–30 m depth range (258 t) and in the 30–50 m range (225 t), with lower values found in the 75–100 m stratum (12 t) (Fig. 2.3.1.1; Table 2.3.1.2).

Project No. BG14MFOP001-1.002-0001 "Collection, management and use of data for the purposes of scientific analysis and implementation of the Common Fisheries Policy for the period 2023-2024", financed by the Maritime, Fisheries and Aquaculture Programme, co-financed by the European Union through the European Fund for maritime, fisheries and aquaculture fund.

Table 2.3.1.1. Area-based method for stock assessment in November 2024 – average catch per unit area (CPUA), biomass (kg), A_x – area, and number of fields.

CPUA average	Strata	Biomass (kg)	Ax Surface	Number of stations
125.3215	15−30	258.8064	2065.14	33
124.128	30−50	225.27	1814.82	29
2.912974	75−100	12.0314	4130.28	66
		496.1078	**8010.24**	**128**

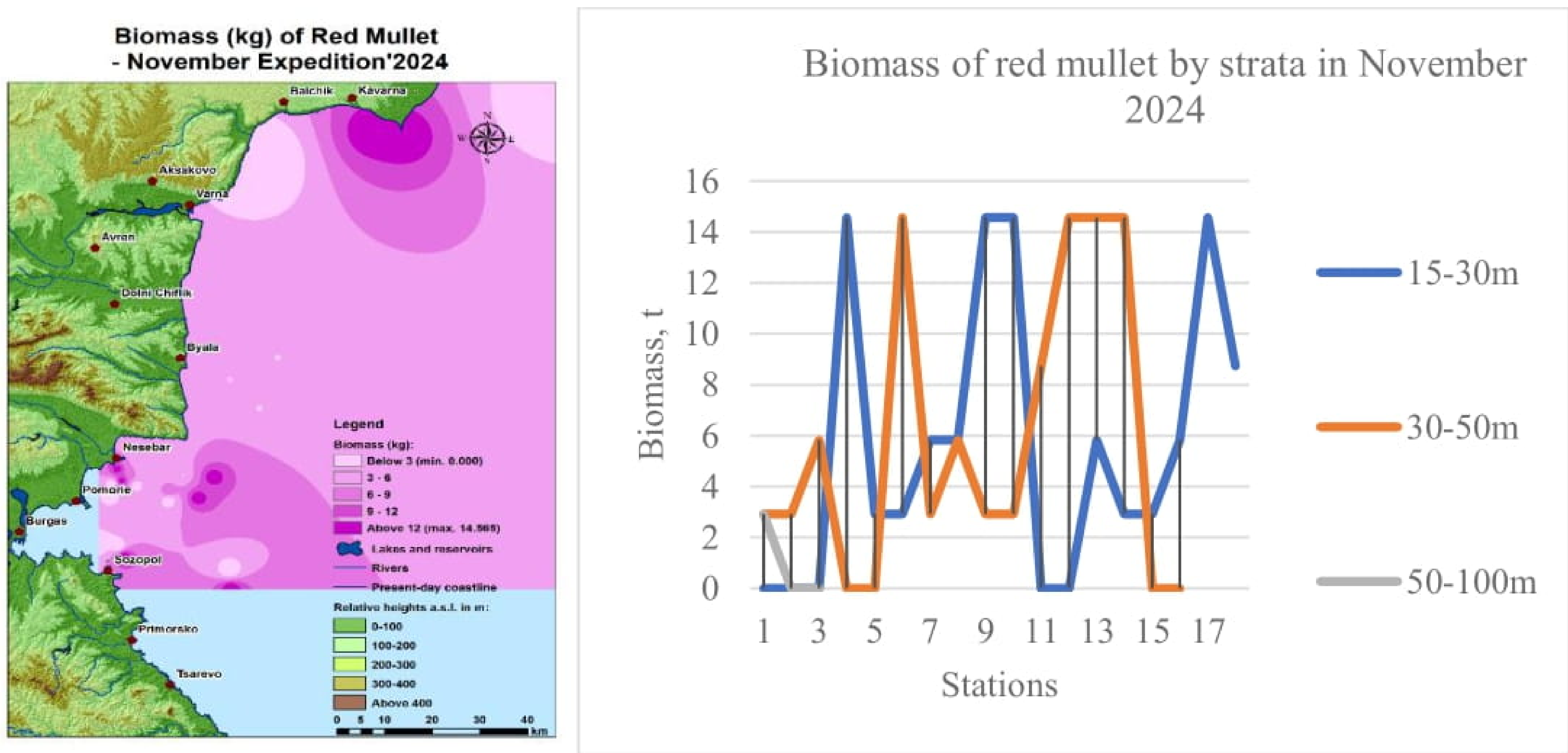

Figure 2.3.1.1. Biomass of red mullet in November 2024

Table 2.3.1.2. Descriptive statistics of the CPUA indices (t) of red mullet in November 2024

	15−30 m	30−50 m	50−100 m
Average	310.320002	93.096001	15.516
Standard error	310.320002	22.882813	15.516
Median	0	46,548	0
Fashion	0	46,548	0

Project No. BG14MFOP001-1.002-0001 "Collection, management and use of data for the purposes of scientific analysis and implementation of the Common Fisheries Policy for the period 2023-2024", financed by the Maritime, Fisheries and Aquaculture Programme, co-financed by the European Union through the European Fund for maritime, fisheries and aquaculture fund.

Standard deviation	537.49001	91,53125	26.874501
Variation	2.89E+05	8.38E+03	7.22E+02
Excess	0	-1.0831885	0
Asymmetry	1.732050808	0,7214863	1.7320508
Range	930.960006	232.74	46.548
Minimum	0	0	0
Maximum	930.960006	232.74	46.548
Amount	930.960006	1489.536	46.548
Number	3	16	3
Greatest Value (1)	930.960006	232.74	46.548
Smallest value (1)	42	16	2
Confidence level (95.0%)		10164.36	15812.07

2.3.2. Catch per unit area (CPUA kg.km^{-2})

The catch per unit area in the 15–30 m stratum was 125 kg.km^{-2}. In the 30–50 m and 50–100 m strata, the values were 124 kg.km^{-2} and 2.9 kg.km^{-2}, respectively. The average catch per unit area ranged between 15–310 kg.km^{-2} (Fig. 2.3.2.1).

From the analysis of catch per unit area and catch per unit effort (Fig. 2.3.2.1 and Fig. 2.3.2.2), it is evident that the highest densities and abundances were recorded in the 30–50 m depth zone, followed by the 15–30 m zone.

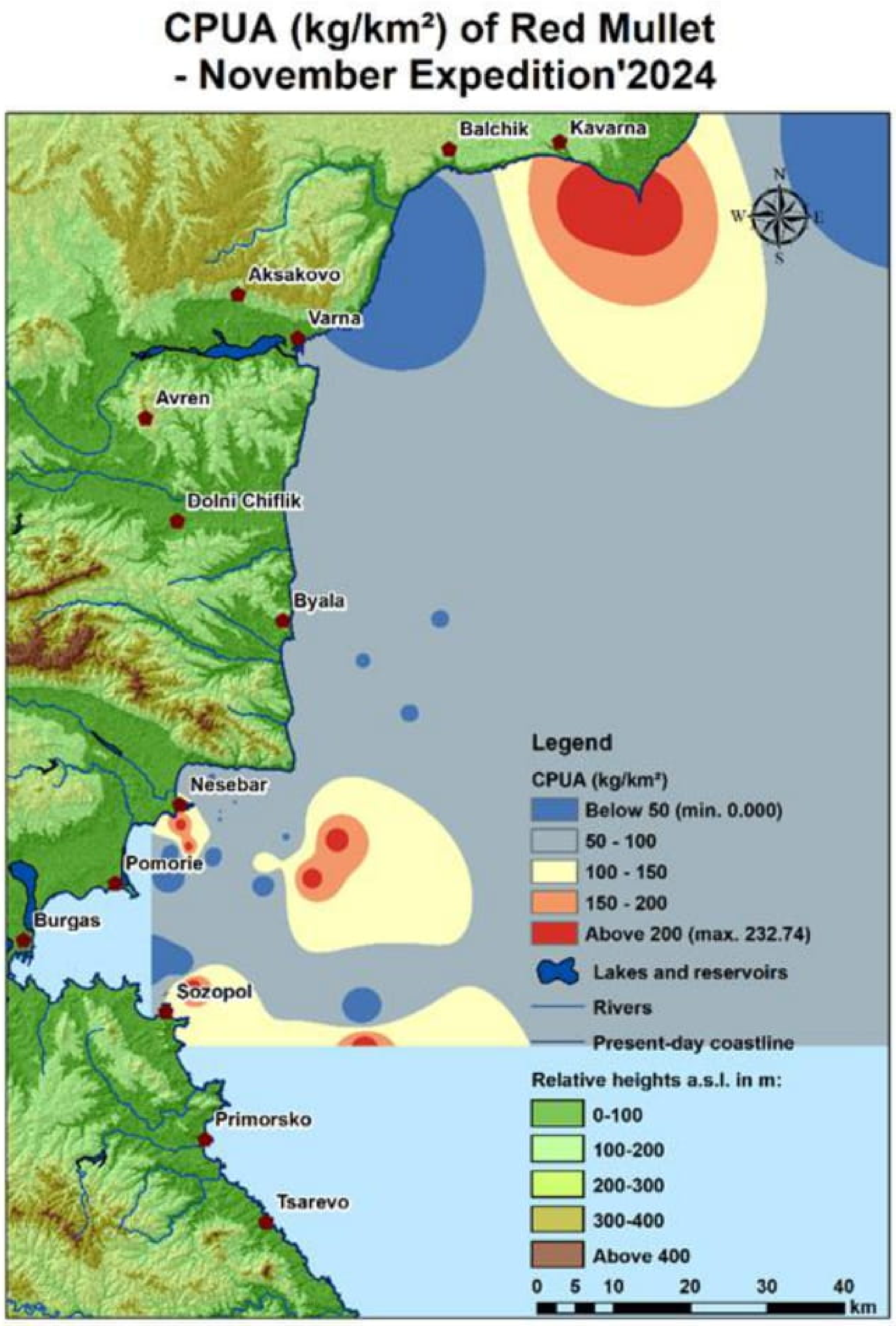

Figure 2.3.2.1. Catch per unit area (CPUA kg.km^{-2}) of red mullet in November 2024

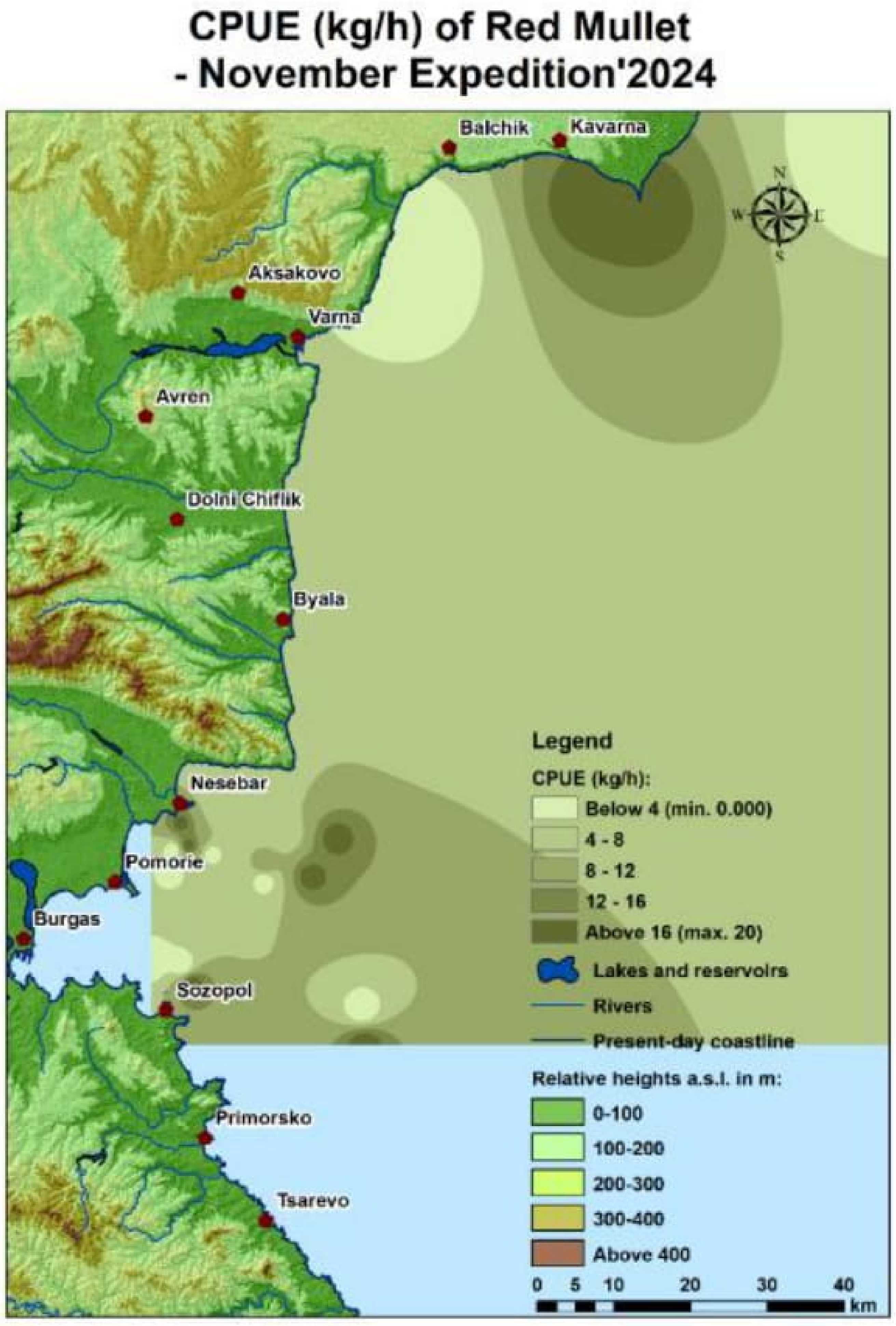

Figure 2.3.2.2. Catch per unit effort (CPUE kg.h^{-1}) of red mullet in November 2024

The length-weight (L–W) analysis of red mullet in November 2024 (Fig. 2.3.2.3) shows a very strong correlation between length and weight, with clearly expressed allometric growth (R^2 = 0.99) and a high determination coefficient (n = 3.11).

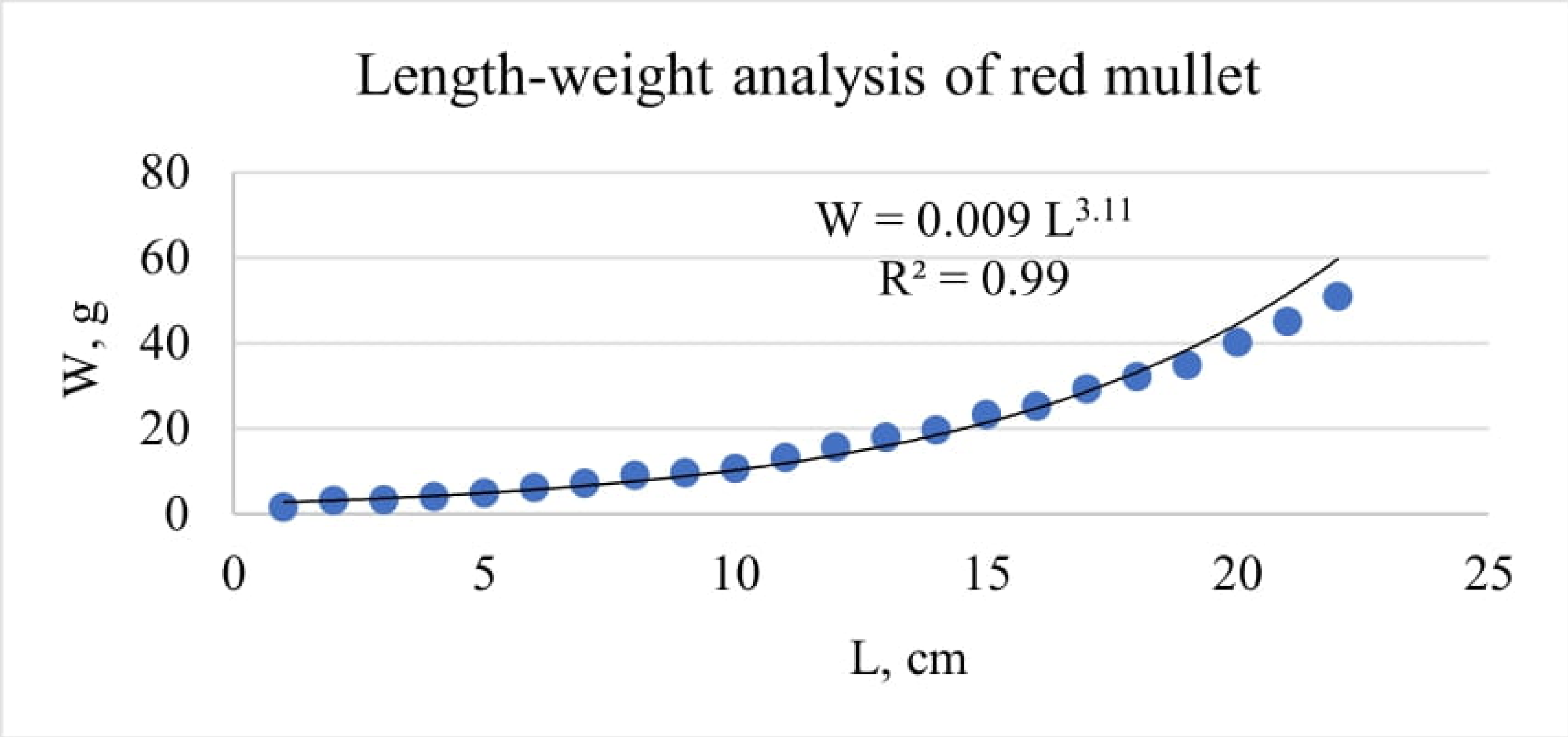

Figure 2.3.2.3. Length-weight analysis of red mullet (L-W) in November 2024

The size structure of red mullet (1200 ind.) is presented in Figure 2.3.2.4. During the survey, the dominant size classes in the catch composition were 11 cm and 13 cm.

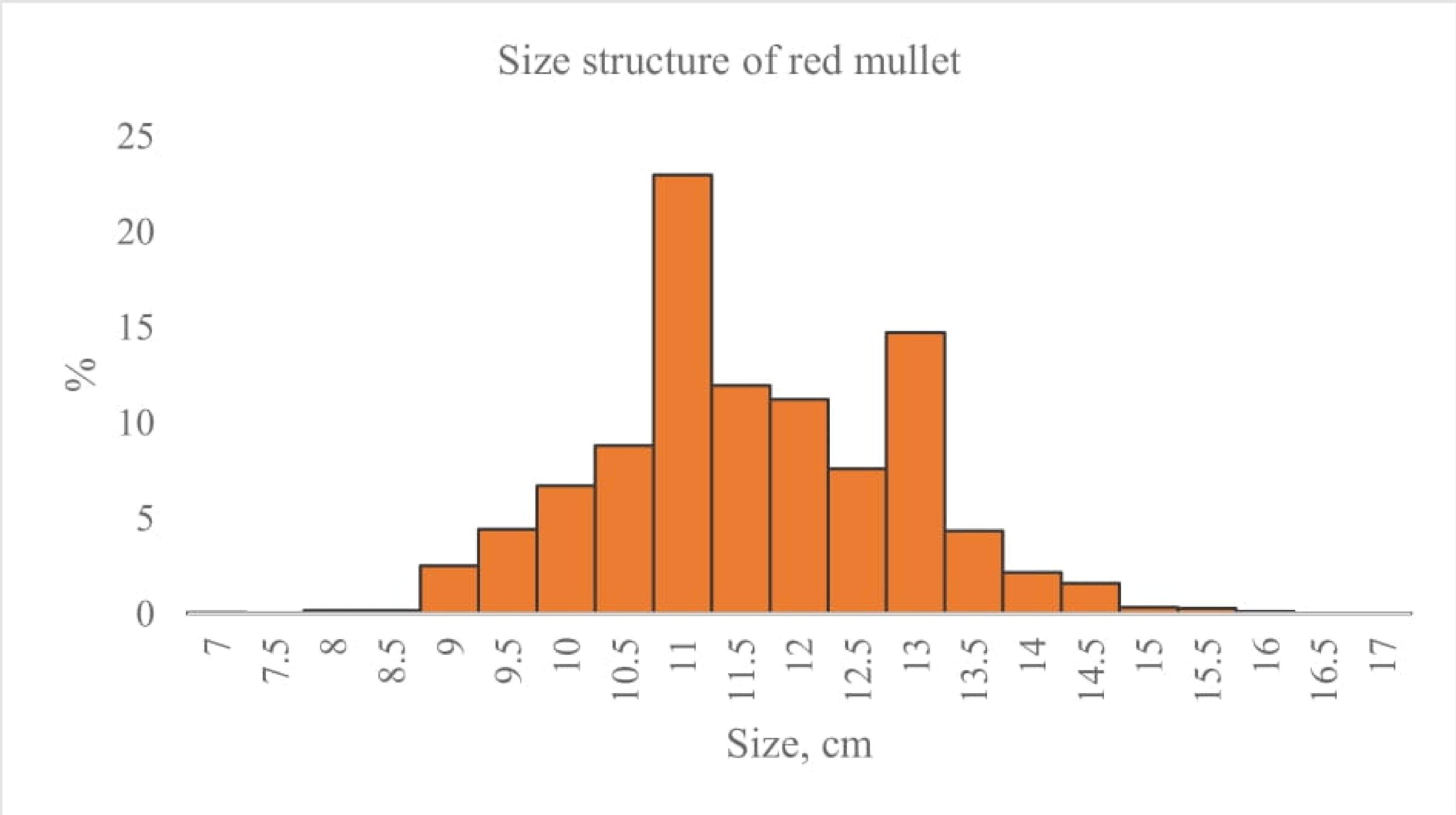

Figure 2.3.2.4. Size structure of red mullet

Project No. BG14MFOP001-1.002-0001 "Collection, management and use of data for the purposes of scientific analysis and implementation of the Common Fisheries Policy for the period 2023-2024", financed by the Maritime, Fisheries and Aquaculture Programme, co-financed by the European Union through the European Fund for maritime, fisheries and aquaculture fund.

Age group 1–1+ years was dominant, followed by 2–2+ and 3–3+ years (500 ind). The remaining age groups had a negligible presence in the catches during November 2024 (Fig. 2.3.2.5).

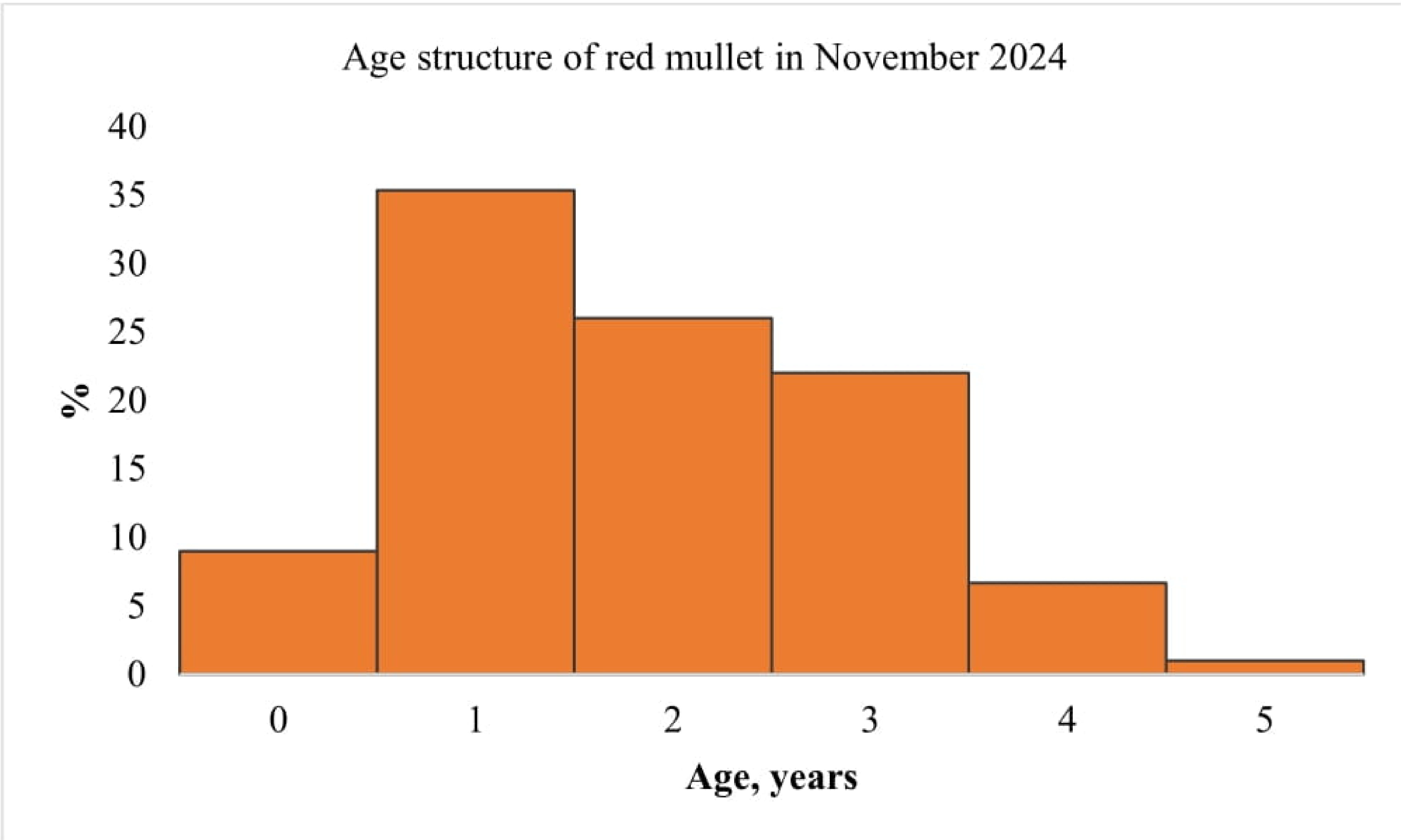

Figure 2.3.2.5. Age structure of red mullet

The growth parameters (1200 ind.) of red mullet, calculated using the von Bertalanffy model, indicate an asymptotic length of 18.41 cm and higher values of the coefficient that defines the rate of approaching the asymptote (Table 2.3.2.1).

Table 2.3.2.1. Von Bertalanffy growth model (VBGF) for red mullet

Species	Asymptotic lenght	Growth rate	Growth parameter	Growth coefficient	Allometric coefficient
M. barbatus	$L\infty = 18.41$	$K = 0.24$	$t_0 = -1.232$	$q = 0.009$	$n = 3.1194$

Somatic growth of red mullet by age did not show any deviations from the norm (Fig. 2.3.2.5).

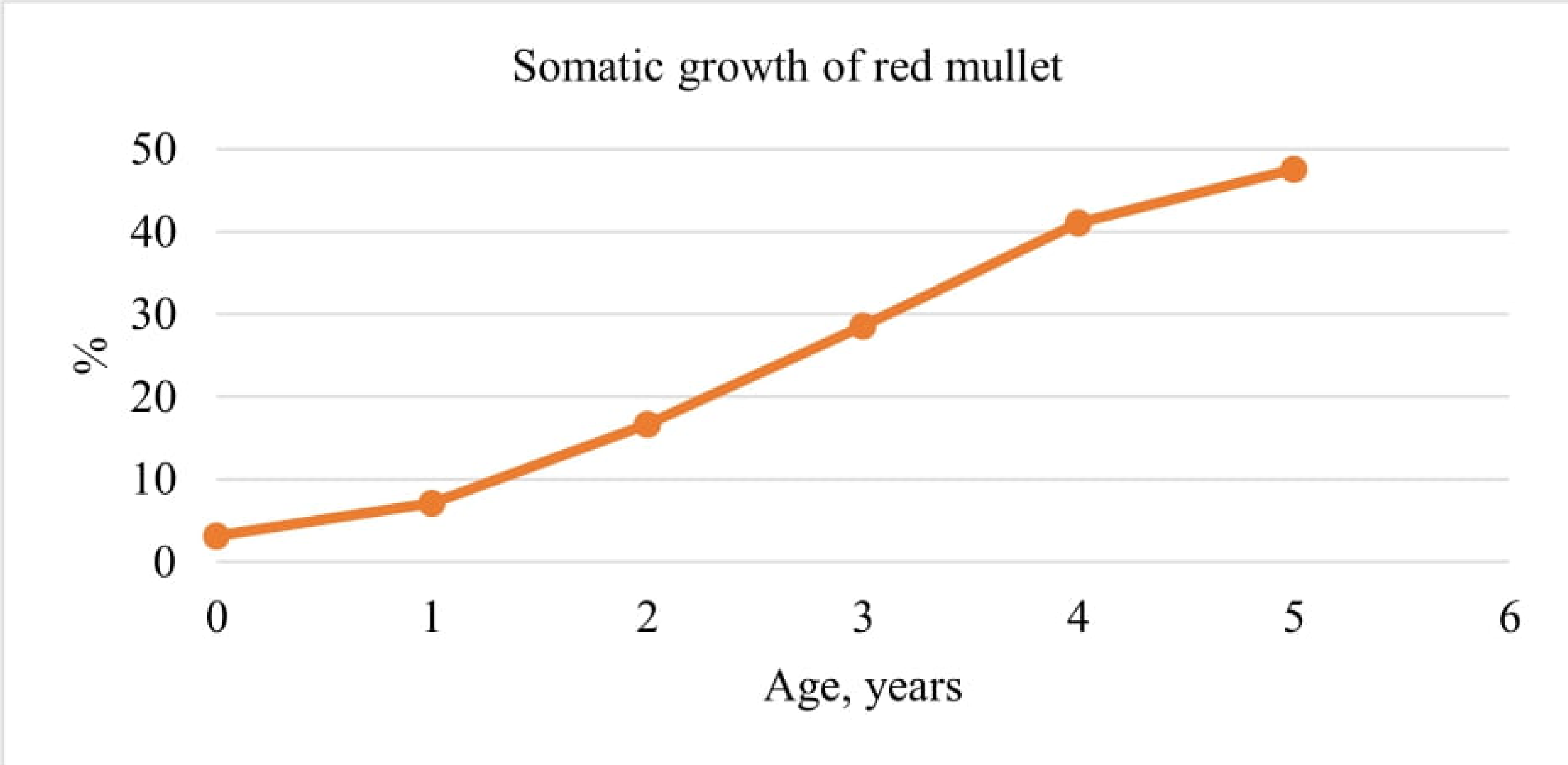

Figure 2.3.2.5. Somatic growth of red mullet by age

2.3.3. Abundance and biomass by length and age classes

The 11 cm and 13 cm length classes dominated the red mullet catches, while larger length classes were represented by a smaller percentage. In November 2024, the 11 cm length class had the highest percentage representation in the catches, followed by the 13 cm length class (Fig. 2.3.3.1; Fig. 2.3.3.2).

Project No. BG14MFOP001-1.002-0001 "Collection, management and use of data for the purposes of scientific analysis and implementation of the Common Fisheries Policy for the period 2023-2024", financed by the Maritime, Fisheries and Aquaculture Programme, co-financed by the European Union through the European Fund for maritime, fisheries and aquaculture fund.

Figure 2.3.3.1. Abundance of red mullet by size classes

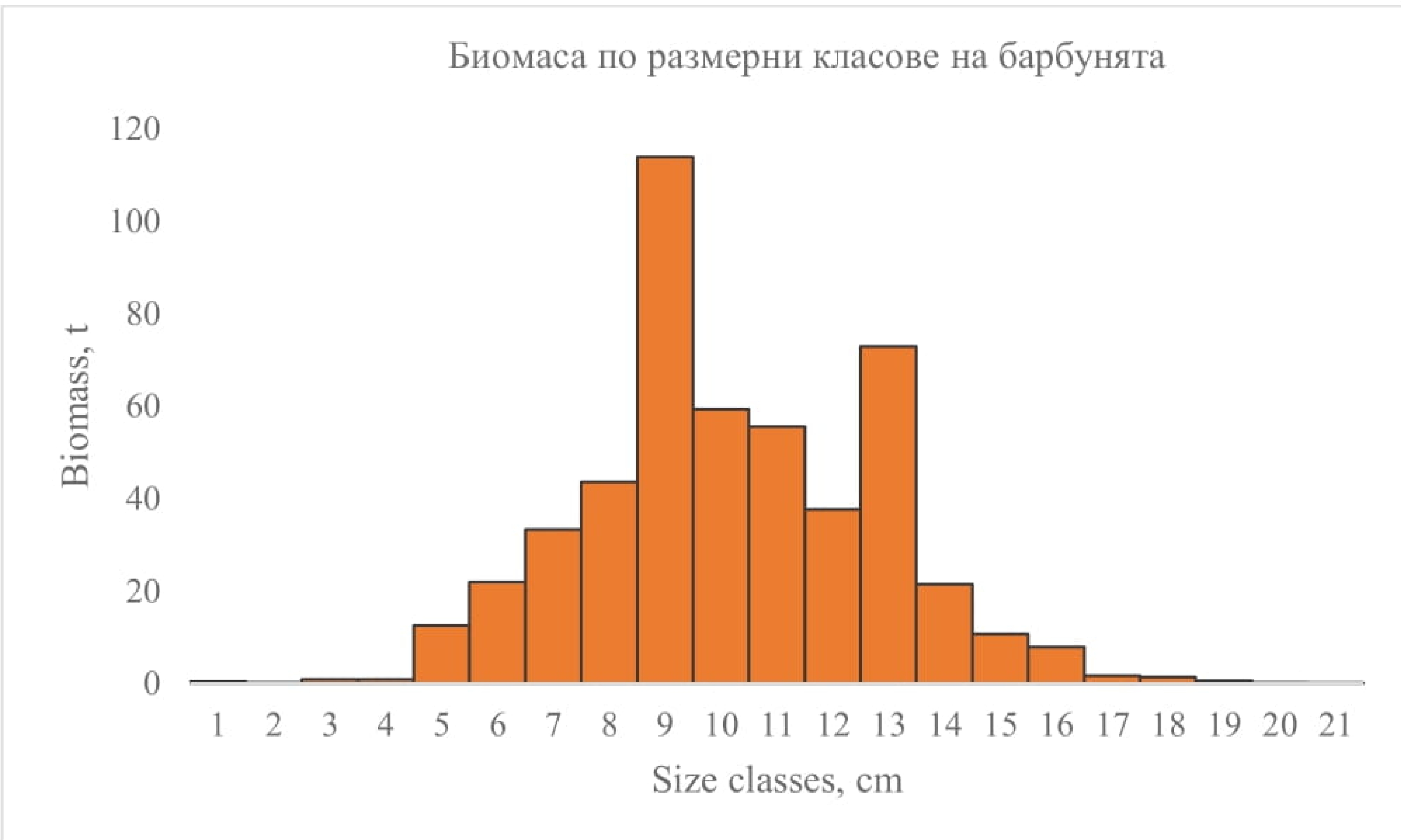

Figure 2.3.3.2. Biomass of red mullet by size classes

Project No. BG14MFOP001-1.002-0001 "Collection, management and use of data for the purposes of scientific analysis and implementation of the Common Fisheries Policy for the period 2023-2024", financed by the Maritime, Fisheries and Aquaculture Programme, co-financed by the European Union through the European Fund for maritime, fisheries and aquaculture fund.

The highest abundance was recorded in the 3–3+ year age group, followed by the 2–2+ year group. In terms of biomass, the 4–4+ year age group was dominant (Fig. 2.3.3.3; Fig. 2.3.3.4).

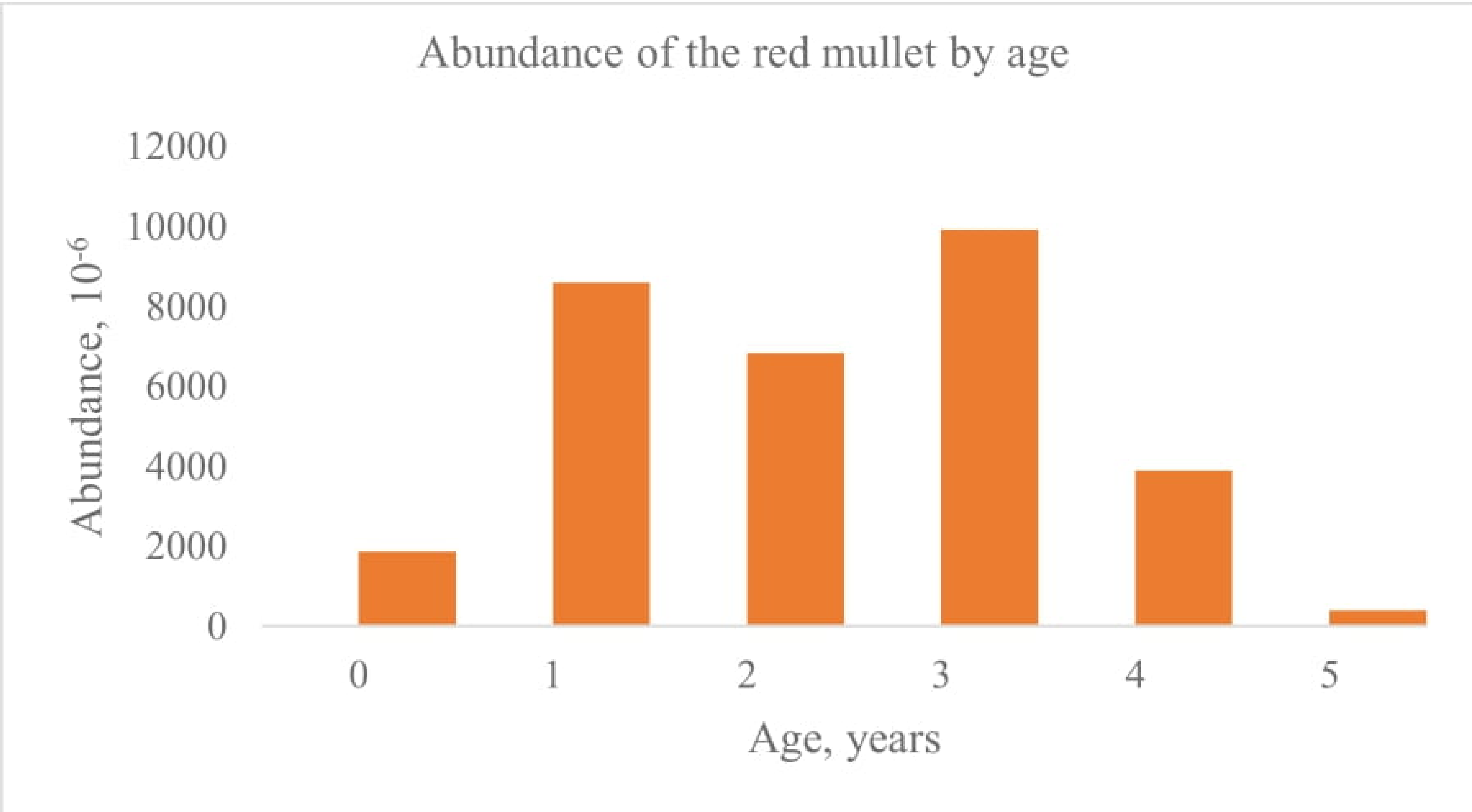

Figure 2.3.3.3. Abundance of the red mullet by age groups

Figure 2.3.3.4. Biomass of red mullet by age groups

Project No. BG14MFOP001-1.002-0001 "Collection, management and use of data for the purposes of scientific analysis and implementation of the Common Fisheries Policy for the period 2023-2024", financed by the Maritime, Fisheries and Aquaculture Programme, co-financed by the European Union through the European Fund for maritime, fisheries and aquaculture fund.

2.3.4. Sex Ratio and Maturity

The percentage representation of females, males, and sexually immature individuals in red mullet was as follows: 48% females, 44% males, and 8% immature (Fig. 2.3.4.1).

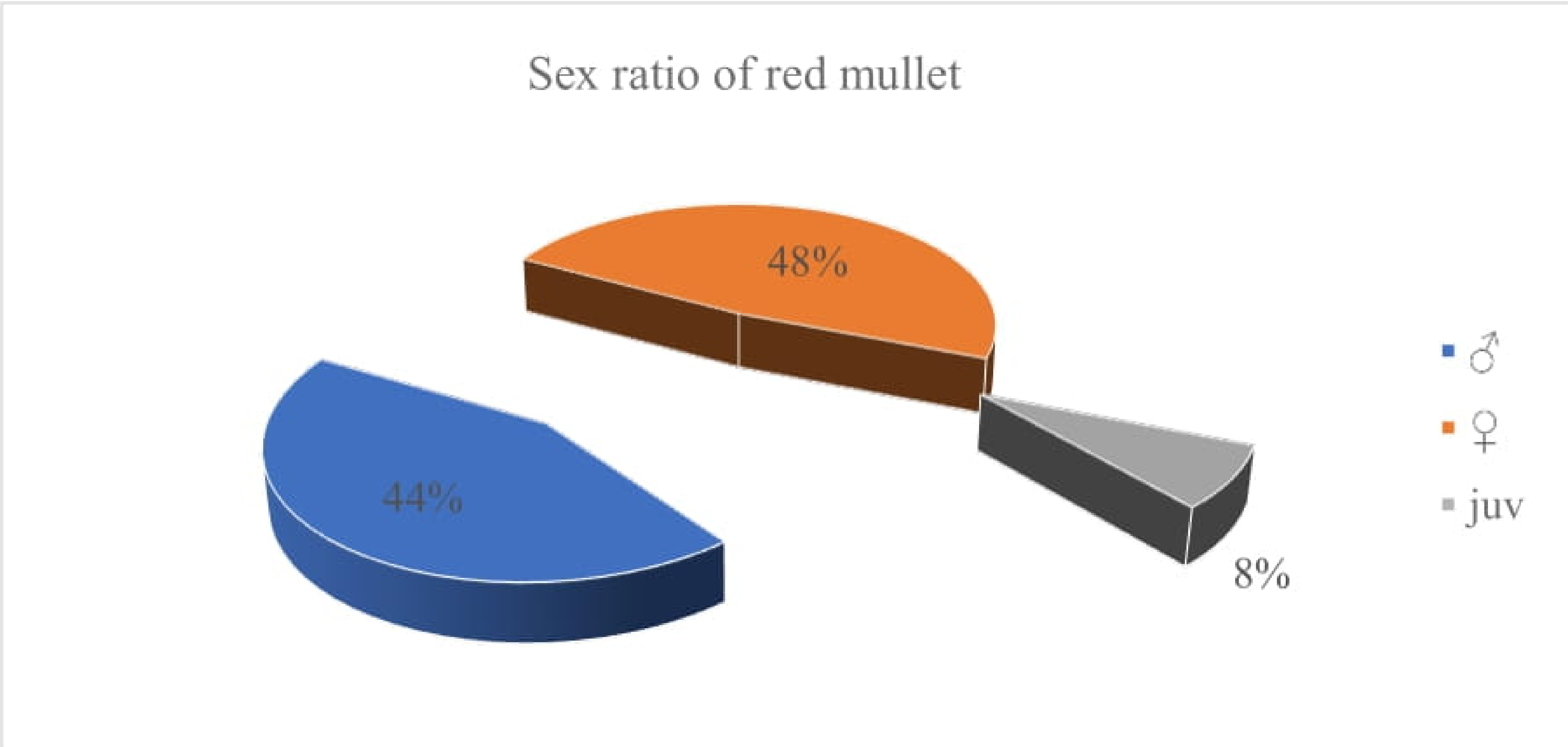

Figure 2.3.4.1. Sex ratio (females – ♀, males – ♂, and juveniles – juv) of red mullet in November 2024

The sexual maturity (250 ind.)of the analyzed species by length classes is presented in Figure 2.3.4.2, and by age groups in Figure 2.3.4.3.

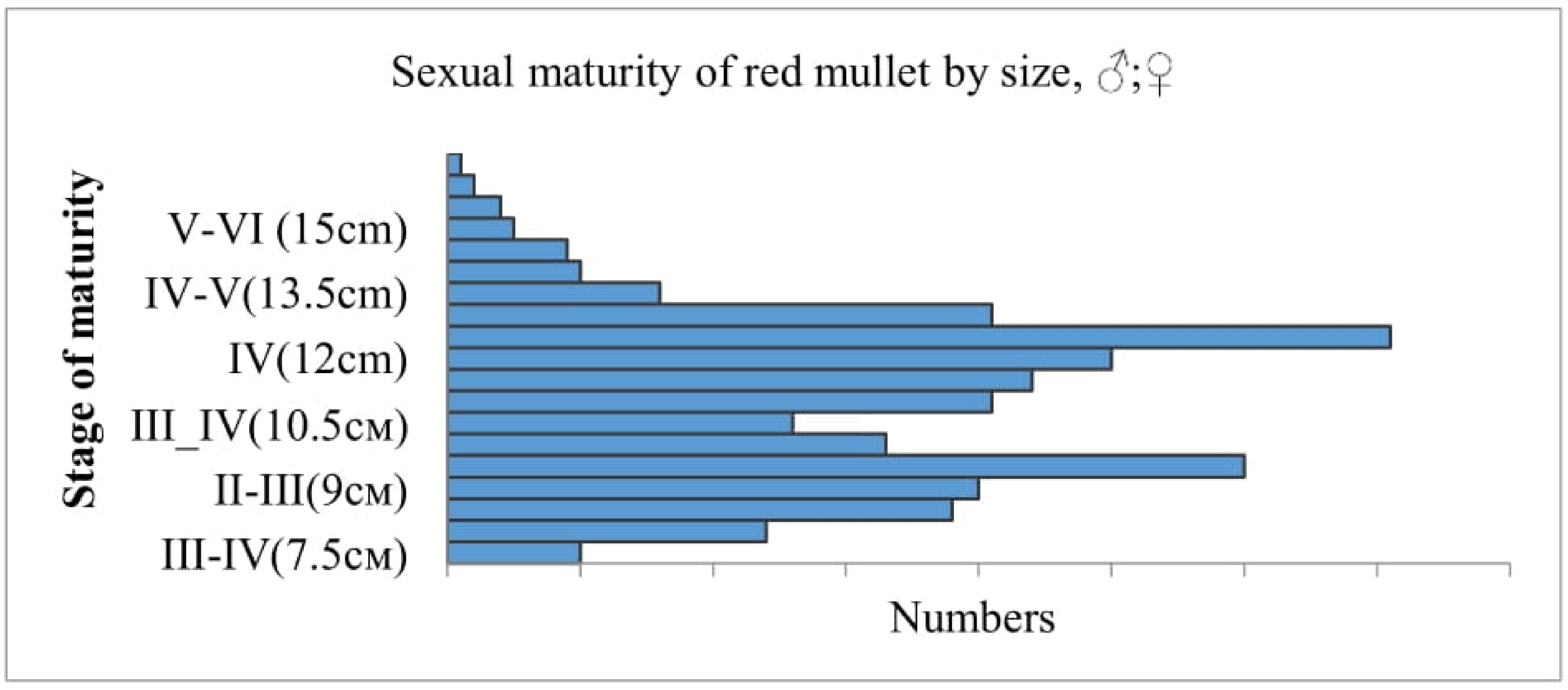

Figure 2.3.4.2. Sexual maturity of the studied species, analysed by size classes (females – ♀ and males – ♂) of red mullet

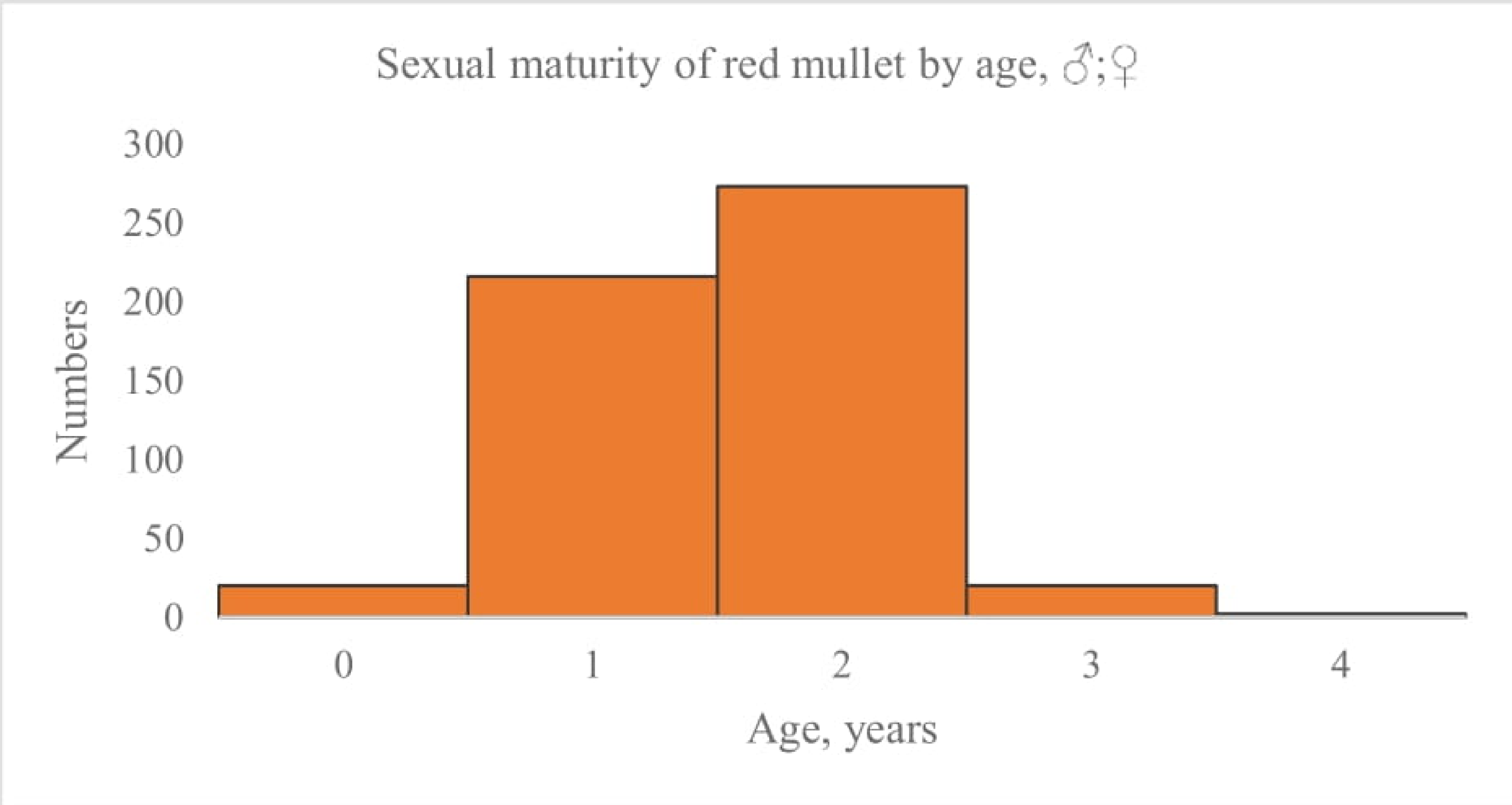

Figure 2.3.4.3. Sexual maturity (females – ♀ and males – ♂) of the studied species, analysedby age groups

2.3.5. Fecundity and Gonado-somatic index (GSI)

Red mullet was in an active phase of gonadal development (250 ind.), likely related to the high sea water temperatures (Fig. 2.3.5.1).

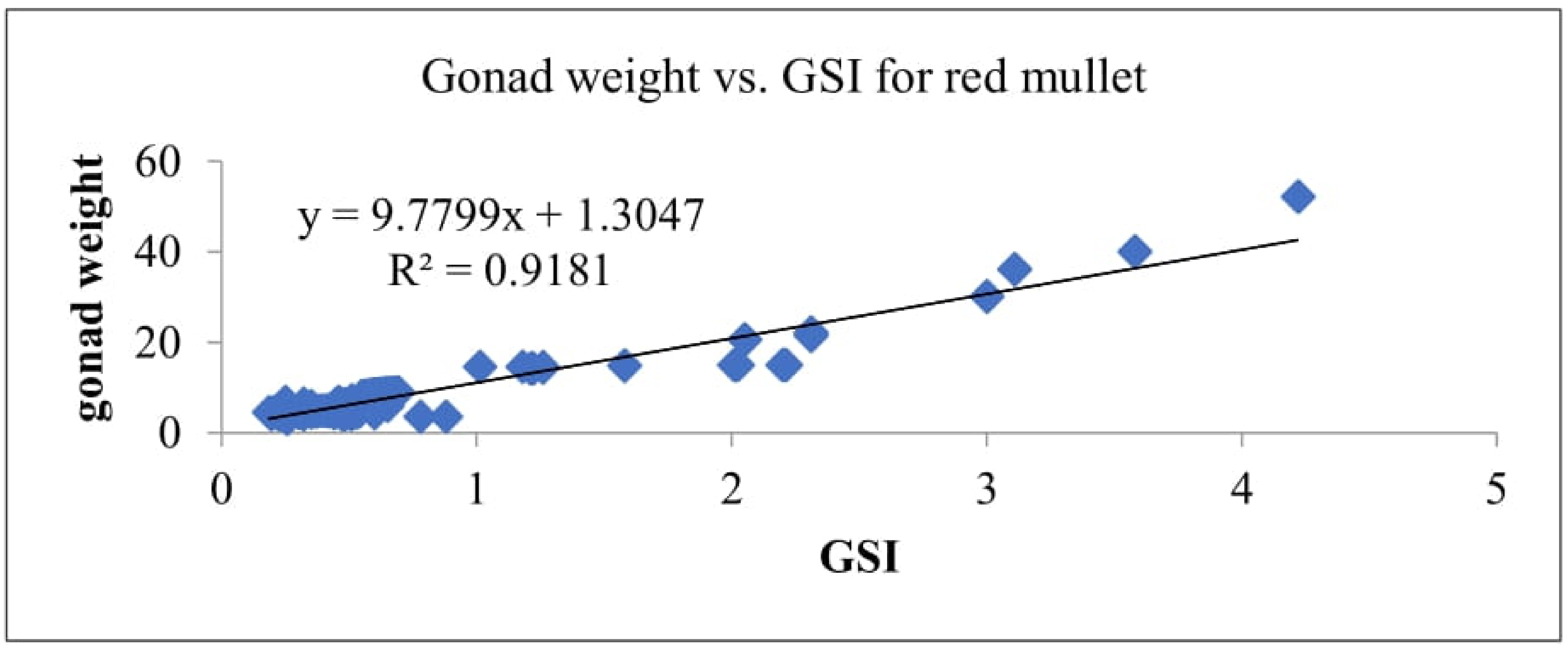

Figure 2.3.5.1. Sexual maturity (females – ♀, males – ♂ and juveniles – Juv) of red mullet bu age groups

Project No. BG14MFOP001-1.002-0001 "Collection, management and use of data for the purposes of scientific analysis and implementation of the Common Fisheries Policy for the period 2023-2024", financed by the Maritime, Fisheries and Aquaculture Programme, co-financed by the European Union through the European Fund for maritime, fisheries and aquaculture fund.

2.3.6. Absolute and relative fecundity of red mullet

Absolute fecundity (measured on 250 ind) at length of 16.5 cm was the highest: 11500 cavier grains. In terms of relative fecundity, the highest was detected at 9,5 cm TL individuals: 769,75. The mean values of absolute and relative fecundity of the whiting were as follows: 8703.94 and 421.7 (Table 2.3.6.1).

Table 2.3.6.1. Absolute and relative fecundity of red mullet

Size classes, cm	Mean weight, w,g)	Mean lenght, (см)	Absolute fecundity F, хайверни зърна	Relative fecundity	No. ♀
9	8.03	9.01	6105±101	759.95±44	**10**
9.5	9.11	9.5	7012±412	769.75±85	**10**
10	11.00	10.12	7099±405	645.42±115	**10**
10.5	13.54	10.55	7212±242	532.68±66	**20**
11	14.80	11	7366±300	497.74±47	**20**
11.5	16.19	11.51	7800±302	481.78±22	**20**
12	18.20	12.33	7866±416	432.20±45	**20**
12.5	21.17	12.62	8150±516	384.98±68	**20**
13	23.00	13.05	8324±555	361.93±58	**20**
13.5	26.20	13.44	9000±444	343.52±61	**20**
14	26.00	14.21	9420±612	362.32±74	**20**
14.5	28.50	14.21	9560±644	335.44±22	**10**
15	33.90	15.11	10215±522	301.33±38	**10**
15.5	38.30	15.49	10325±412	269.59±101	**10**
16	45.00	16.25	10688±444	237.52±87	**10**
16.5	47.23	17	11500±977	243.49±34	**10**
17	49.33	17.22	10325±842	209.31±	**10**
средно			8703.941	**421.70**	250

2.4. Whiting (*Merlangius merlangus*)

The species was represented in the catches by single specimens, with catches of 1 kg each at two of the stations. It was not possible to make a spatial and quantitative assessment of the species' distribution based on the autumn 2024 survey.

2.4.1. Size structure

The size distribution of whiting (1200 ind.) showed a normal pattern, with peaks at 11.5 cm and 14.5 cm (Fig. 2.4.1.1).

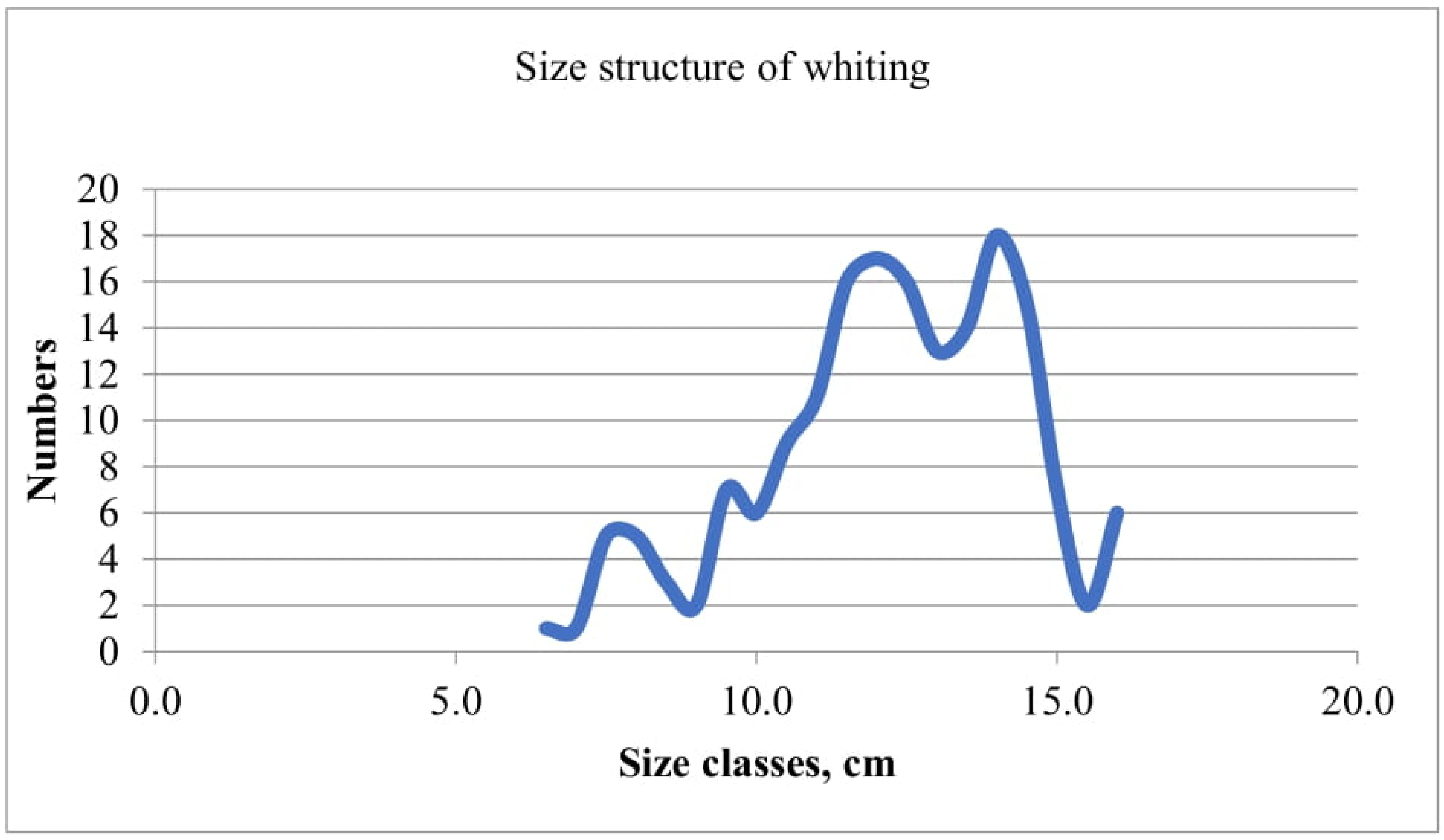

Figure 2.4.1.1. Size structure of whiting in November 2024

The weights of the whiting specimens (1200 ind.) ranged from 3.22 to 26.8 g in the present study (Fig. 2.4.1.2).

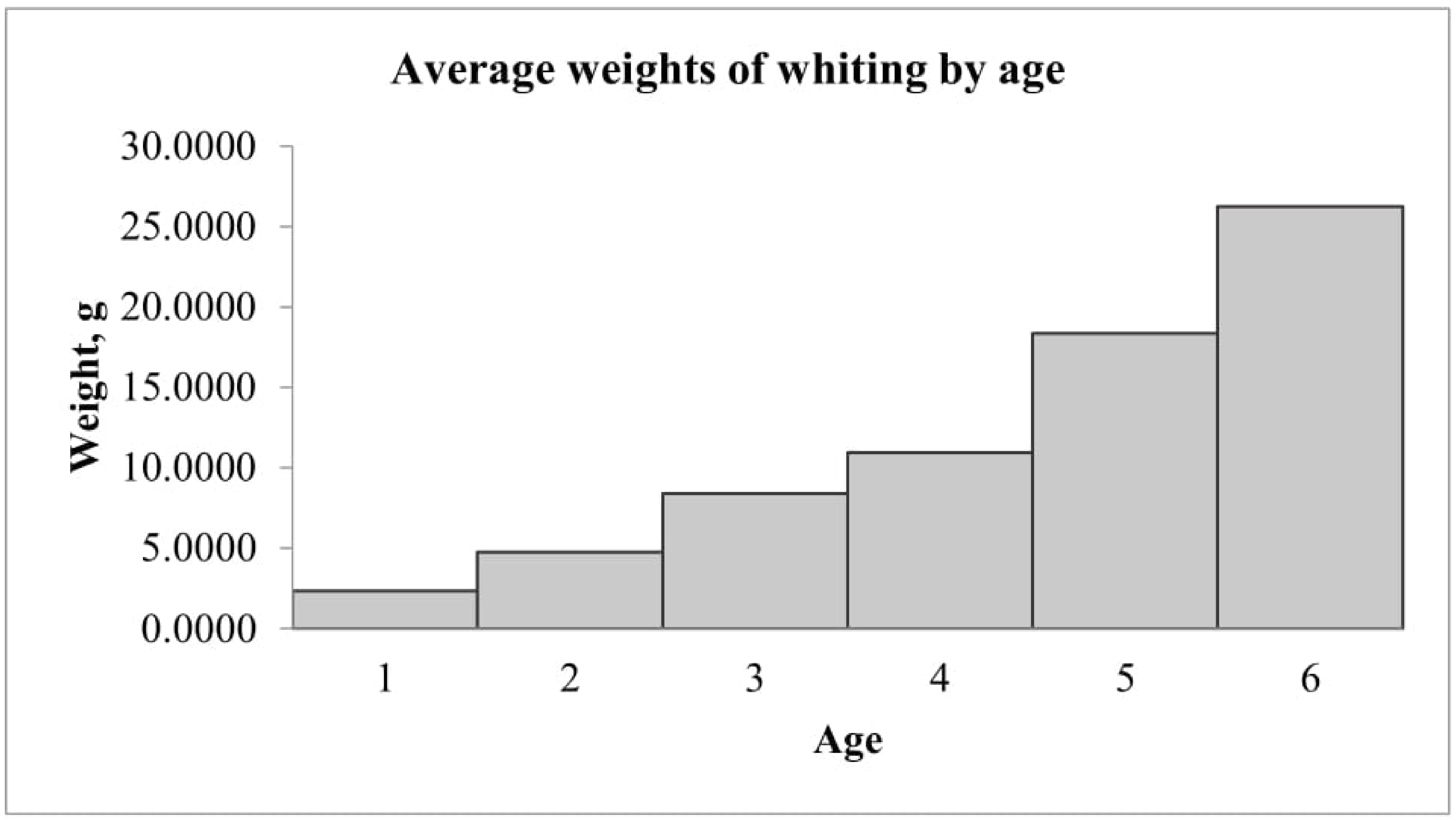

Figure 2.4.1.2. Average weights of whiting by age in November 2024

In the catches from the autumn 2024 survey, individuals aged 4–4+ years (38%) and 5–5+ years (20%) were predominant based on the sampling of 1200 individuals (Fig. 2.4.1.3).

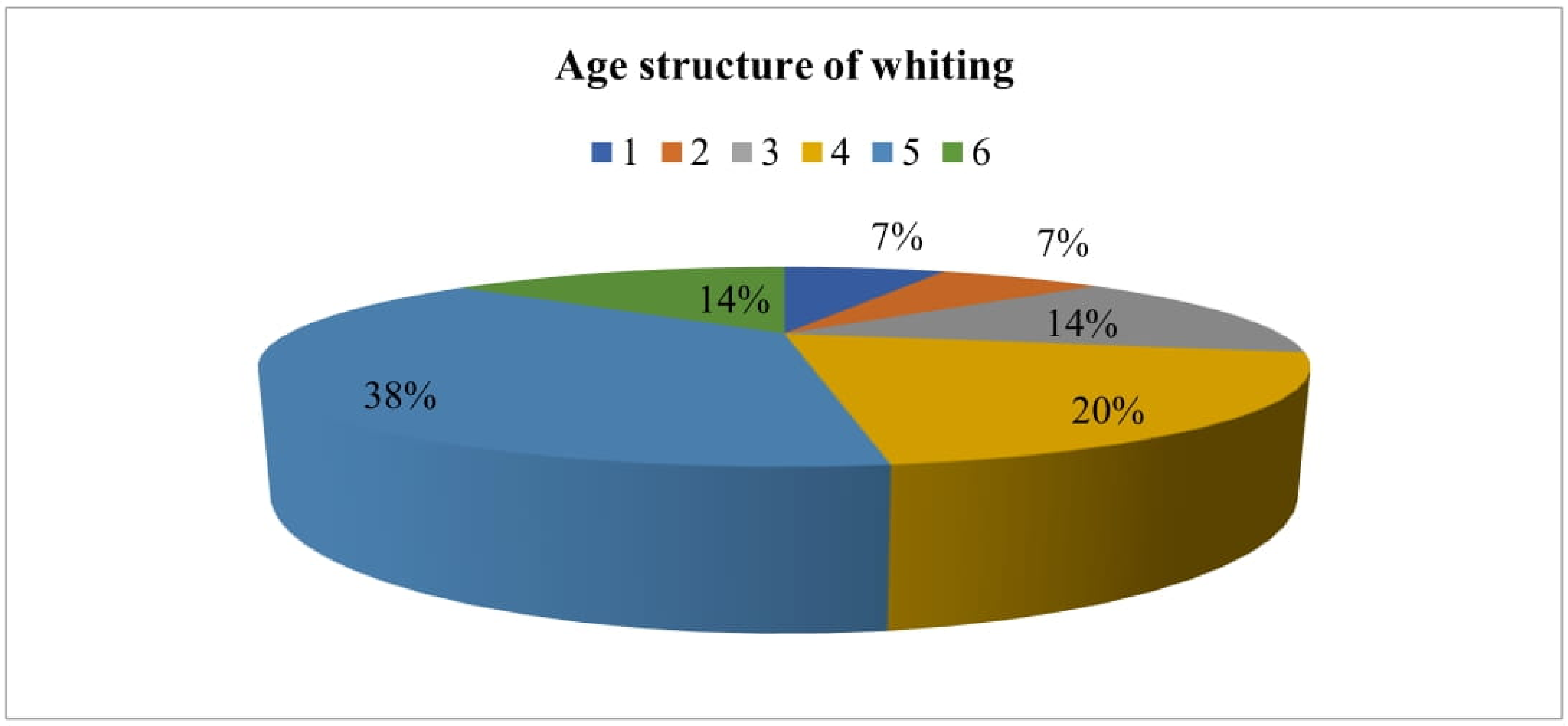

Figure 2.4.1.3. Age distribution of whiting in November 2024

Project No. BG14MFOP001-1.002-0001 "Collection, management and use of data for the purposes of scientific analysis and implementation of the Common Fisheries Policy for the period 2023-2024", financed by the Maritime, Fisheries and Aquaculture Programme, co-financed by the European Union through the European Fund for maritime, fisheries and aquaculture fund.

The length–weight relationship for the species showed a very high degree of reliability (R^2 = 0.955) (Fig. 2.4.1.4).

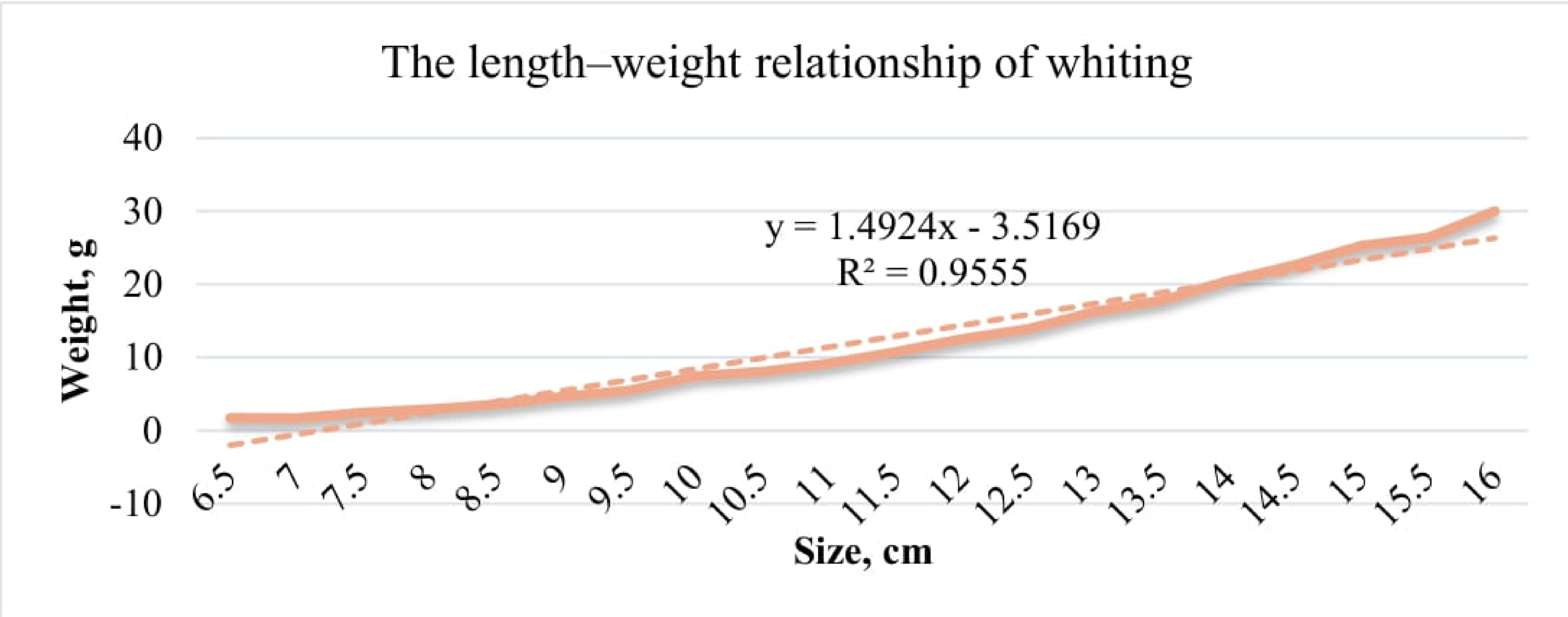

Figure 2.4.1.4. The length–weight relationship of whiting in November 2024

To determine the growth parameters, the von Bertalanffy Growth Function (VBGF) was applied. The calculated growth parameters (1200 ind.) are presented in Table 2.4.1.1. The asymptotic length reached 27.55 cm, with a growth rate that can be classified as low (k = 0.23) (Table 2.4.1.1).

Table 2.4.1.1. von Bertalanffy Growth Function of whiting

Species	Asymptotic lenght	Growth rate	Growth parameter	Growth coefficient	Allometric coefficient
M. merlangus	$L\infty = 27.55$	K = 0.23	$t_0 = -2.0112$	a = 0.009	n = 3.11

In terms of sex ratio, females made up 50%, males 49%, and larvae 1% of the population (Fig. 2.4.1.5).

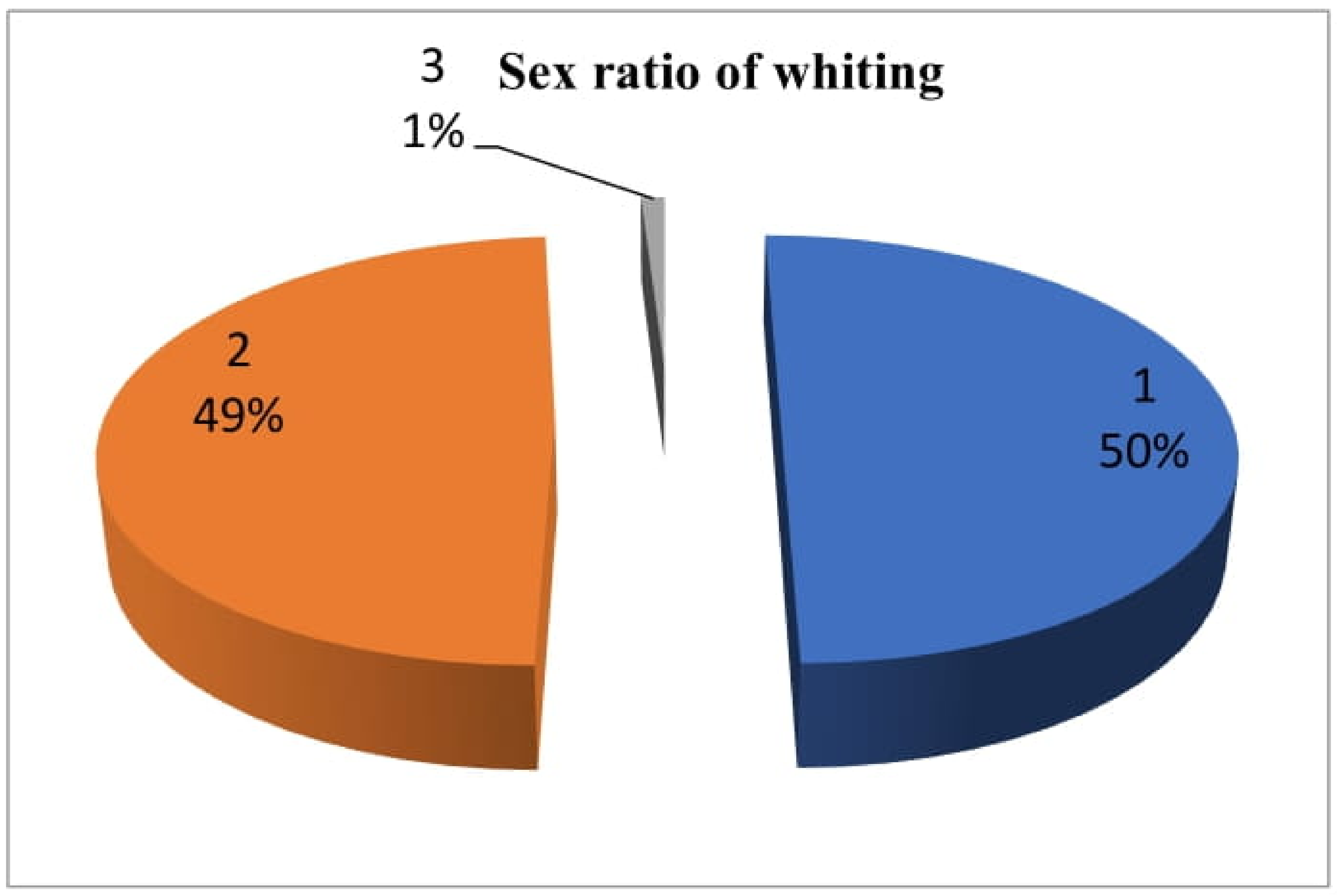

Figure 2.4.1.5. Sex ratio of whiting in November 2024

2.4.2. Fecundity and gonadosomatic index (GSI)

The maturation of the gonads indicates the beginning of the species' active reproductive period. Due to the warmer weather, the spawning process is likely to intensify in the coming months, even at relatively lower sea water temperatures. The analysis of gonadal maturity in whiting (based on 250 ind.) showed that the gonads were in stages 2a to 3b, with no dominance of a particular size group exhibiting a specific degree of gonad development. No deviations from the norm were observed in gonadal maturation, which, in terms of stage and intensity, corresponds to the species' active reproductive period (Fig. 2.4.2.1.).

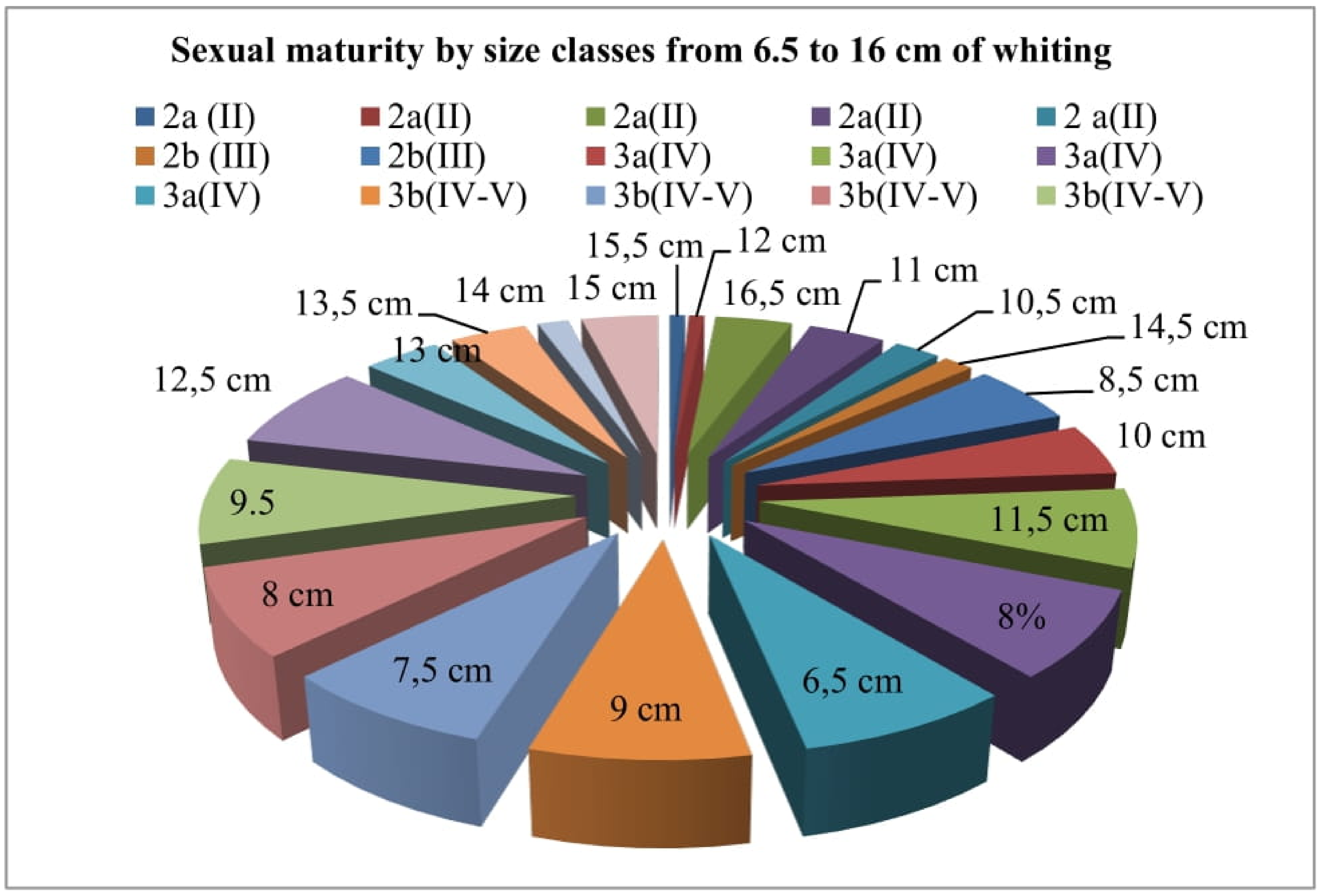

Figure 2.4.2.1. Sexual maturity of whiting analysed by size classes in November 2024

Male and female individuals of whiting aged 4–4+ years had the highest presence in the catches, with a maturity stage of III (2.4.2.2).

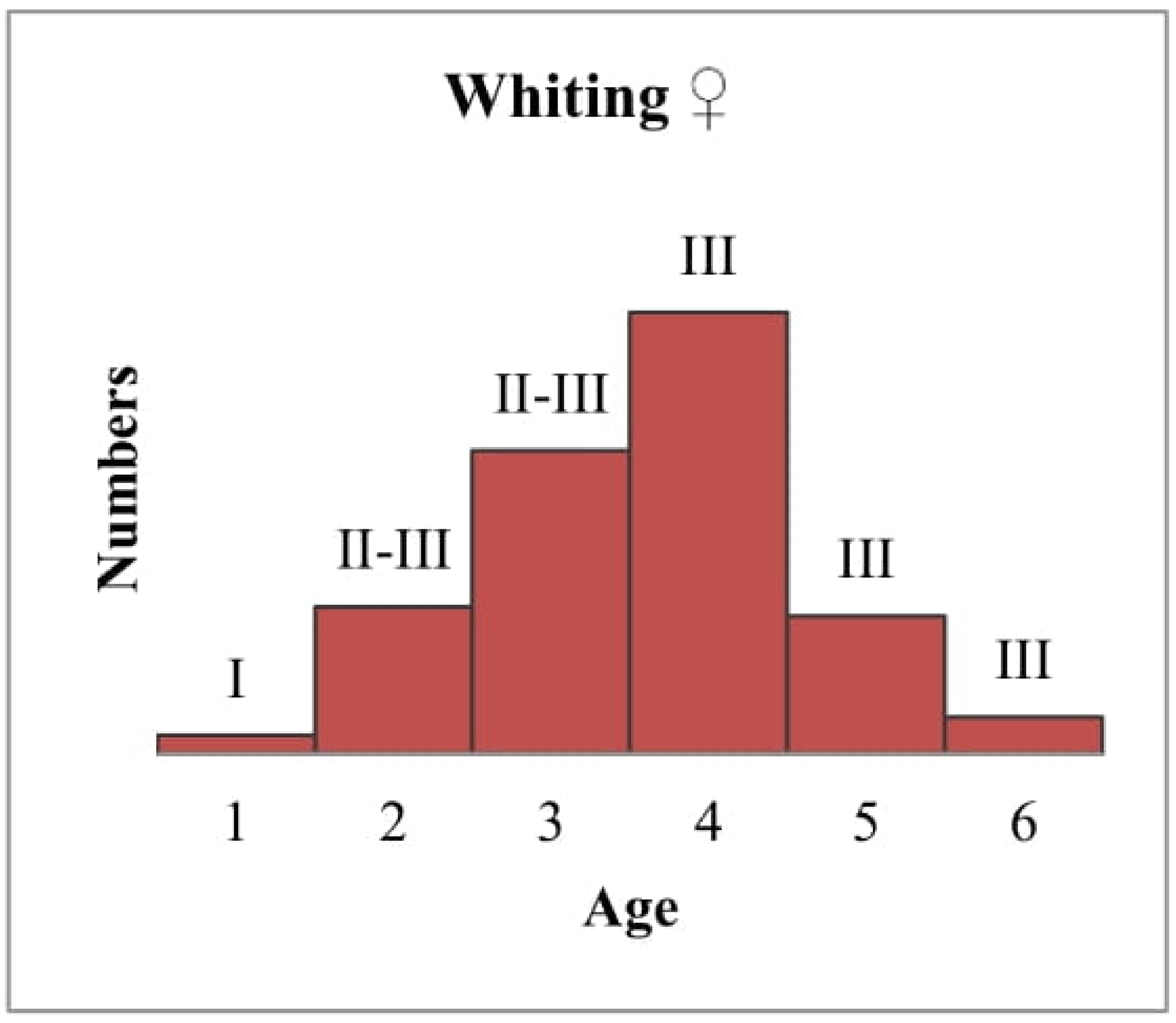

Figure 2.4.2.2. Maturity of whiting analysed by age groups

Project No. BG14MFOP001-1.002-0001 "Collection, management and use of data for the purposes of scientific analysis and implementation of the Common Fisheries Policy for the period 2023-2024", financed by the Maritime, Fisheries and Aquaculture Programme, co-financed by the European Union through the European Fund for maritime, fisheries and aquaculture fund.

The weight of the gonads, compared to the gonadosomatic index, showed a high degree of reliability (R^2= 0.83) (Fig. 2.4.2.3).

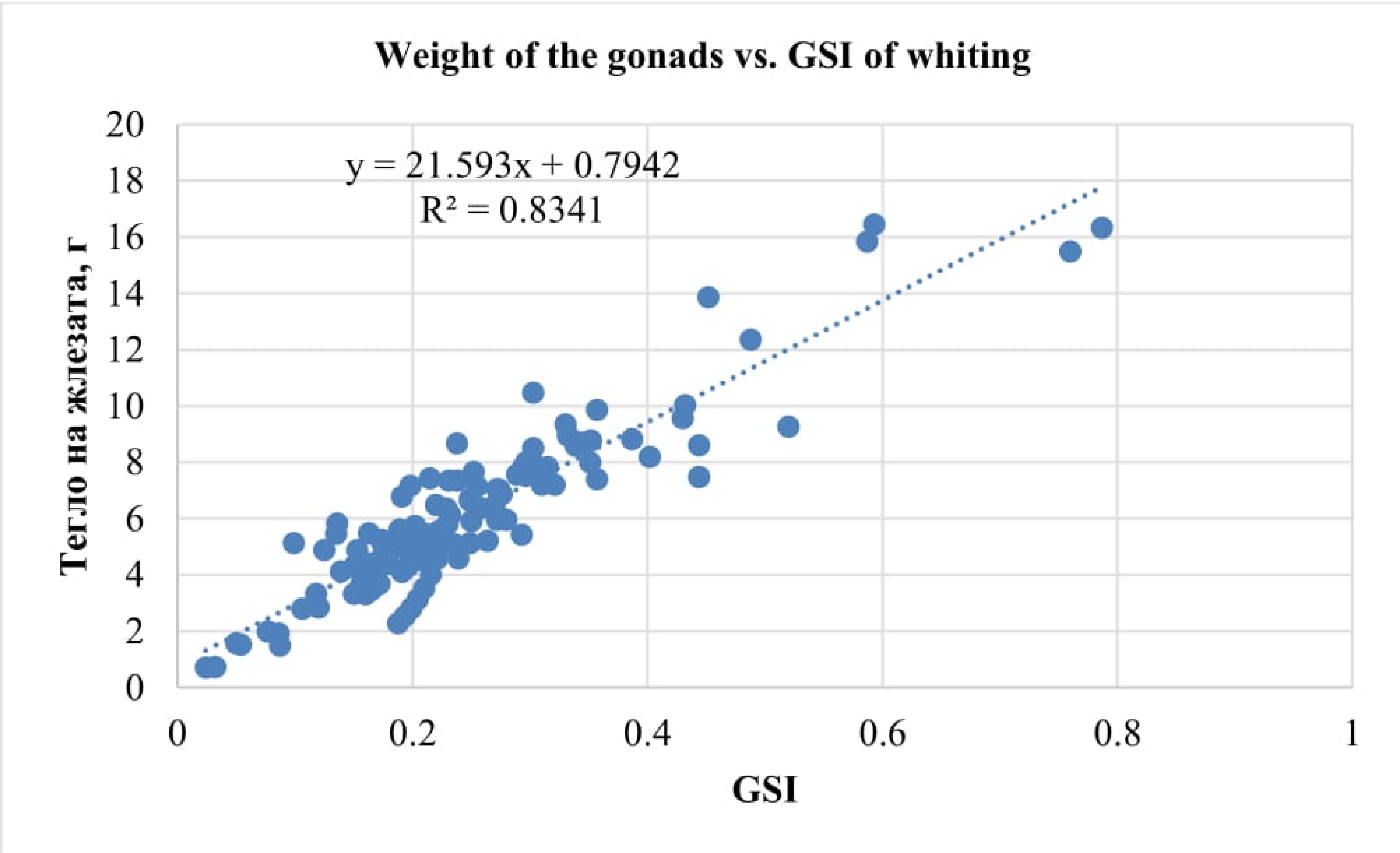

Figure 2.4.2.3. Weight of the gonads, compared to the gonadosomatic index of whiting in November 2024

2.4.3. Absolute and relative fecundity

Absolute fecundity (measured on 250 ind) at length of 17.5 cm was the highest: 60 212 cavier grains. In terms of relative fecundity, the highest was detected at 14 cm TL individuals: 3247,66. The mean values of absolute and relative fecundity of the whiting were as follows: 37159.88 and 1557.92 (Table 2.4.3.1).

Table 2.4.3.1. Absolute and relative fecundity of whiting, November 2024

Size class	Average body weight (W, g)	Absolute fecundity (F, caviar grains)	Relative fecundity	Number
10	7.16	8400±242	1172.48±106	10
10.5	8.37	8512±112	1017.57±111	10
11	9.18	9835±212	1071.61±211	10
11.5	10.66	11706±146	1098.42±99	20
12	15.20	14800±112	973.68±77	20
12,5	14.60	28120±241	1926.03±112	20
13	15.63	36035±356	2305.02±89	20
13.5	17.70	44200±388	2497.18±111	20
14	17.50	56834±412	3247.66±146	10
14.5	27.30	50112±455	1835.60±256	20
15	28.34	52418±652	1849.61±199	20
15.5	31.23	51115±705	1636.73±56	20
16	33.45	56405±1184	1686.25±63	10
16.5	34.00	46332±922	1362.71±58	10
17	49.10	36898±602	751.49±45	10
17.5	55.40	60212±512	1086.86±99	10
18	61.90	59784±521	965.82±77	10
		37159.88	1557.92	250

2.5. Picked dogfish

The species picked dogfish (Squalus acanthias) were presented with 6 individuals incidently caught. The parameters of individual growth are given in Table 2.5.1.

Project No. BG14MFOP001-1.002-0001 "Collection, management and use of data for the purposes of scientific analysis and implementation of the Common Fisheries Policy for the period 2023-2024", financed by the Maritime, Fisheries and Aquaculture Programme, co-financed by the European Union through the European Fund for maritime, fisheries and aquaculture fund.

Table 2.5.1. Picked dogfish from November 2024

Sex	Total length, cm	Weight, kg
male	115	5.91
male	122	6.265
female	118	6.02
male	118	6.02
male	121	6.15
female	118	6.055

2.6. Planktivorous fish species feeding

2.6.1. Length-weight relationships (LWR), index of stomach fullness (ISF)

For the measured sprat specimens, the average total length is 10.03 cm ± 0.37 (SD), with an average weight of 5.87 g ± 0.99 (SD). Respectively, the average length of horse mackerel is 9.81 cm ± 1.49 (SD), with an average weight of 7.93 g ± 3.86 (SD) (Table 2.6.1.1.).

Table 2.6.1.1. Summary data for length (L, cm), weight (W, g), and ISF (% of BW) of plankton-eating fish: sprat (1) and horse mackerel (2), as determined by stomach content analysis in November 2024

1. Sprat

	L, cm	W, g	ISF, % BW
Average value	10.030	5.870	0.223
Standard error	0.117	0.316	0.038
Median	10.000	5.800	0.219
Mode	10.000	6.900	#N/A
Standard deviation	0.371	0.998	0.120
Sample Variance	0.138	0.996	0.014
Kurtosis	0.065	-1.877	-1.114
Skewness	0.193	-0.137	0.281

Range	1.200	2.400	0.356
Minimum	9.500	4.600	0.057
Maximum	10.700	7.000	0.413
Confidence interval (95.0%)	0.266	0.714	0.086

2. Horse mackerel

	L, cm	W, g	ISF, % BW
Average value	9.812	7.929	0.519
Standard error	0.135	0.353	0.059
Median	9.800	7.200	0.315
Mode	10.000	7.100	#N/A
Standard deviation	1.484	3.862	0.644
Sample Variance	2.201	14.916	0.415
Kurtosis	1.082	3.292	16.442
Skewness	0.500	1.582	3.511
Range	7.500	20.500	4.732
Minimum	6.500	2.000	-0.041
Maximum	14.000	22.500	4.691
Confidence interval (95.0%)	0.268	0.698	0.116

The relationship between weight (W, g) and linear size (L, cm) was derived for the studied horse mackerel and sprat specimens as follows:

(1) Horse mackerel: $W(g)=0.0069*L(cm)^{3.055}$; ($R^2=0.98$, $p<0.001$, Fig. 2.6.1.1 (1))

(2) Sprat: $W(g)=0.0013*L(cm)^{3.6296}$; ($R^2=0.56$, Fig. 2.6.1.1 (2))

The growth of horse mackerel and sprat is positively allometric, with a coefficient b>3.

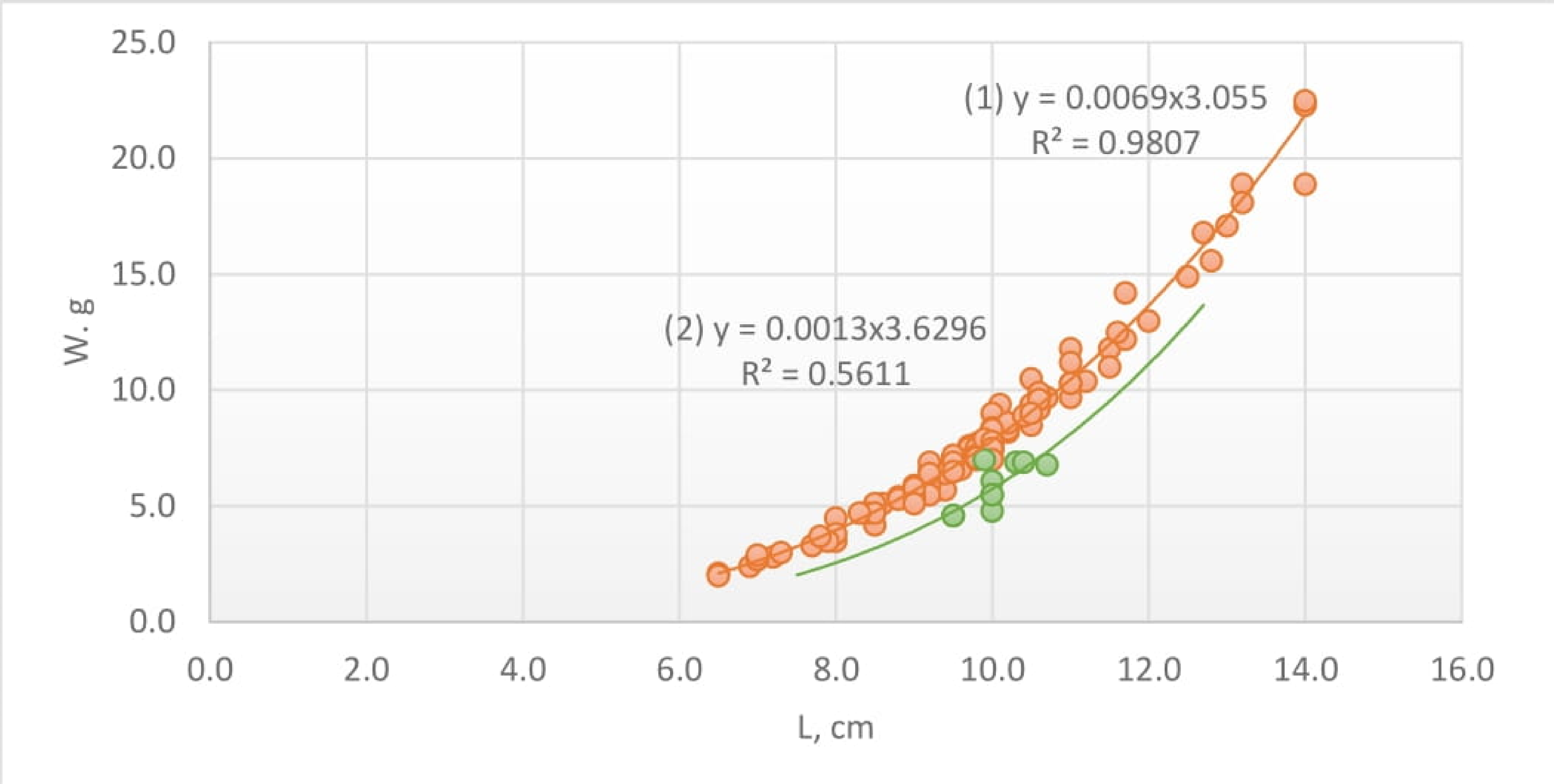

Figure 2.6.1.1. Linear-weight relationships for horse mackerel (orange) and sprat (green) specimens in November 2024

The average value of the stomach fullness index for sprat is 0.22 % BW ± 0.04 (SD), and for horse mackerel it is 0.52 % ± 0.06 (SD) (Fig. 2.6.1.2.).

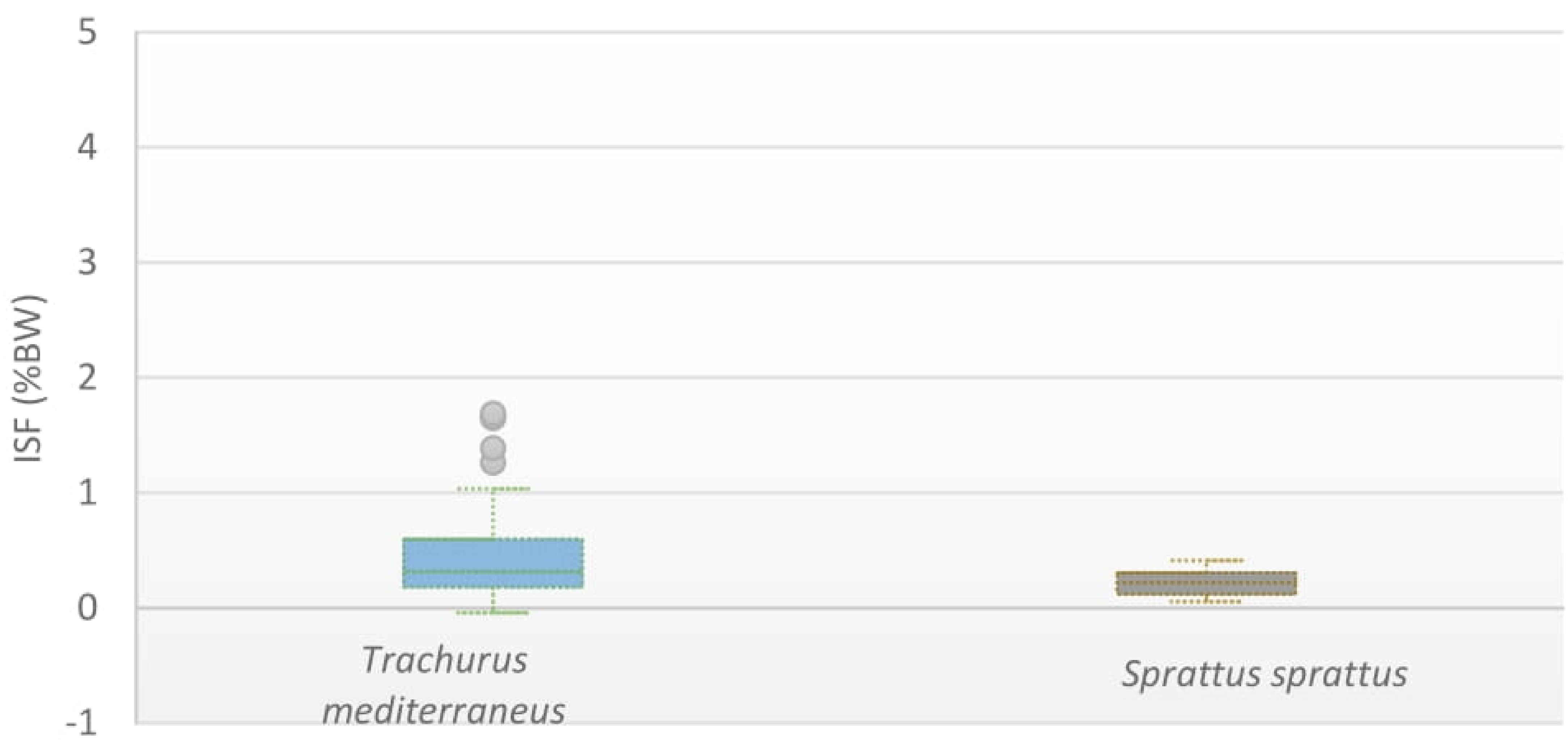

Figure 2.6.1.2. Box plot: ISF values (% BW) by species in November 2024 (median, range of values: 25–75%; minimum and maximum values are indicated)

Accordingly, the autumn value of the stomach fullness index (ISF) for sprat in 2024 was 0.73 % BW, while for horse mackerel, an average value of 0.37 % BW ± 1.24 SD was recorded. The present study observes a higher stomach fullness index for horse mackerel, but a lower ISF value for sprat compared to the data from 2023.

An analysis of the spatial distribution of ISF (% BW) can only be performed for horse mackerel data, as the samples for sprat and anchovies were insufficient during the study season. More intensive feeding of horse mackerel was observed off the central coasts of Cape Galata and Cape Emine (Fig. 2.6.1.3.).

.

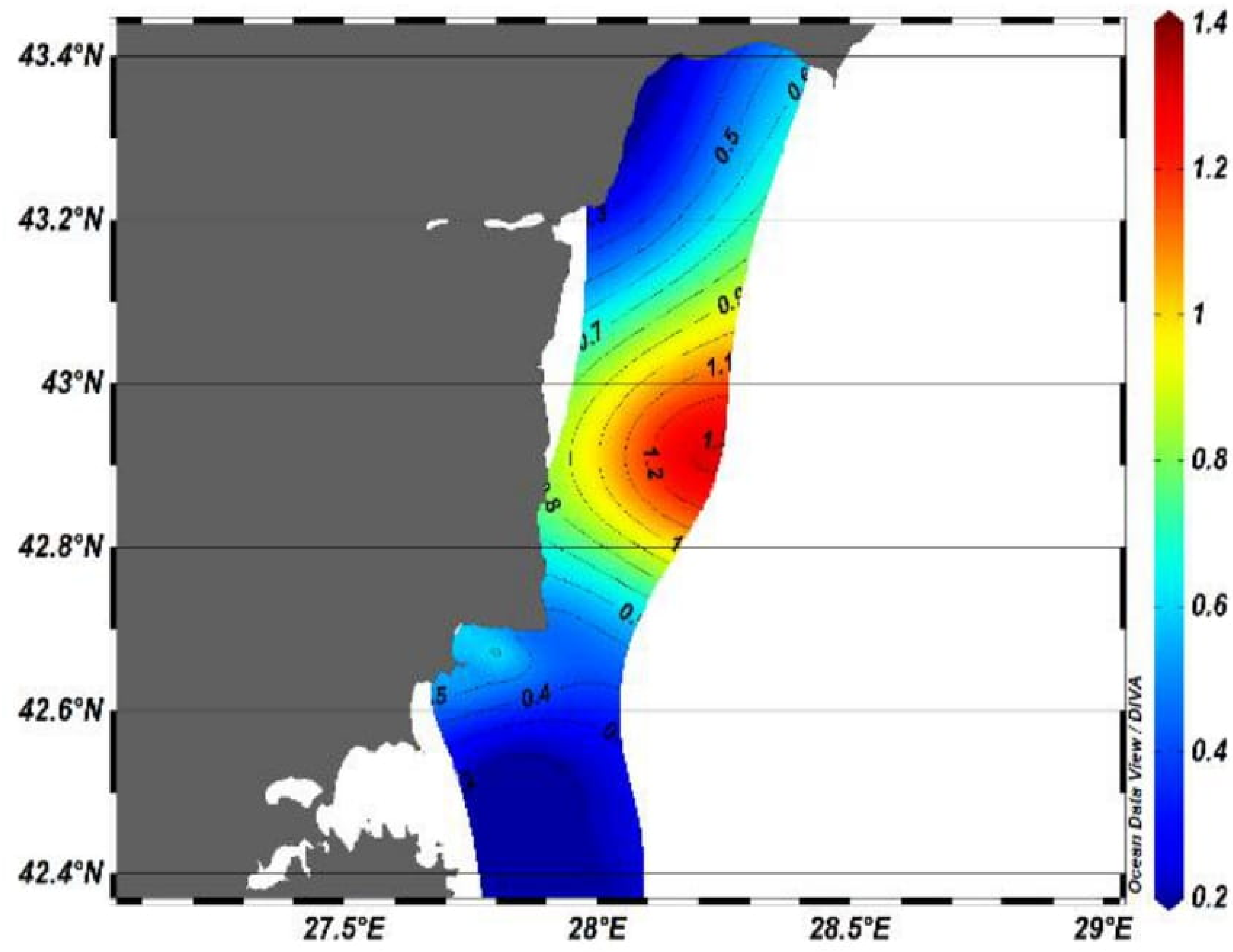

Figure 2.6.1.3. Spatial distribution of ISF (% BW) of horse mackerel in November 2024

2.6.2. Prey number (PN), species composition of food and relative importance index (IRI) of zooplankton

The highest average number of prey items was recorded for horse mackerel at 88.58 ind/stomach ± 11.88 SE, with a maximum number of food organisms reaching 624 ind/stomach, primarily due to the consumption of *Cirripedia larvae*. The average number of prey items in the diet of sprat was 6.70 ind/stomach ± 1.90 SE (Fig. 2.6.2.1.).

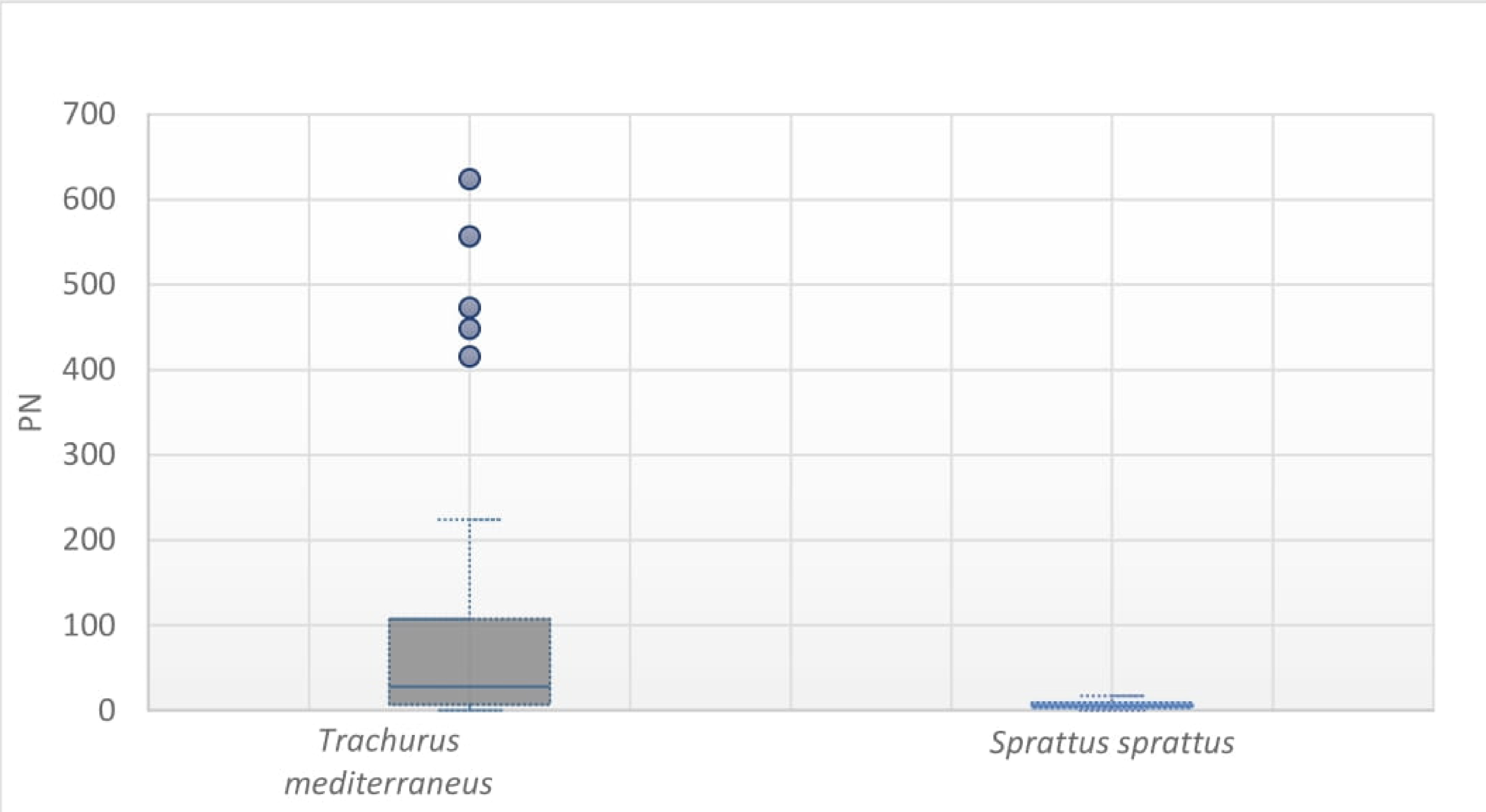

Figure 2.6.2.1. Box plot: Number of prey (PN, ind/stomach) in the stomach contents of surveyed specimens by species in November 2024 (median, range of values: 25–75%; minimum and maximum values are indicated)

In the zooplankton samples from the marine environment, 25 species/groups were identified, with a significant portion (20 species/groups) being present as components in the diet of horse mackerel and 2 species/groups in the diet of sprat.

The following groups and species are present in the sprat diet: Copepoda, mainly the species *Calanus euxinus*, and meroplankton larvae of *Cirripedia*.

Accordingly, the horse mackerel diet consisted of the following groups and species: *Mysida-Paramysis* spp.; Malacostraca - *Upogebia pusilla*; Copepoda - *Calanus euxinus, Pseudocalanus elongatus, Paracalanus parvus, Acartia clausi, Oithona davisae, Centropages ponticus, Harpacticoida spp*.; Diplostraca – *Pleopis polyphemoides, Penilia avirostris*, meroplankton - *Lamellibranchia veliger, Gastropoda veliger, Cirripedia larvae, Decapoda larvae*; the class Appendicularia is represented by the species *Oicopleura dioica*; the type

Annelida is represented by larvae of the class Polychaeta, the type Protozoa of the species *Noctiluca scintillans*; type Chaetognatha - from *Parasagitta setosa*, and from Chordata fish eggs and larval stages are found.

The indices of relative importance for the main dietary components, their percentage contribution by abundance and biomass, as well as their frequency of occurrence, are presented in Table 2.6.2.1. for the studied pelagic fish species.

Table 2.6.2.1. The diet composition of pelagic fish species (XI. 2024)

1. **Sprat**

Food composition	*N (%, of the total abundance)*	*M (%, of total biomass)*	*FO - Frequency of Occurrence*	*IRI - Relative Importance Index*
Calanus euxinus	95.5	99.9	80.0	15631.7
Cirripedia cypris	4.5	0.1	20.0	92.1
Total	**100.00**	**100.00**		

2. **Horse mackerel**

Food composition	*N (%, of the total abundance)*	*M (%, of total biomass)*	*FO - Frequency of Occurrence*	*IRI - Relative Importance Index*
Cirripedia cypris	24.83	13.08	100.00	3790.79
Acartia clausi	9.12	16.51	100.00	2562.64
Cirripedia nauplii	17.32	9.90	91.67	2495.10
Paracalanus parvus	14.18	7.88	100.00	2205.91
Lamellibranchia veliger	13.14	1.85	100.00	1499.26
Calanus euxinus	5.90	19.06	66.67	1664.13
Parasagitta setosa	5.46	24.01	50.00	1473.41
Pseudocalanus elongatus	4.00	4.14	100.00	813.40
others	6.06	3.57		
Total	100.00	100.00		

In the analysed samples, the diet of sprat is predominantly composed of Copepoda - specifically *Calanus euxinus*. The diet of horse mackerel is dominated by meroplankton larvae, including *Cirripedia cypris* and *nauplii*, as well as copepods (Table 2.6.2.1., Fig. 2.6.2.2.).

Project No. BG14MFOP001-1.002-0001 "Collection, management and use of data for the purposes of scientific analysis and implementation of the Common Fisheries Policy for the period 2023-2024", financed by the Maritime, Fisheries and Aquaculture Programme, co-financed by the European Union through the European Fund for maritime, fisheries and aquaculture fund.

1. 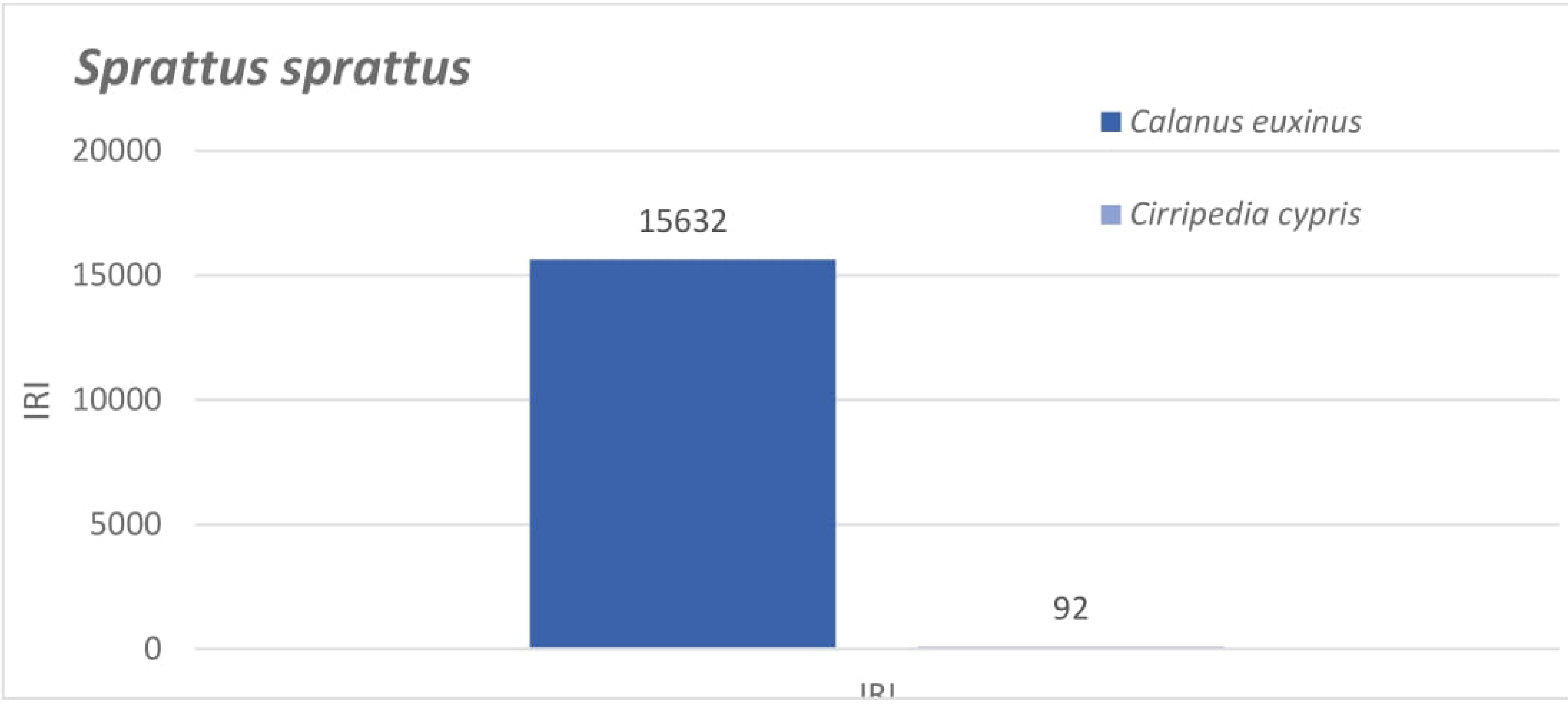

2. 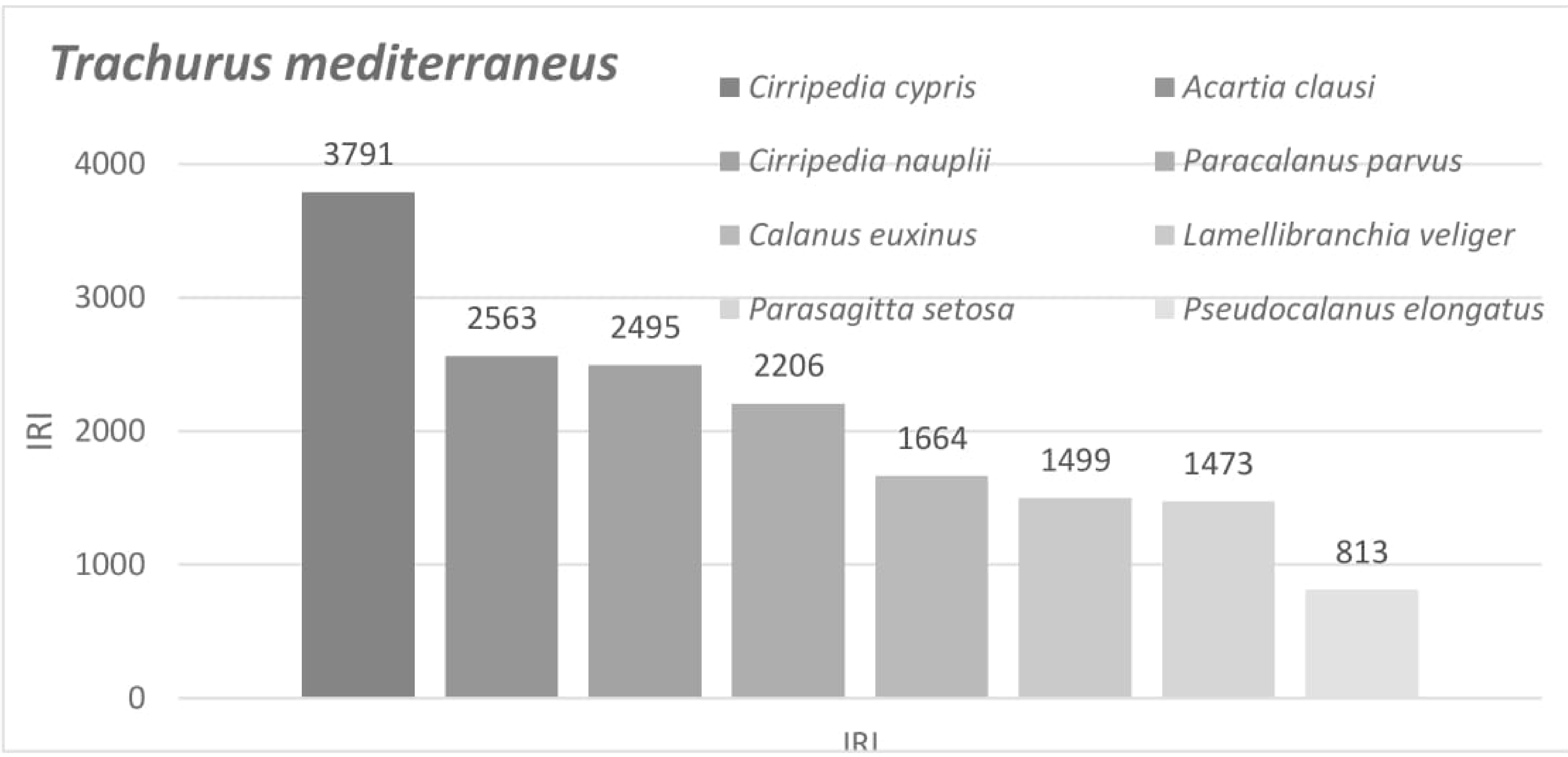

Figure 2.6.2.2. Average relative importance index (IRI) of the main species in the diets of sprat (1) and horse mackerel (2) in November 2024

Project No. BG14MFOP001-1.002-0001 "Collection, management and use of data for the purposes of scientific analysis and implementation of the Common Fisheries Policy for the period 2023-2024", financed by the Maritime, Fisheries and Aquaculture Programme, co-financed by the European Union through the European Fund for maritime, fisheries and aquaculture fund.

2.6.3. Species composition and quantities of zooplankton in the marine environment

During the study period, zooplankton biodiversity was comprised of 25 species and groups of organisms (Table 2.6.3.1.).

Table 2.6.3.1. Species composition of zooplankton

	Species
1.	*Noctiluca scintillans*
2.	*Aurelia autria*
3.	*Beroe ovata*
4.	*Pleurobrachia pileus*
5.	*Calanus euxinus*
6.	*Pseudocalanus elongatus*
7.	*Oithona similis*
8.	*Oithona davisae*
9.	*Acartia clausi*
10.	*Centropages ponticus*
11.	*Pontella mediterranea*
12.	*Harpacticoida* spp.
13.	*Pleopis polyphemoides*
14.	*Penilia avirostris*
15.	*Polychaeta larvae*
16.	*Lamellibranchia veliger*
17.	*Gastropoda veliger*
18.	Cirripedia larvae
19.	Decapoda larvae
20.	Phoronis larvae
21.	Bryozoa larvae
22.	Ascidia larvae
23.	*Parasagitta setosa*
24.	*Oicopleura dioica*
25.	Pisces ova, larvae

Project No. BG14MFOP001-1.002-0001 "Collection, management and use of data for the purposes of scientific analysis and implementation of the Common Fisheries Policy for the period 2023-2024", financed by the Maritime, Fisheries and Aquaculture Programme, co-financed by the European Union through the European Fund for maritime, fisheries and aquaculture fund.

Copepoda (50.23 %), Diplostraca (20.34 %), and meroplankton (18.97 %) played a dominant role in forming the mesozooplankton biomass (Table 2.6.3.2. and Fig. 2.6.3.1.). Gelatinous zooplankton are represented by three species: *Aurelia aurita, Pleurobrachia pileus*, and *Beroe ovata*, with *Aurelia aurita* being the most dominant (Fig. 2.6.3.1.). In terms of abundance, the dominant groups were Protozoa (70.79 %), Copepoda (18.15 %), and meroplankton (6.22 %) (Fig. 2.6.3.1.).

Table 2.6.3.2. Percentages (%, relative to biomass mg.m^{-3}) of the major zooplankton groups by station in November 2024

station	*Cope-poda*	*Clado-cera*	*Mero-plankton*	*Chaeto-gnatha*	*Appen-dicularia*	*Noctilucales*	*Jellyfish*
T9	2.03	1.50	0.87	0.45	0.21	87.80	7.15
T10	0.48	0.30	0.33	0.06	0.02	39.96	58.85
T11	0.53	0.33	0.42	0.27	0.04	88.56	9.85
T14	1.30	0.41	0.46	0.42	0.05	82.16	15.21
T16	3.30	0.81	1.02	0.37	0.21	18.02	76.26
T18	0.37	0.28	0.51	0.06	0.02	44.83	53.92
T20	0.10	0.02	0.04	0.02	0.00	4.24	95.58
T22	3.31	0.97	0.83	0.06	0.17	94.28	0.37
T24	1.91	0.96	0.97	0.44	0.03	32.66	63.03
T26	2.51	0.44	0.28	0.45	0.08	11.84	84.40
T28	1.29	0.34	0.24	0.25	0.06	24.15	73.65
T32	17.21	8.63	2.70	0.05	0.54	70.87	0.00
T34	46.70	22.23	8.81	1.64	2.70	17.93	0.00
Avg	**6.23**	**2.86**	**1.34**	**0.35**	**0.32**	**47.48**	**41.41**

Project No. BG14MFOP001-1.002-0001 "Collection, management and use of data for the purposes of scientific analysis and implementation of the Common Fisheries Policy for the period 2023-2024", financed by the Maritime, Fisheries and Aquaculture Programme, co-financed by the European Union through the European Fund for maritime, fisheries and aquaculture fund.

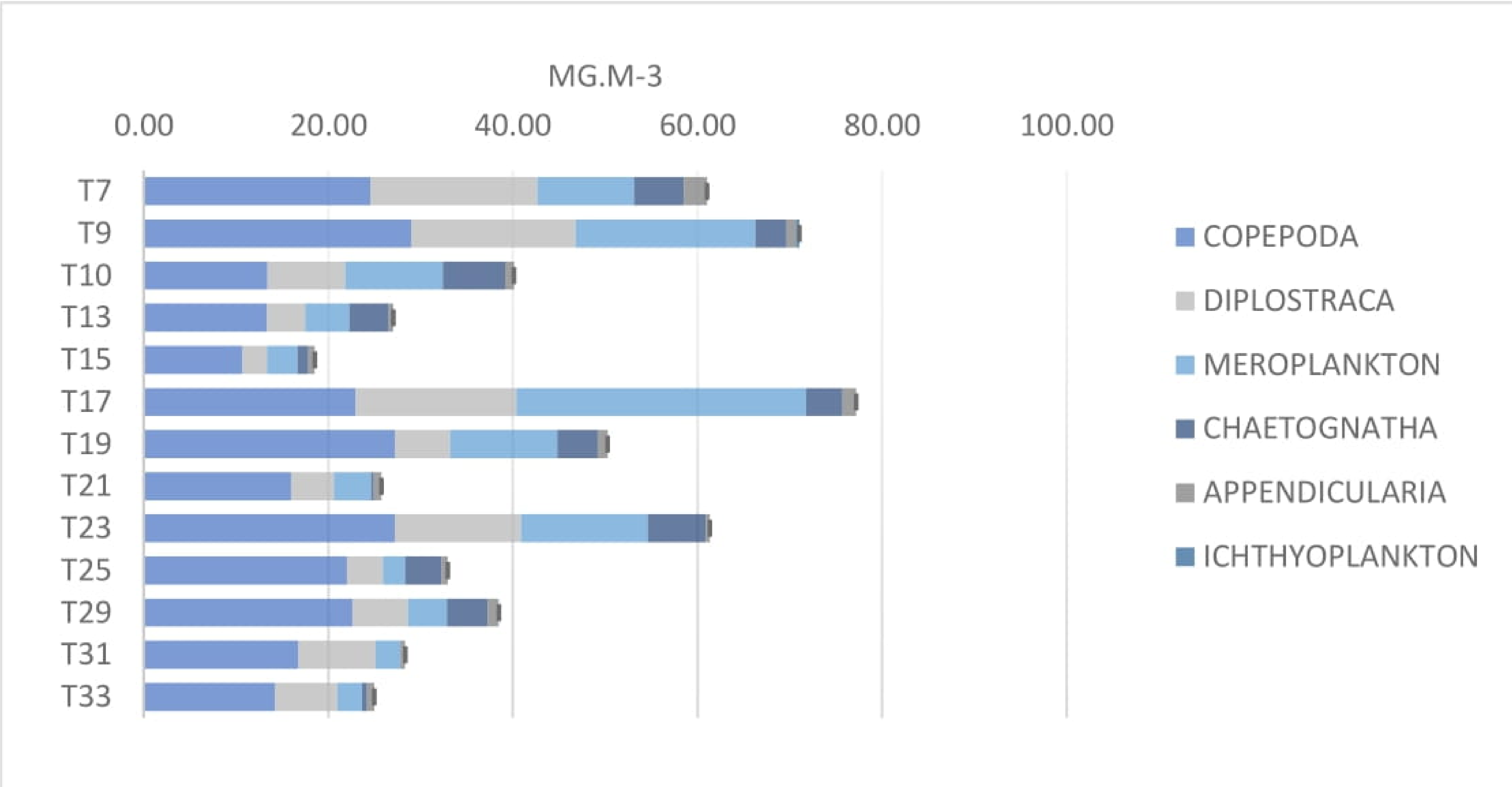
MG.M-3
0.00
20.00
40.00
60.00
80.00
100.00
T7
T9
T10
T13
T15
T17
T19
T21
T23
T25
T29
T31
T33
COPEPODA
DIPLOSTRACA
MEROPLANKTON
CHAETOGNATHA
APPENDICULARIA
ICHTHYOPLANKTON

1.

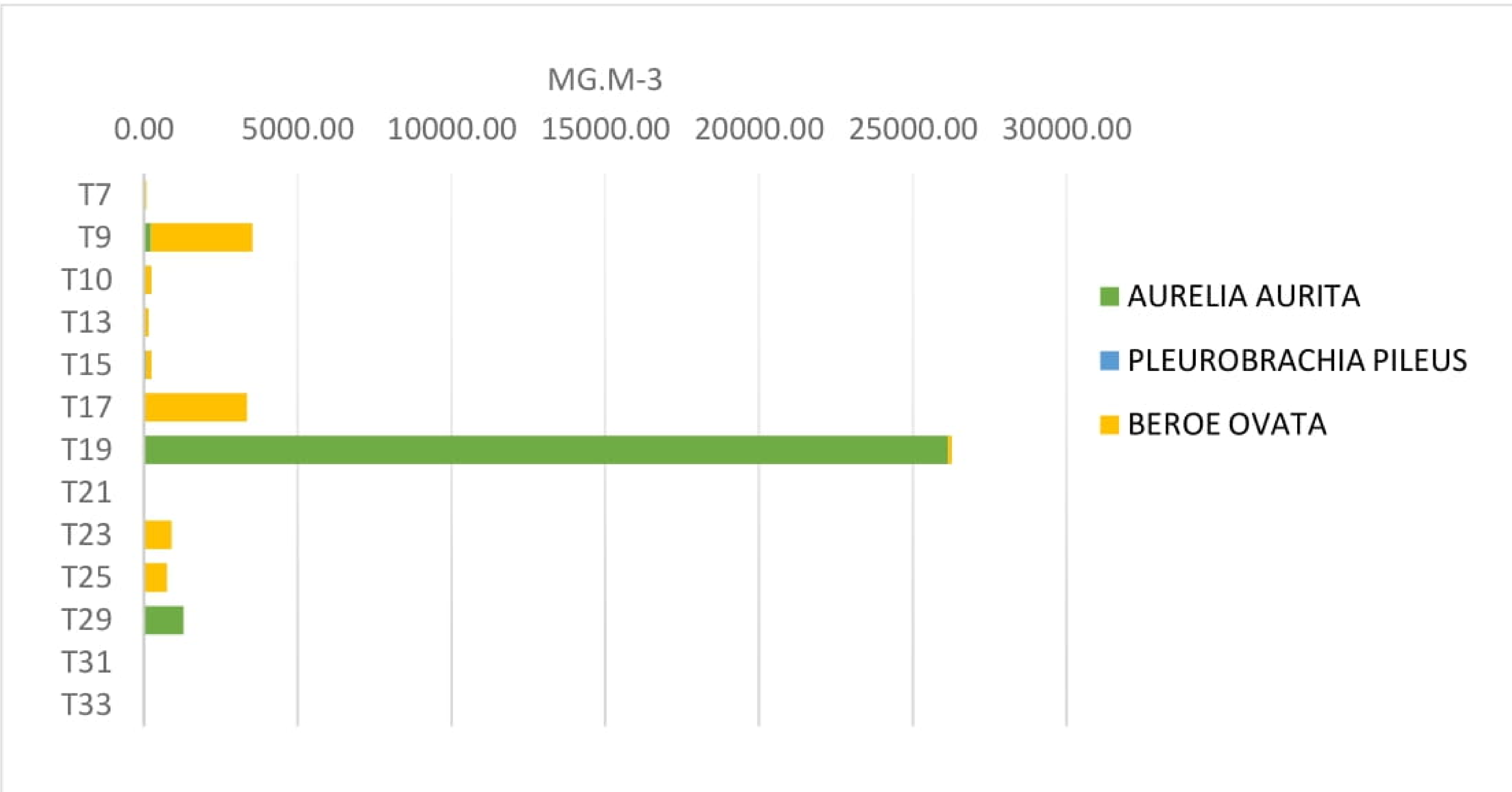
MG.M-3
0.00
5000.00
10000.00
15000.00
20000.00
25000.00
30000.00
T7
T9
T10
T13
T15
T17
T19
T21
T23
T25
T29
T31
T33
AURELIA AURITA
PLEUROBRACHIA PILEUS
BEROE OVATA

2.

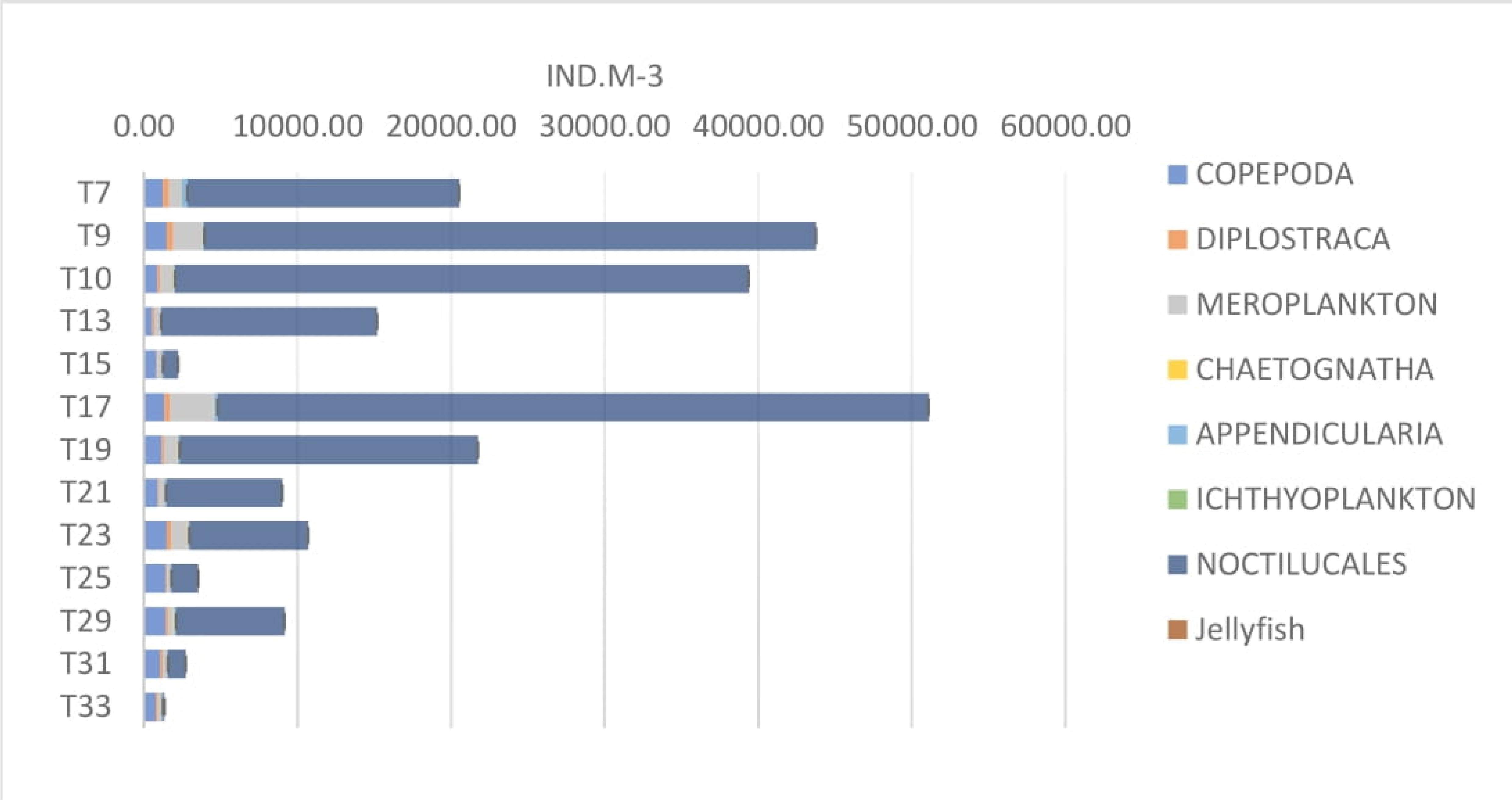

3.

Figure 2.6.3.1. Distribution of mesozooplankton biomass (1, mg.m^{-3}) and gelatinous zooplankton (2, mg.m^{-3}), and abundance of major zooplankton groups (3, ind.m^{-3}) by station in November 2024

Table 2.6.3.3 presents summarized the statistical data on the total biomass of zooplankton and its main constituent subgroups: mesozooplankton, gelatinous zooplankton, and protozoa. The total zooplankton biomass has average levels of 3800 mg·m^{-3} ± 2051.76 (SE) and is primarily formed by gelatinous species (2830.131 mg·m^{-3} ± 1981.43 (SE). The biomass of mesozooplankton (42.86 mg·m^{-3}) is comparable to the seasonal average.

Table 2.6.3.3. Summary data on the total biomass (mg.m^{-3}) of zooplankton and the major groups in November 2024

	Meso - zooplankton	*Gelatinous zooplankton*	*Protozoa*	*Total zooplankton biomass*
Mean	42.855	2830.131	927.420	3800.406
Standard error	5.365	1981.434	266.596	2051.759
Median	38.476	249.308	464.220	1208.669

Standard deviation	19.344	7144.161	961.226	7397.724
Kurtosis	-1.065	12.061	-0.413	10.592
Skewness	0.578	3.433	0.975	3.170
Minimum	18.536	0.000	5.460	30.447
Maximum	77.198	26265.486	2778.480	27480.715
Confidence interval (95.0%)	11.689	4317.173	580.863	4470.400

During the study, the mesozooplankton biomass reaches its highest values of approximately 77.20 mg·m^{-3} off the northern part of the coast (Fig. 2.6.3.2.(1)). The quantities of Protozoa increased in the northern region, with a maximum of 2778 mg·m^{-3}, as well as in Burgas Bay (Fig. 2.6.3.2.(2)). The concentration of gelatinous zooplankton increased off the central and northern parts of the coast, reaching a maximum of 26 g·m^{-3} (Fig. 2.6.3.2.(3)).

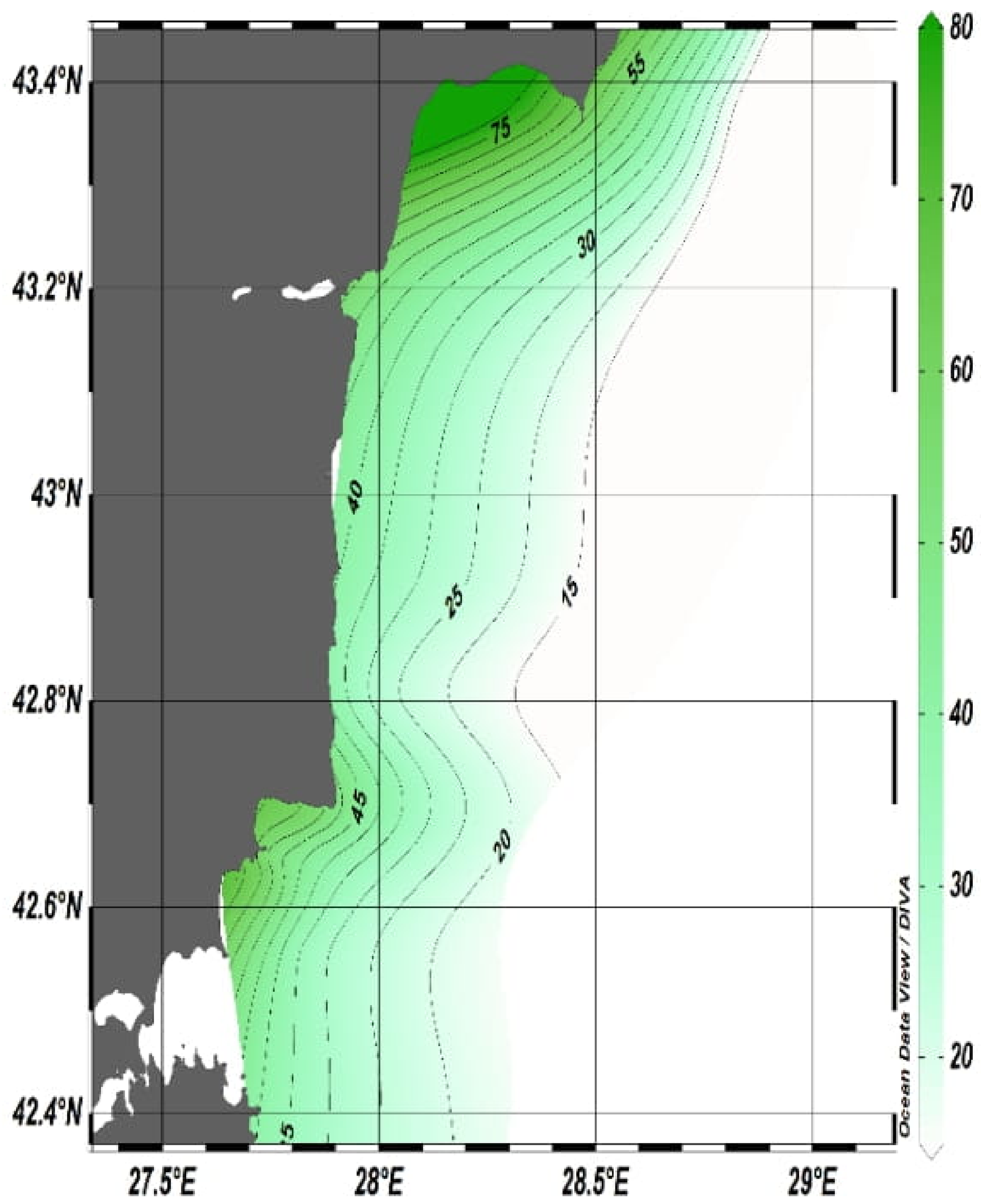

1 .

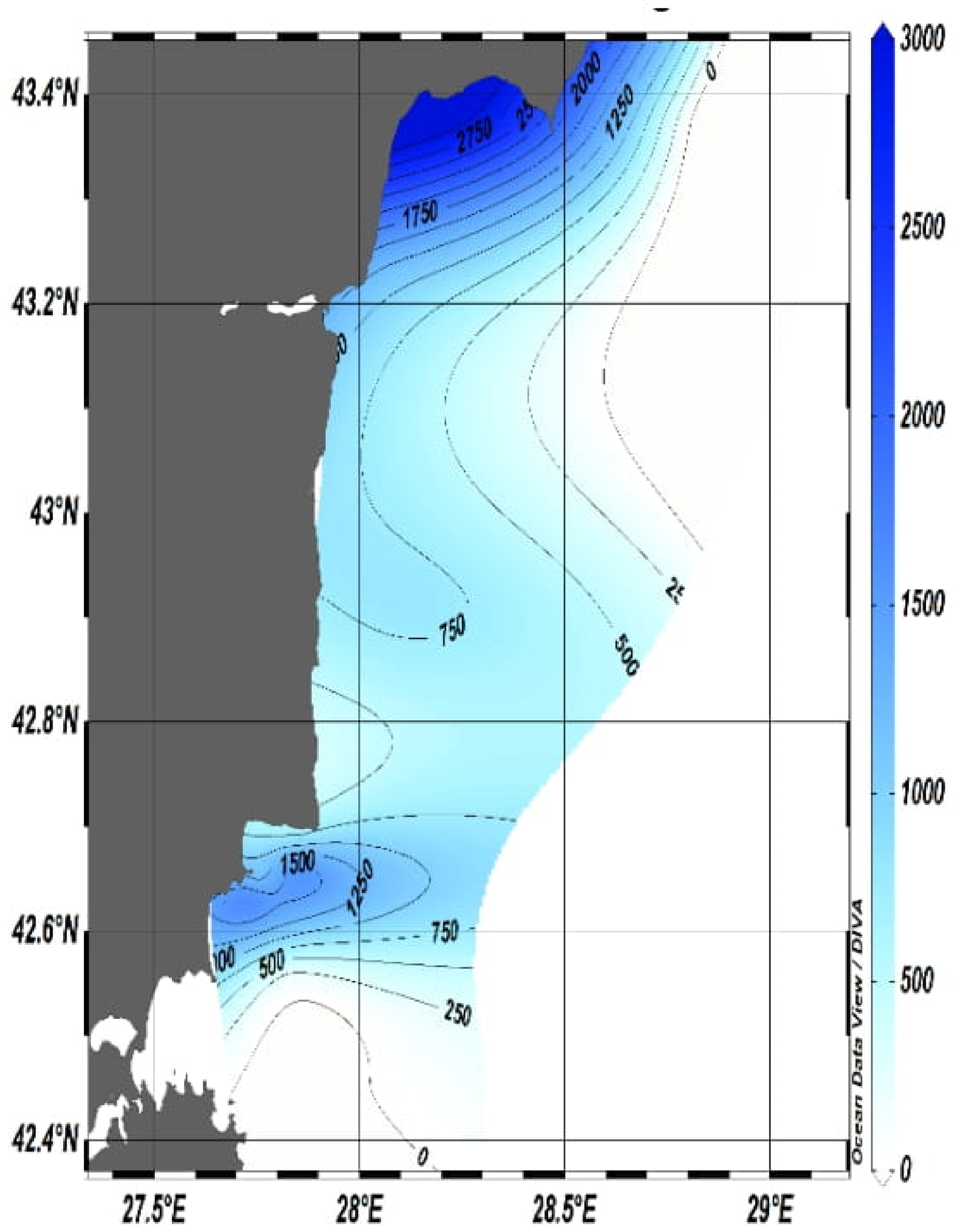

2.

3.

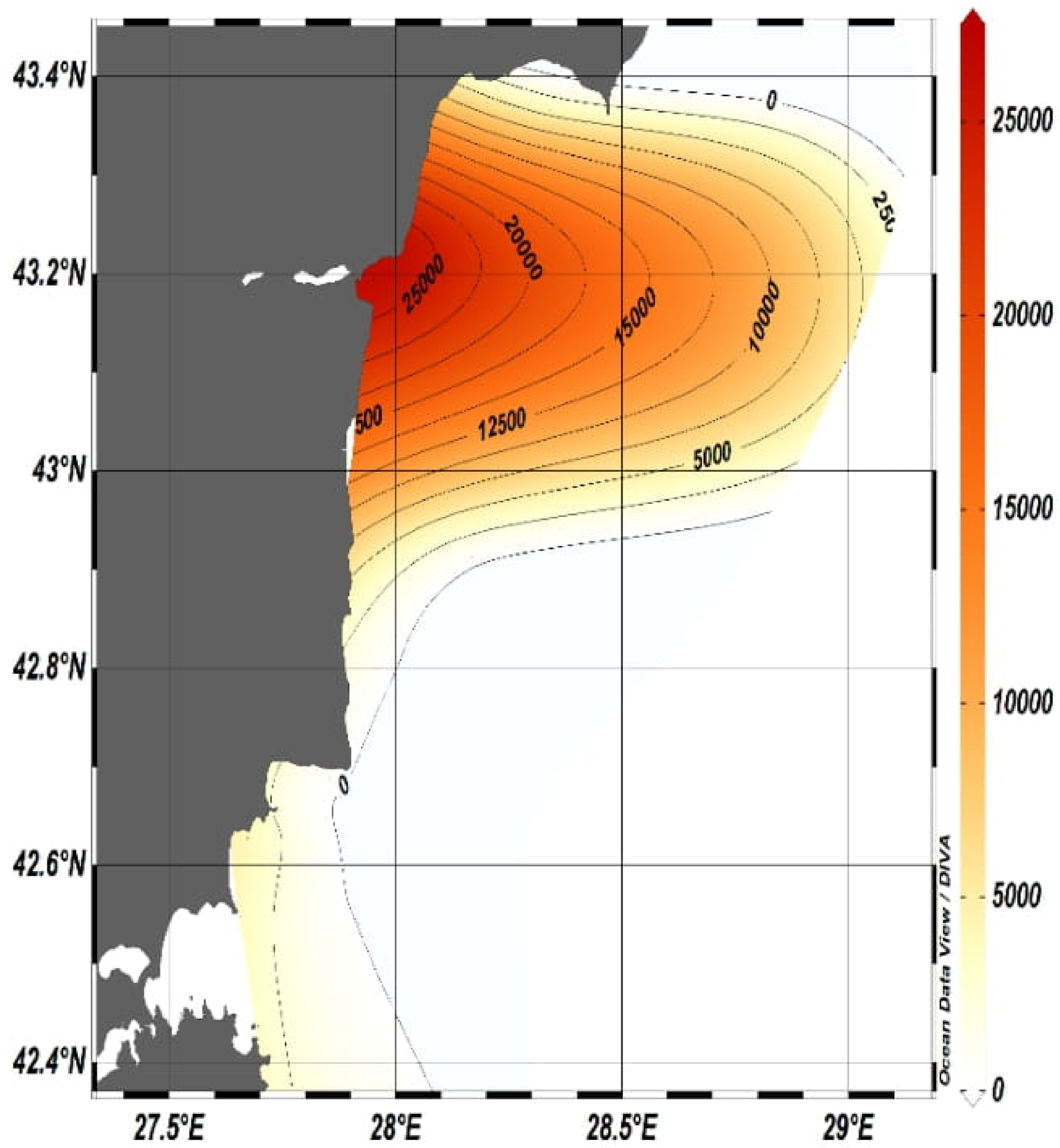

Figure 2.6.3.2. Spatial distribution of the biomass (mg.m^{-3}) of mesozooplankton (1), protozoa (2), and gelatinous zooplankton (3) in November 2024

3. Conclusions

- During the study period, 36 trawl hauls were conducted in the Bulgarian sector of the Black Sea aboard the R/V HaitHabu. The survey took place in November 2024. The trawling duration ranged between 30 and 40 minutes at depths between 15 m and 100 m in the area between Ahtopol, Kiten, and Durankulak. Sprat (*Sprattus sprattus*) was observed at depths greater than 18 m.
- A total of 24 species were identified during the survey, including 17 fish species, 2 crustaceans, 2 mollusks, and 3 macrozooplankton species. The most frequently encountered species in the trawl catches (presence/absence) were *T. mediterraneus* (45.76%), *M. barbatus* (24.66%), and *M. merlangus* (10.4%). *Sprattus sprattus* was observed sporadically in the catches. Other species such as *A. immaculata*, *N. melanostomus*, *G. niger*, *M. batrachocephalus*, *Z. ophiocephalus*, *R. clavata*, *D.*

pastinaca, *P. lascaris*, *U. scaber*, *T. draco*, *S. maximus*, *Sq.. acanthias*, and *A. stellatus* had negligible presence in the catches.

- Sprat (*Sprattus sprattus*) – although one of the most widespread pelagic species in the Black Sea – was represented by single specimens during the study period. This is most likely related to the migration of predatory species and the scattered nature of the sprat schools. High sea water temperature is a significant factor contributing to the dispersed distribution of small pelagic fish schools, such as sprat.
- Four goby species (*G. niger*, *N. melanostomus*, *M. batrachocephalus*, and *Z. ophiocephalus*) and isolated specimens of *A. immaculata* were observed in the catches. A quantitative assessment was not possible due to the low number of different species found in individual trawls.

Horse mackerel

- During the survey, horse mackerel was observed to be widely distributed, with the highest biomass values recorded in the 30–50 m depth layer: 1589.8 t, followed by 1030.6 t (30–50 m) and 472.8 t (15–30 m).
- The total surveyed area was 8010.24 km², and the estimated total biomass of horse mackerel was 3093.2 tonnes. The densest aggregations were observed off the coast of Byala and in the Bay of Nesebar. The highest biomass was recorded in the 30–50 m depth stratum: 2138 t, followed by 1511.35 t (15–30 m) and 1281.71 t (50–100 m).
- In November 2024, horse mackerel was well represented in the catch composition, with the highest density of distribution recorded in the waters of the Nesebar Bay, Obzor, and Burgas Bay.
- The highest values of CPUA (catch per unit area) were recorded in the 30–50 m depth layer – 1178.3 $kg.km^{-2}$, with an average of 731 $kg.km^{-2}$. In the 15–30 m depth layer, CPUA was 731 $kg.km^{-2}$, and in 50–100 m – 310.3 $kg.km^{-2}$, where the species was found in isolated trawls.
- The highest CPUE (catch per unit effort, $kg.h^{-1}$) values were observed off Obzor and in Nesebar Bay.
- The length distribution of horse mackerel samples followed a normal (Gaussian) pattern, with a bell-shaped curve. The most frequent lengths were in the range of 8.5–10.5 cm, with a peak at the 10.5 cm size group.
- The dominant age group of horse mackerel during the study period was 2–2+ years (37.33%), followed by 1–1+ years (26%). Juvenile recruitment accounted for 7.66%.

The age structure ranged from 0 to 5+ years, with significant representation of the 3–3+ year group (21.33%).

- The length–weight relationship was described by the model $W = 0.009*L^{2.99}$, indicating a positive allometric growth coefficient (> 3). The nonlinear model showed a high degree of determination ($R^2 = 0.9903$).
- Growth parameters calculated using the von Bertalanffy growth model showed an asymptotic length of 22.45 cm and a relatively high growth coefficient, indicating a faster approach to asymptotic size.
- The average weights of horse mackerel ranged from 7.3 to 29.9 g.
- The 10.5–12.5 cm size classes dominated the catches, while larger size classes were represented in smaller proportions. In November 2024, the 12.5 cm size class had the highest percentage in the catches, followed by the 10.5 cm size class.
- Biomass, like abundance, was dominated by the 125 mm size group.
- The gonadosomatic index (GSI %) of horse mackerel indicated a later stage of spawning activity. The correlation between gonad weight and GSI was strong ($R^2 = 0.3353$), suggesting active spawning and sexual maturity during the study period.
- The sex ratio of horse mackerel was as follows: females – 50%, males – 45%, and immature individuals – 5%.
- Maximum Sustainable Yield (MSY):

Based on the current biomass:

Bmsy = 0.5 × 3093.174 t = 1546.6 t

Based on maximum estimated biomass:

Bmsy = 0.5 × 4931.361 t = 2,465.68 t

According to FAO (1995), following the precautionary approach:

Bpr (2/3 MSY) = 1644 t

The maximum allowable catch of horse mackerel in the Bulgarian sector of the Black Sea should be approximately 1600 tonnes.

Project No. BG14MFOP001-1.002-0001 "Collection, management and use of data for the purposes of scientific analysis and implementation of the Common Fisheries Policy for the period 2023-2024", financed by the Maritime, Fisheries and Aquaculture Programme, co-financed by the European Union through the European Fund for maritime, fisheries and aquaculture fund.

Red Mullet

- The total surveyed area was 8010.24 km², and the estimated total biomass of red mullet was 496 tonnes.
- The densest aggregations were observed off Cape Kaliakra, in Nesebar Bay, and Burgas Bay of at depths of 30–50 m, and west of Sozopol at depths of 50–100 m. The species was recorded at 24 out of 36 stations, with the highest density in the 30–50 m stratum.
- The length–weight relationship for red mullet showed a strong positive allometry, with a high coefficient of determination (n = 3.114), $R^2 = 0.9944$.
- Catch per unit area (CPUA) in the 15–30 m stratum was 125 kg.km^{-2}; in the 30–50 m stratum – 124 kg/km², and in the 50–100 m stratum – 2.9 kg.km^{-2}. Average CPUA values ranged between 15 and 310 kg.km^{-2}.
- Analysis of CPUA and CPUE (catch per unit effort) showed that the highest densities and abundances were found in the 30–50 m depth zone, followed by the 15–30 m zone.
- Length–weight analysis (L–W) for red mullet in November 2024 showed a very strong dependence between size and weight, with well-defined allometric growth (R^2 = 0.9944).
- The dominant size classes in the catches during the survey were 11 cm and 13 cm.
- The most abundant age group was 1–1+ years, followed by 2–2+ and 3–3+ years. Other age groups had negligible representation in the catches in November 2024.
- Growth parameters calculated using the von Bertalanffy growth model showed an asymptotic length of 18.41 cm and relatively high growth coefficient values, indicating faster attainment of the asymptotic size.
- The 11.0 cm and 13.0 cm size classes dominated the red mullet catches, while larger size classes were represented in lower proportions. In November 2024, the 11 cm size class had the highest share in the catches, followed by the 13 cm class.
- The numerical abundance of 3–3+ year-old individuals was the highest, followed by the 2–2+ age group. However, in terms of biomass, the 4–4+ age group dominated.
- The sex ratio for red mullet was as follows: females – 48%, males – 44%, and immature individuals – 8%.
- Red mullet was in an active phase of gonadal maturation, likely due to high sea water temperatures.
- Maximum allowable catch as a proportion of the current biomass for red mullet:

Project No. BG14MFOP001-1.002-0001 "Collection, management and use of data for the purposes of scientific analysis and implementation of the Common Fisheries Policy for the period 2023-2024", financed by the Maritime, Fisheries and Aquaculture Programme, co-financed by the European Union through the European Fund for maritime, fisheries and aquaculture fund.

B_{msy} = 0.5*496.11 t = 248.05 t

According to FAO (1995), following the precautionary approach:

B_{pr} (2/3 MSY) = 165.4 t

The maximum allowable catch of red mullet in the Bulgarian part of the Black Sea should be approximately 165 tonnes.

Whiting

- The species was represented in the catches by single specimens, with catches of 1 kg each at two of the stations. It was not possible to make a spatial and quantitative assessment of the species' distribution based on the autumn 2024 survey.
- The size distribution of the specimens showed a normal pattern, with peaks at 11.5 cm and 14.5 cm.
- In the catches from the autumn 2024 survey, individuals aged 4–4+ years (38%) and 5–5+ years (20%) were predominant.
- The length–weight relationship showed a very high degree of reliability (R^2 = 0.955).
- The von Bertalanffy Growth Function (VBGF) was applied to determine growth parameters. The asymptotic length ($L\infty$) reached 27.55 cm, and the growth rate was classified as low (k = 0.23).
- The sex ratio was 50% females, 49% males, and 1% larvae.
- The maturation of the gonads indicates the onset of the species' active reproductive period. Due to the warmer weather, the spawning process is likely to intensify in the coming months, even at relatively lower sea temperatures.
- The relationship between gonad weight and the gonadosomatic index showed a high level of reliability (R^2 = 0.83).
- The low number of specimens caught did not allow for a more detailed spatial analysis to determine the biomass and abundance of the species during the study period. As a result, it was not possible to conduct analyses or draw conclusions regarding sustainable exploitation measures for the autumn 2024 period.

Project No. BG14MFOP001-1.002-0001 "Collection, management and use of data for the purposes of scientific analysis and implementation of the Common Fisheries Policy for the period 2023-2024", financed by the Maritime, Fisheries and Aquaculture Programme, co-financed by the European Union through the European Fund for maritime, fisheries and aquaculture fund.

Feeding

- In autumn 2024, the diet of horse mackerel included 20 species/groups, while the diet of sprat contained two species/groups. Sprat primarily fed on Copepoda, specifically *Calanus euxinus*. The diet of horse mackerel was more diverse, including various species of Mysida, Copepoda, Diplostraca, meroplankton, Appendicularia, Chaetognatha, and fish larvae.
- The Copepoda species *C. euxinus* dominated the diet of sprat (IRI = 15631.7). In horse mackerel, meroplanktonic larvae, particularly Cirripedia larvae (IRI = 6285.89), as well as the copepod *Acartia clausi* (IRI = 2,562.64), were predominant.
- The mean ISF varied among species: sprat – 0.22% BW ± 0.12 (SD) and horse mackerel – 0.52% BW ± 0.64 (SD). The current study recorded a higher stomach fullness index for horse mackerel, but a lower ISF value for sprat compared to data from 2023.
- Horse mackerel stomachs contained the highest average number of prey items (88.58 ind/stomach ± 11.88 SE), with a maximum of 624 ind/stomach, mainly due to the consumption of Cirripedia larvae. In contrast, sprat had an average of 6.70 ind/stomach ± 1.90 SE.
- The average biomass of zooplankton in the marine environment was 3800 $mg.m^{-3}$ ± 2051.76 (SE), composed mainly of gelatinous species – 2830.13 $mg.m^{-3}$ ± 1981.43 (SE). The biomass of edible zooplankton was comparable to the seasonal average – 42.86 $mg.m^{-3}$, with maximum values of ~77.2 $mg.m^{-3}$ recorded along the northern coasts.

Project No. BG14MFOP001-1.002-0001 "Collection, management and use of data for the purposes of scientific analysis and implementation of the Common Fisheries Policy for the period 2023-2024", financed by the Maritime, Fisheries and Aquaculture Programme, co-financed by the European Union through the European Fund for maritime, fisheries and aquaculture fund.

4. References

1. Bertalanffy L. VON 1938. A quantitative theory of organic growth (Inquiries on growth laws. II). Human Biol. 10: 181-213.
2. Gulland J.A., 1966. Manual of sampling and statistical methods for fisheries biology. Part I: Sampling methods. FAO Manuals in Fisheries Science No. 3, Rome.
3. FAO: Precautionary approach to fisheries. FAO Fish. Tech. Paper N. 350 (1), 1995.
4. ICES. 2011. Report of the Workshop on Sexual Maturity Staging of Herring and Sprat (WKMSHS), 20-23 June 2011, Charlottenlund, Denmark. ICES CM 2011/ACOM:46. 143pp.
5. Kasapoglu, N., Duzgunes, E. 2014. Otolith Atlas for the Black Sea. Journal of Environmental Protection and Ecology 16, No 1, 133–144
6. Korshenko, A., Alexandrov B., 2013. Manual for mesozooplankton sampling and analysis in the Black Sea monitoring (Black Sea Zooplankton Manual) Online: http://bsc.ath.cx/documents/ExpertNetwork/default.asp?I=/Expert%20Network%20-%20 Zooplankton
7. Laevastu, T., 1965. Manual methods in fisheries biology. Observations on the chemical and physical environment. Chemical analysis of water FAO. Marine Physiological Sci., 6: 86-86.
8. Mordukhay-Boltovskoy, F.D. (Ed.). 1968. The identification book of the Black Sea and the Sea of Azov Fauna.- Kiev: Naukova Dumka Publ., T. 1 (Protozoa, Porifera, Coelenterata, Ctenophora, Nemertini, Nemathelminthes, Annelida, Tentaculata), 423 pp. (in Russian).
9. Pinkas L.,. Oliver M.S, Iverson I.L.K., 1971. Food habits of albacore, bluefin tuna and bonito in Californian waters. California Fish Game 152:1-105.
10. Pısıl, Y., 2006. Karadeniz'de Yaşayan Çaça Balığı (Sprattus sprattus (L., 1758))'nda Kemiksi Yapıları ve Uzunluk-Frekans Metodu ile Yaş Tayini. 19 Mayıs Üniversitesi, Fen Bilimleri Enstitüsü, Y. Lisans Tezi, 32 s.
11. Simon, K.D., Y. Bakar, A.G. Mazlan, C.C. Zaidi and A. Samat et al., 2012. Aspects of the reproductive biology of two archer fishes Toxotes chatareus, (Hamilton, 1822) and Toxotes jaculatrix (Pallas, 1767). Environ. Biol. Fish., 93: 491-503.